Proceedings of the
Annual Stability Conference
Structural Stability Research Council
Baltimore, Maryland, April 10-13, 2018

Distortional Failure and DSM Design of Cold-Formed Steel Lipped Channel Beams under Non-Uniform Bending

Isis Cler Depolli[1], Alexandre Landesmann[2], Dinar Camotim[3], André Dias Martins[4]

Abstract

Recently, Martins *et al.* (2017a) reported an in-depth numerical investigation that providing solid evidence that the current Direct Strength Method (DSM) beam distortional strength curve overestimates the ultimate strength of cold-formed steel simply supported beams, thus leading to unsafe designs – the beams analyzed were uniformly bent (mostly about the major-axis). Moreover, the above authors used the distortional failure moment data obtained to propose new DSM beam distortional design curves, differing visibly from the current one for moderate-to-high slenderness – these curves were already successfully employed in the context of the design of uniformly bent beams undergoing local-distortional interaction (Martins *et al.* 2017b). The work reported in this paper, which may be viewed as a continuation of the aforementioned investigation, concerns the distortional post-buckling behavior and DSM design of simply supported cold-formed steel beams buckling and failing in distortional modes under non-uniform bending due to unequal end moments – five bending moment diagrams (including uniform bending, for comparison purposes) are considered. As in previous studies, two beam simply supported end conditions are considered, differing in the end cross-section warping and local displacements/rotations, which may be either completely free or fully prevented. The beams analyzed buckle and fail in modes exhibiting various half-wave numbers. After acquiring in-depth insight on how the bending moment diagram influences the beam distortional buckling and post-buckling behaviors, an extensive numerical (shell finite element) parametric study is carried out in order to gather significant distortional failure moment data concerning lipped channel beams with various cross-section dimension ratios and yield stresses (to enable covering wide distortional slenderness ranges). These failure moments, together with additional values collected from the literature, are then employed to assess the merits of the available DSM beam distortional strength curves in predicting them, and also to propose slight adjustments/modifications aimed at achieving DSM design curves able to provide accurate failure moment predictions that take into account the variation of the bending moment diagram.

1 Introduction

Cold-formed steel structures are currently widely used by the construction industry for a plethora of different applications, such as (i) low rise official, residential and industrial buildings, (ii) high storage

[1] M.Sc. Student, Civil Engineering Program, COPPE, Federal University of Rio de Janeiro, Brazil. <isis@coc.ufrj.br>
[2] Associate Professor, Civil Engineering Program, COPPE, Federal University of Rio de Janeiro, Brazil. <alandes@coc.ufrj.br>
[3] Professor, CERIS, ICIST, DECivil, Instituto Superior Técnico, Universidade de Lisboa, Portugal. <dcamotim@civil.ist.utl.pt>
[4] Ph.D. Student, CERIS, ICIST, DECivil, Instituto Superior Técnico, Universidade de Lisboa, Portugal. <andrerdmartins@ist.utl.pt>

structures and (iii) roof trussed structures. The combined usage of high-strength steel grades and very slender cross-sections is responsible for rendering those structural systems highly susceptible to several instability phenomena – it is well known that distortional buckling is one of them, often governing the structural response and collapse of "intermediate members", *i.e.*, members with "intermediate lengths". The most advanced current design specifications for cold-formed steel structures include provisions dealing with the distortional strength and failure of columns and beams with or without perforations. In particular, most of these provisions concern the application of the Direct Strength Method (DSM – *e.g.*, Schafer 2008, Camotim *et al.* 2016), which appears prominently in the latest versions of the North-American (AISI 2016), Australian/New Zealand (AS/NZS 2005) and Brazilian (ABNT 2010) specifications for cold-formed steel structures. The application of such provisions requires only knowing the member distortional buckling and yield load/moments. In the specific case of cold-formed steel beams, a fair amount of research work has been devoted to the development/improvement of DSM-based design methodologies – for instance, the works of Yu & Schafer (2005, 2006, 2007), Bebiano *et al.* (2007), Dinis & Camotim (2010), Wang & Young (2014), Landesmann & Camotim (2016) and Martins *et al*. (2017a). At this point, it should be noted that the currently codified DSM curve was calibrated almost exclusively against experimental (uniform) failure moments of beams with small-to-moderate distortional slenderness (λ_D<1.5) (Yu & Schafer 2005) – this design curve, corresponding to an equation defined in Section 4 (see Eq. (1)), is plotted in Figure 1. In order enable the application of this DSM strength curve to "practical situations"[5], Yu & Schafer (2005) employed shell finite element analyses (SFEA) to investigate how the presence of a moment gradient (due to unequal applied end moments) influences the distortional buckling, post-buckling and ultimate strength behaviors of cold-formed steel beams. The numerical analyses simulations carried out by these authors were quite sophisticated, since they aimed at simulating a rather complex 4-point bending experimental set-up previously employed by them to test uniformly bent beams (more details provided in Section 3.2). They considered (i) two moment gradients, corresponding to $\psi=0$ and $\psi=0.5$ (ψ is the ratio between the end moments of the beam segment under scrutiny – see Figs. 6(a)-(c)), (ii) two cross-section shapes (lipped channels and zed-sections) with *9* distinct dimensions (1LC + 8Z), (iii) *5* yield stresses, associated with small-to-moderate distortional slenderness (λ_D<1.5), and (iv) "warping continuity" at cross-sections connecting adjacent beam segments – *i.e.*, warping support conditions lying in-between "completely free" and "fully prevented".

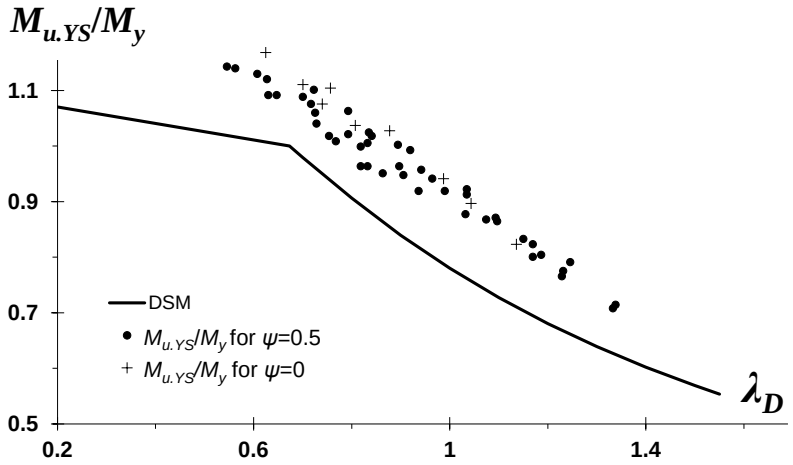

Figure 1. Comparison between ($M_{u.YS}/M_y$) values concerning the numerical failure moments reported by Yu & Schafer (2005) for beams subjected to moment gradients and the currently codified DSM beam distortional strength curve

[5] Only very rarely involving uniform bending moment diagrams.

Figure 1 (i) plots the ($M_{u.YS}/M_y$) values corresponding to the *55* numerical failure moments reported by Yu & Schafer (2005) for beams subjected to moment gradients, against the distortional slenderness $\lambda_D=(M_y/M_{crD})^{0.5}$ and (ii) compares them with the currently codified DSM beam distortional strength curve[6] – while M_{crD} and $M_{u.YS}$ and are the beam numerical distortional buckling and failure moments, M_y is the cross-section yield moment. Yu & Schafer readily concluded that their numerical failure moments were clearly underestimated by the (then available) distortional strength curve. Nevertheless, probably because the distortional failure moment estimates were all safe, no further action was ever taken to improve this situation, *i.e.*, to ensure more accurate DSM-based failure moment predictions for beams subjected to moment gradients.

On the other hand, a very recent numerical (SFE) investigation carried out by Martins *et al*. (2017a), who analyzed more than *4000* simply supported uniformly bent cold-formed steel beams exhibiting (i) three cross-section shapes (lipped channels, zed-sections and hat-sections), (ii) several geometries (cross-section dimensions and lengths), and (iii) the two end support conditions considered in this work, termed SCA and SCB – warping and local displacements/rotations completely free and fully prevented, respectively. These authors (i) showed that the currently codified DSM beam distortional design curve (originally proposed by Yu & Schafer 2005 and later modified to exhibit a sloped line in the low slenderness range) failed to predict adequately part of the numerical distortional failure moments obtained (those concerning slender beams) and (ii) proposed novel DSM-based distortional design curves that exhibit a much better prediction quality, particularly in the high slenderness range. The objective of the present work is to extend the scope of the above study by investigating beams subjected to non-uniform major-axis bending (caused by unequal end moments), namely their (i) buckling, post-buckling and ultimate strength behaviors and (ii) DSM-based design. The beams analyzed are acted by five distinct linear bending moment diagrams (including uniform bending, for comparison proposes).

The paper begins by addressing the beam geometry selection, carried out by means of sequences of "trial-and-error" buckling analyses. It aims at identifying beam geometries (cross-section dimensions and lengths) that ensure, as much as possible, "pure" distortional buckling and failure modes for both uniform and non-uniform bending (*i.e.*, the selected beams exhibit distortional critical buckling uniform and non-uniform moments significantly lower than their local and global counterparts). Then, the shell finite element model employed to perform the geometrically and materially non-linear ANSYS (SAS 2009) analyses is briefly described and validated, by reproducing simulations reported by Yu & Schafer (2005). Next, illustrative numerical results concerning the simply supported beam distortional post-buckling behavior and ultimate strength are presented and discussed, paying particular attention to the combined influence of the (i) end support conditions (SCA or SCB) and (ii) bending moment diagram (via the ψ value) – elastic and elastic-plastic numerical results are addressed separately. Finally, the numerical failure moment data obtained in this work, together with additional values collected from the literature (Yu & Schafer 2005), are used to assess the merits of the available DSM beam distortional design curves, namely (i) the one currently codified in North America (AISI 2016), (ii) those recently proposed by Martins *et al.* (2017a) and (iii) their modifications proposed in this work. It is clearly shown that such modifications improve the failure moment prediction quality, thus providing encouragement to continue the search for an efficient and reliable DSM-based design approach for beams failing in distortional modes under uniform or non-uniform bending.

[6] Note that this strength curve is only included in the latest version of the North-American specification (AISI 2016) – in all other versions, the strength curve exhibits a horizontal plateau for λ_D <0.673. The replacement of this plateau by the inclined straight line displayed in Figure 1 stems from the output of the investigation carried out by Shifferaw & Schafer (2012).

2 Buckling Behavior – Beam Geometry Selection

The first task in this work consists of carefully selecting the cross-section dimensions and lengths of the cold-formed steel single-span simply supported (with respect to major and minor-axis bending) lipped channel beams to be analyzed, which (i) are subjected to the five bending moment diagrams depicted in Figure 2 ($\psi=M_1/M_2=+1.0, +0.5, 0.0, -0.5, -1.0$, where M_1 and M_2 are the two end moments), and (ii) exhibit SCA or SCB end support conditions, which were defined earlier – physically speaking, the latter correspond to rigidly attaching thick plates to the beam end cross-sections (see Fig. 5).

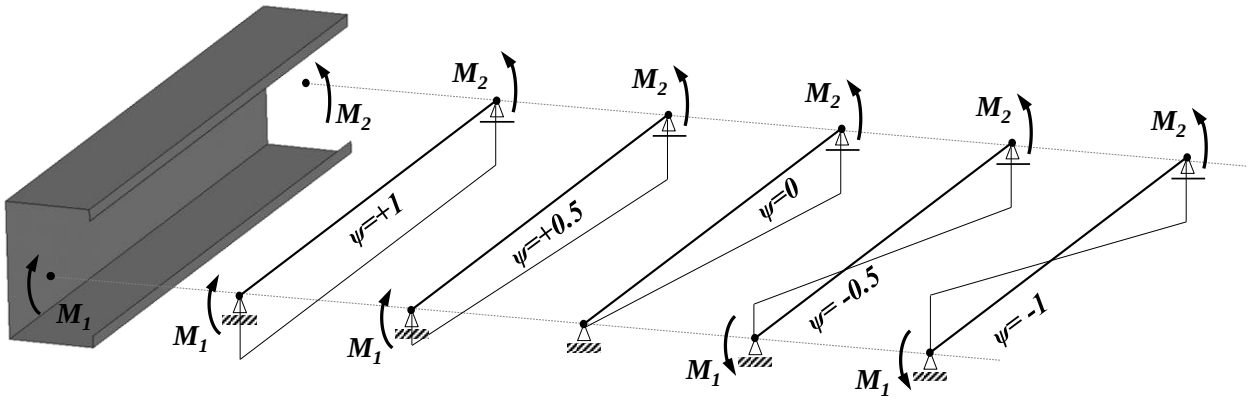

Figure 2. Bending moment diagrams considered for the lipped channel beams and corresponding ψ values

As done in previous works, the selection procedure is carried out by means of sequences of "trial-and-error" buckling analyses, performed in the code GBTUL (Bebiano *et al.* 2018), based on Generalized Beam Theory (GBT) and taking advantage of its modal nature, which makes it possible to obtain buckling moments associated with "pure" distortional modes. This selection procedure aims at satisfying the following goals/requirements:

(i) Beams buckling in "pure" distortional modes and also exhibiting distortional collapses. This goal is achieved by ensuring that the critical buckling moment (i_1) corresponds to a clear distortional mode and (i_2) falls considerably below the local and global lowest bifurcation moments.

(ii) Cross-section (lipped channel) dimensions commonly used in practice and associated with "pure" distortional failures for the five ψ values and two end support conditions considered – only the beam lengths are not the same.

(iii) As much as possible, beam lengths (iii_1) associated with single half-wave distortional buckling modes and (iii_2) close to the SCA beam values (corresponding to minimum distortional critical buckling moments).

The output of the above effort are the *15* lipped channel cross-sections whose dimensions (b_w, b_f, b_l, t – see the schematic figure in Table 2) are given in Table 1, which also displays their area (A) and major-axis elastic (S) and plastic (Z) moduli. Moreover, Tables A1-A5, included in Annex A, provide, for each ψ value considered, (i) the critical distortional buckling lengths (L_D) and moments (M_{crD}), (ii) the ratios M_{crL}/M_{crD} and M_{crG}/M_{crD} (M_{crL} and M_{crD} are the lowest local and global bifurcation moments), and (iii) the critical buckling mode half-wave numbers (n_D) for the *30* selected beams (*15* cross-section dimension sets and *2* end support conditions) – all buckling/bifurcation moments were for $E=210\,GPa$ and $v=0.3$ (typical steel Young's modulus and Poisson's ratio values). It is worth mentioning that (i) the overwhelming majority of the beams selected exhibit single half-wave critical distortional buckling modes and (ii) M_{crL}/M_{crD} and M_{crG}/M_{crD} lie in the ranges *1.18-4.19* and *5.48-154.3* (SCA beams) and

Table 1. Cross-section dimensions, areas and elastic/plastic moduli of the selected lipped channel beams

Beam	b_w (mm)	b_f (mm)	b_l (mm)	t (mm)	*Area* (cm²)	S (cm³)	Z (cm³)
C01	75	65	5	2	4.3	12.3	13.3
C02	90	75	6.25	1.8	4.5	15.5	16.7
C03	120	75	10	3	8.7	37.2	41.1
C04	120	80	10	2.5	7.5	32.5	35.8
C05	130	80	10	3	9.3	43.0	47.5
C06	135	75	10	2.7	8.2	38.7	43.0
C07	135	85	10	2.8	9.1	43.9	48.4
C08	140	100	10	2.5	9.0	46.2	50.5
C09	150	80	10	2.5	8.3	42.7	47.6
C10	150	100	10	2.5	9.3	50.2	55.1
C11	150	120	10	3.5	14.4	80.7	87.6
C12	160	100	10	2.2	8.4	47.7	52.6
C13	165	85	10	2.4	8.5	48.1	53.7
C14	225	90	12	2.9	12.4	90.2	102.8
C15	275	110	13	3	15.6	138.3	157.7

1.13-3.04 and *9.72-137.2* (SCB beams), respectively. For illustrative purposes, the sets of signature curves M_{cr} vs. L (logarithmic scale) depicted in Figures 3(a)-(b) provide the variation of the elastic critical buckling moment with the beam length and bending moment diagram for the SCA and SCB C01 beams (see Table 1) – the (distortional) critical buckling modes of the selected beams. The observation of these two sets of plots leads to the following comments:

(i) As expected and also previously observed by Yu & Schafer (2005), the beam critical buckling mode exhibits either (i_1) a symmetric single half-wave ($\psi=1$ – uniform bending), (i_2) an asymmetric single half-wave ($\psi=+0.5;0;-0.5$ – the asymmetry, towards the most loaded end, grows as ψ decreases) or (i_3) two anti-symmetric half-waves ($\psi=-1$ – double curvature).

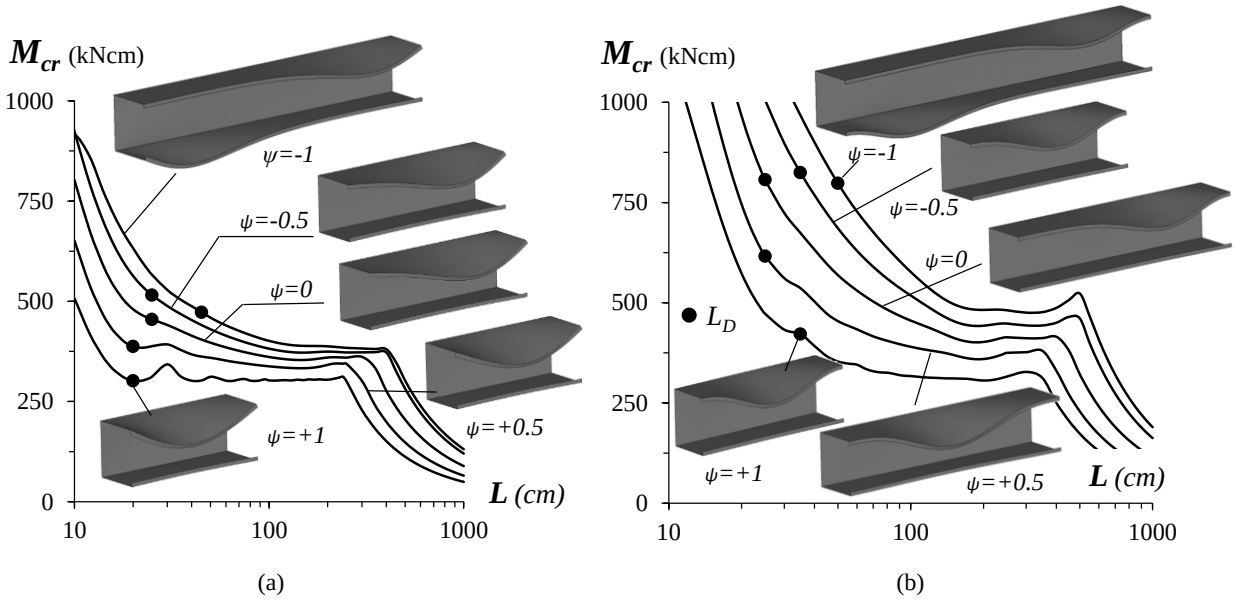

Figure 3. Variation of M_{cr} with L and ψ for (a) SCA and (b) SCB C01 beams

(ii) Regardless of the end support conditions (SCA or SCB) the beam signature curves are logically ordered in descending sequence as ψ varies between *–1* and *+1*. Moreover, the "vertical distances" between two consecutive curves are roughly the same.

(iii) Figures 4(a)-(b), dealing with the SCA and SCB selected beams, make it possible to assess the influence of ψ on M_{crD}. The plotted $\bar{m}$ values stand for ratios between the distortional critical buckling moments of identical beams subjected to non-uniform ($\psi \neq 1$) and uniform ($\psi=1$) bending – the corresponding M_{crD} values can be found in Tables A2-A5 and Table A1, respectively. Naturally, for each beam geometry and end support conditions the smallest and largest distortional critical buckling moments are associated with $\psi=+1$ (uniform bending) and $\psi=-1$ (highest moment gradient). For the selected beam geometries, the average difference/increase is equal to 58% (SCA beams) and 69% (SCB beams)[7] – moreover, the vertical dispersion of the $\bar{m}$ values is more pronounced for the SCB beams than for their SCA counterparts.

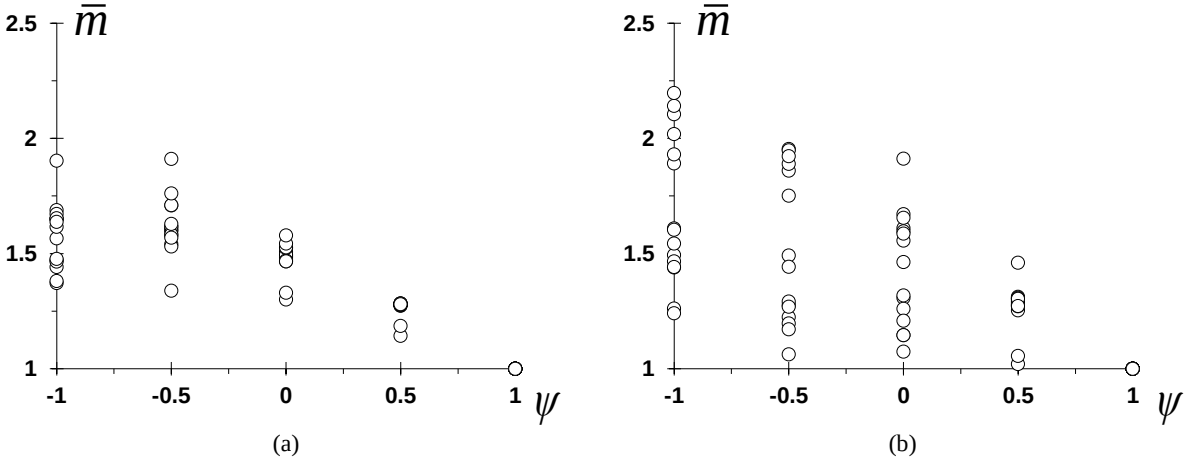

Figure 4. Assessment of the influence of ψ on M_{crD} for the (a) SCA and (b) SCB selected beams

3 Distortional Post-Buckling Behavior

After briefly addressing the ANSYS shell finite element model adopted and its validation, numerical results concerning the combined influence of the end support conditions (SCA or SCB) and bending moment diagram (ψ value) on the beam distortional post-buckling behavior and ultimate strength are presented and discussed – the elastic and elastic-plastic results are dealt with separately.

3.1 Numerical model

The beam distortional post-buckling equilibrium paths and ultimate strength values were determined through ANSYS (2009) geometrically and materially non-linear shell finite element analyses (SFEA), employing models similar to those used in recent studies (*e.g.*, Martins *et al.* 2017a). The beams were discretized into SHELL181 elements (ANSYS nomenclature – *4*-node shear deformable thin-shell elements with six degrees of freedom per node and full integration). The analyses were performed by means of an incremental-iterative technique combining Newton-Raphson's method with an arc-length control strategy. As stated earlier, the simply supported beams analyzed exhibit two end support conditions, differing in the warping displacements and local displacements/rotations, which can be either free (SCA beams) or prevented (SCB beams) – see Figures 5(a)-(b). The latter are modeled by attaching rigid

[7] For $\psi= -1$ beam with boundary conditions similar to the SCA ones, Yu & Schafer (2005) reported differences/increases comprised between 30% and *50%*.

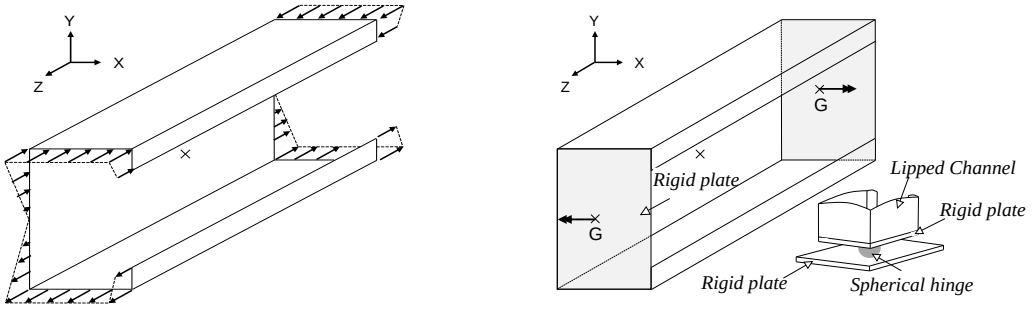

(a) (b)

Figure 5. End support and loading conditions concerning the (a) SCA and (b) SCB beams (Martins *et al*. 2017a)

plates to the beam end cross-sections. The various bending moment diagrams are achieved through the application of either (equal or unequal) (i) sets of concentrated forces acting on the nodes of both end cross-sections section (SCA beams) or (ii) two concentrated moments acting on the rigid end plates (SCB beams). The force/moment application is made in small increments, taking advantage of the ANSYS automatic "load stepping procedure". Moreover, all the materially non-linear analyses assumed an elastic-perfectly plastic steel material behavior following Prandtl-Reuss's plasticity model, which combines von Mises yield criterion with its associated flow rule.

All the beams contained initial geometrical imperfections with a critical-mode (distortional) shape and small amplitude (*10%* of the wall thickness *t*). These initial imperfections involve inward compressed flange-lip motions, since they are known to be the most detrimental, in the sense of leading to lower post-buckling strengths (Dinis & Camotim 2010, Martins *et al*. 2017a) – obviously, this distinction does not make sense for the $\psi = -1$ beams, since their flange-lip motions are always opposite (one outward and the other inward). Each critical buckling mode shape is obtained by means of a preliminary ANSYS buckling analysis, performed with exactly the same shell finite element mesh employed to carry out the subsequent non-linear (post-buckling) analysis – this procedure makes it very easy to "transform" the buckling analysis output into a non-linear analysis input. It is still worth noting that no strain-hardening, residual stresses and/or corner strength effects were considered in this work.

3.2 Validation Studies

In order to validate the use of the ANSYS shell finite element model to assess the distortional post-buckling behavior and strength of cold-formed steel beams, one begins by replicating numerical simulations reported by Yu & Schafer (2005), concerning cold-formed steel lipped channel beams that were experimentally tests carried out by these authors[8]. The cross-section dimensions considered are given in Table 2 and consist of the mean values of the dimensions/angles adopted by Yu & Schafer (2005) in their extensive numerical investigation, which included a large number of beams never experimentally tested – all beams subjected to moment gradients fall into this category.

Since the primary goal of Yu & Schafer was to simulate real experimental tests, they modeled the whole experimental set-up, comprising the cold-formed steel beams, steel decking and hot-rolled tubes – Figure 6(a), taken from Yu & Schafer (2005), provides an overall view of the experimental test set-up, which was used exclusively to test beams under uniform bending. On the other hand, Figures 6(b)-(c) depict the two structural systems considered to obtain failure moments of cold-formed steel beams subjected to moment gradients – they are intended to simulate $\psi = 0.5$ and $\psi = 0$ beams.

[8] Note that the SFE element model employed in this work (described in Section 3.1) was previously used by Landesmann & Camotim (2016) to satisfactorily replicate failure moments reported by Yu & Schafer (2005), but exclusively for beams under uniform bending.

Table 2. Beam cross-section dimensions selected from the extended numerical investigation of Yu & Schafer (2005)

Cross-section	b_w (mm)	b_f (mm)	b_l (mm)	t (mm)	r (mm)	θ_l (deg)
8C097	204.216	52.832	14.097	2.4892	7.11	85.7

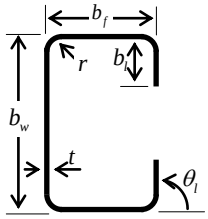

(a)

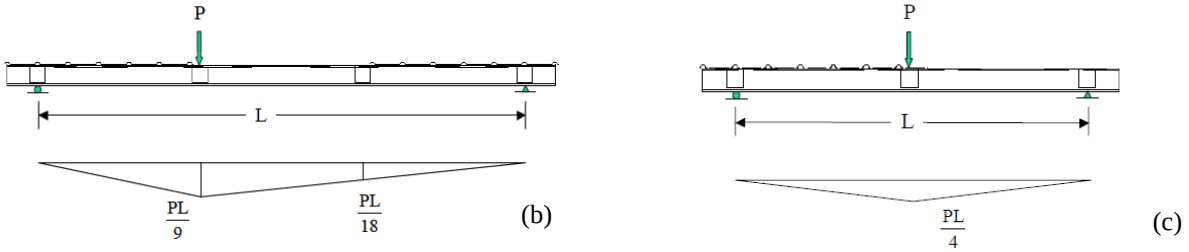

(b) (c)

Figure 6. Yu & Schafer (2005) (a) experimental test set-up and structural systems concerning the (b) $\psi=0.5$ and (c) $\psi=0$ beams

The first system (Fig. 6(b)) is inspired on four-point bending tests of beams formed by assemblies of two identical lipped channel members (i) with an overall length (L) of *487.68 cm* (*i.e., 3x64 in* spans), (ii) connected together back-to-back (to avoid torsion) by means of *4* (rigid) hot-rolled tubes placed *162.56 cm* (*64 in*) apart, bolted to both webs and located at the ends (two of them) and third points (the other two), thus also avoiding shear and web crippling failures, and (iii) exhibiting the central 1/3-span (of length of *162.56 cm*) basically unrestrained[9]. Since the through-fastened steel decking is attached (screwed) to stabilize the compression flange along the two outer spans, the application of a single point load P at one 1/3 point, as depicted in Fig. 6(a), induces in the beam unrestrained central span a bending moment diagram associated with $\psi=0.5$. The second system (Fig. 6(c)) is similar to the first one and corresponds to three-point bending. The main differences are: (i) a shorter length (L) of *325.12 cm* (only *2x64 in* spans), (ii) connection through *3* tubes (instead of *4*), also located *162.56 cm* (*64 in*) apart, (iii) steel deck attached (screwed) to stabilize the compression flange along only half the beam length, and (iv) a point load P applied at the beam mid-span, thus inducing two "triangular" bending moment diagrams ($\psi=0$), as shown in Figure 6 (c). Both structural systems were analyzed in the code ABAQUS – the beam and hot-rolled tubes were discretized by means of *25.4 mm×25.4 mm* meshes of S4R

[9] This experimental set-up, ensures that the two lipped channel beam "work almost independently" in their central spans – the word "almost" stems from the fact that small angles (*1¼×1¼×0.057 in*) were attached (screwed) to the tension flanges every *12 in* (see Fig. 6(a)).

shell finite elements (ABAQUS nomenclature: 4-node isoparametric thin-shell elements with six degrees of freedom per node and reduced shear integration). The steel material properties adopted in the numerical simulation were: *E=203.4 GPa* (*29500 ksi*), *v=0.3* and σ_y*=227.53-303.37-386.80-428.85-506.08 MPa* (*33-44-56.1-62.2-73.4 ksi*). Finally, all beams contained critical-mode (distortional) initial geometrical imperfections with *0.94t* amplitude – residual stresses and corner strength effects were neglected.

On the other hand, the numerical analyses carried out in this work were performed in the code ANSYS and adopted the simulation models briefly described in Section 3.1 – the underlying structural models are obviously much simpler, mainly because the end support conditions are very well defined. Indeed, the models adopted in this work merely consist of a single-span simply supported lipped channel beam (not two back-to-back beams) (i) with length *L=162.56 cm* (like the unrestrained span of the beams analyzed by Yu & Schafer) and the cross-section dimensions given in Table 2, (ii) exhibiting an elastic-perfectly plastic material behavior with five yield stresses (as also considered by Yu & Schafer – see Table 3), (iii) acted by unequal end moments (in order to ensure ψ values of *0.5* and *0*) and (iv) containing critical-mode (distortional) initial geometrical imperfections with amplitude equal to *94%* of the wall thickness (as also considered by Yu & Schafer). Concerning the end support conditions, SCB beams (see Section 3.1) are analyzed and, in order to replicate more closely the experimental set-up used by Yu & Schafer, the minor-axis flexural rotations are prevented – *i.e.*, as far as the global flexural deformations are concerned, the beam is simply supported for major-axis bending and fixed for minor-axis bending. In addition, the rounded corners were included in the cross-section model (radius values given in Table 2)[10]. The failure moments obtained in this work ($M_{u.obt}$) are compared with those reported by Yu & Schafer (2005) ($M_{u.YS}$) in Table 3, for beams with the five yield stresses σ_y*=227.53-303.37-386.80-428.85-506.08 MPa* and subjected to the two moment gradients under consideration. Figures 7(a_1)-(b_2) show the distortional critical buckling modes and failure mode shapes (plus the von Mises stress contours at the peak load) of the beams with σ_y*=386.80 MPa*, for ψ*=0.5* or ψ*=0*. The percentage differences between the $M_{u.obt}$ and $M_{u.YS}$ values, also given in Table 3, never exceed either *2.2%* (ψ*= –0.5*) or *6.5%* (ψ*=0*) – in view of this comparison, it seems fair argue that the shell finite element model employed in this work may be deemed as adequately validated. Nevertheless, it should be noticed that, with one exception, the $M_{u.obt}$ values are lower than their $M_{u.YS}$ counterparts, particularly for the ψ*=0* beams. This is a bit surprising, since the $M_{u.obt}$ values were obtained under the assumption of full restraint of the minor-axis flexural rotations and warping displacements at the end cross-sections – most likely, this discrepancy stems from the fact that the structural systems tested by Yu & Schafer (2005) exhibit some degree of major-axis flexural rotation restraint (due to the beam continuity), which is completely absent in the SCB support conditions.

Table 3. Comparison between the failure moments obtained (SCB beams) and reported by Yu & Schafer (ψ*=0.5* + ψ*=0*)

σ_y (*MPa*)	ψ*=0.5*			ψ*=0*		
	$M_{u.YS}$ (*kNcm*)	$M_{u.obt}$ (*kNcm*)	$\frac{M_{u.YS}-M_{u.obt}}{M_{u.YS}}$	$M_{u.YS}$ (*kNcm*)	$M_{u.obt}$ (*kNcm*)	$\frac{M_{u.YS}-M_{u.obt}}{M_{u.YS}}$
227.53	1163.74	1137.90	2.2%	1229.27	1149.20	6.5%
303.37	1484.62	1460.30	1.6%	1585.18	1487.30	6.2%
386.80	1795.33	1783.40	0.7%	1916.22	1822.60	4.9%
428.85	1933.17	1926.80	0.3%	2063.10	1973.00	4.4%
506.08	2186.26	2191.30	–0.2%	2345.57	2259.00	3.7%

[10] The inclusion of the rounded corners is restricted to this validation study – in all the remaining numerical results presented and discussed in this work, this effect is ignored and sharp corners are considered.

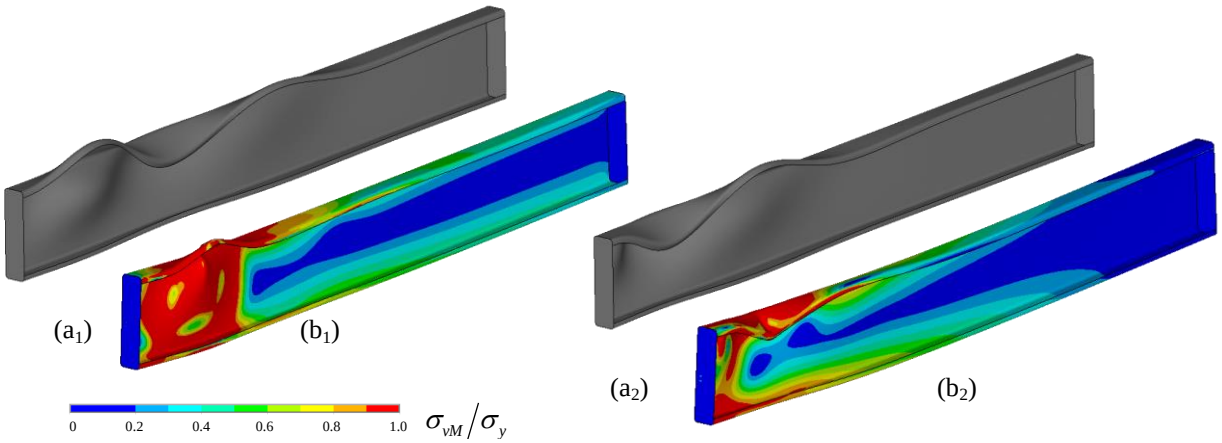

Figure 7. 8C097 beam distortional (a) critical buckling and (b) failure mode shapes for (1) ψ=0.5 and (2) ψ =0 (σ_y =*386.80MPa*)

3.3 Elastic Post-Buckling Behavior and Strength

The validated ANSYS shell finite element model is now used to obtain illustrative elastic post-buckling equilibrium paths[11], intended enable assessing how the beam elastic distortional post-buckling behavior is influenced by the combined effect of the (i) end support conditions (SCA or SCB), and (ii) moment gradient moment (ψ value). Figures 8(a_1)-(b_2) show post-buckling equilibrium paths of the C02 beams (cross-section dimensions and lengths given in Tables 1 and A1-A5, respectively). These equilibrium paths plot the absolute (M – Figs. 8(a_1)+(b_1)) and normalized *w.r.t.* M_{crD} (M/M_{crD} – Figs. 8(a_2)+(b_2)) applied moments against the normalized displacement $|\delta|/t$, where $|\delta|$ is the maximum absolute vertical displacement occurring along the flange-stiffener longitudinal edges and t is the wall thickness. The observation of these distortional post-buckling equilibrium paths leads to the following conclusions:

(i) First of all, the comparison between Figures 8(a_1)-(b_1) and 8(a_2)-(b_2) amply confirms the expected much higher stiffness and strength exhibited by the SCB beams, regardless of the ψ value. Naturally, this suggests that, like in the uniform bending case, different design/strength curves are needed to predict adequately the SCA and SCB beam failure moments, particularly for high slenderness values.

(ii) As it would be logical to expect, the beam absolute (non-normalized) post-buckling strength increases as ψ decreases for both the SCA and SCB beams (see Figs. 8(a_1)+(b_1)) – the differences are clearly more pronounced in the latter.

(iii) However, the picture surprisingly changes when dealing with the normalized post-buckling strength, as shown in Figures 8(a_2)+(b_2). Indeed, the previous post-critical strength sequence (increase as ψ decreases) (iii_1) is kept for the SCB beams, with the various curves visibly apart, and (iii_2) is fully reversed for the SCA beams, with the various curves quite close (those concerning "non-positive" ψ values practically coincide). In mechanical terms, this means that a ψ decrease changes the SCA beam buckling moment and post-critical strength reserve in completely opposite ways, increasing the former and decreasing the latter (the last feature is already well perceptible in the equilibrium paths displayed in Fig. 8(a_1)). Obviously, the above findings will have implications on the design of beams subjected to non-uniform bending moments caused by unequal applied end moments.

(iv) In spite of its limited scope (only lipped channel beams with *15* geometries analyzed), the output of this elastic post-buckling investigation, showing that both the end support conditions and the moment gradient influence considerably the beam equilibrium path characteristics, makes it possible to

[11] As mentioned in Section 3.1, all beams contain (distortional) critical-mode initial imperfections exhibiting the most detrimental shape (inward motions of the compressed flange-lip assembly) and amplitude equal to 0.1*t*.

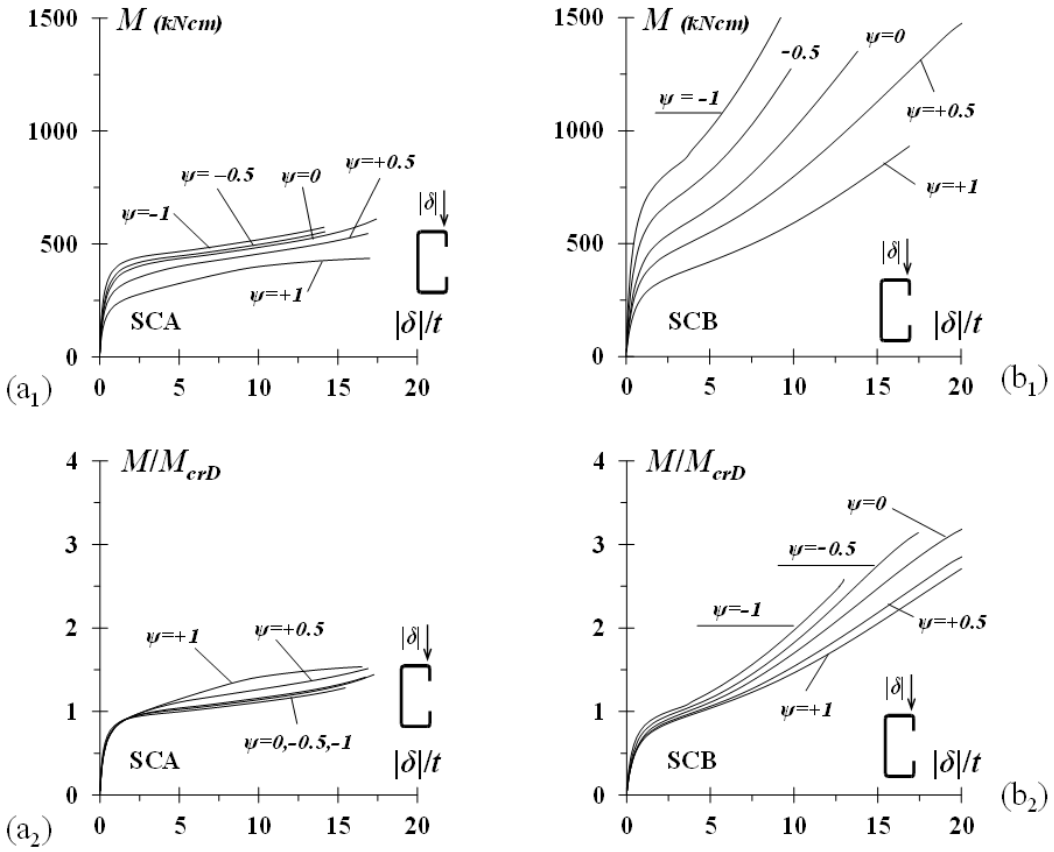

Figure 8. Elastic equilibrium paths (a) M *vs.* $|\delta|/t$ and (b) M/M_{crD} *vs.* $|\delta|/t$ concerning the ($_1$) SCA and ($_2$) SCB C02 beams

anticipate that their combined effect will have non-negligible implications on the corresponding (elastic-plastic) failure moment and, therefore, also on its prediction by means of design methods. This issue will be thoroughly discussed ahead in the paper.

3.4 Elastic-Plastic Post-Buckling Behavior and Strength

Attention is now turned to investigate the elastic-plastic post-buckling behavior of the beams considered in this work (SCA and SCB beams buckling and failing in distortional modes when subjected to various moment gradients). Moreover, it is also intended to gather fairly considerable failure moment data, which will be subsequently used to assess the adequacy of the currently codified DSM beam distortional design curve in predicting them. The numerical results presented and discussed concern a total of *1200* lipped channel beams, combining (i) the *15* geometries defined in Table 1 (together with the corresponding lengths, given in Tables A1 to A5 of Annex A), (ii) the two end support conditions dealt with (SCA and SCB), (iii) *5* ψ values considered in this work (ψ=+1/+0.5/0/–0.5/–1) and (iv) *8* yield stresses, which enable covering wide distortional slenderness ranges (λ_D varies between *0.3* and *4.9* for both the SCA and SCB beams). The full set of numerical failure moments obtained in this parametric study is provided in Tables B1 to B15, included in Annex B. Each table concerns one cross-section geometry (C01 to C15) and include results of SCA and SCB beams with five ψ values – these results consist of the beam (i) distortional slenderness (λ_D), (ii) yield, plastic and failure moments (M_y, M_p and M_u), and (iii) M_u/M_y ratio.

Figures 9(a)-(b) show a sample of the elastic and elastic-plastic (the latter for $0.5 \leq \lambda_D \leq 4.0$) post-buckling equilibrium paths M/M_{crD} vs. $|\delta|/t$, obtained for SCA and SCB C01 beams with *5* ψ values – the elastic paths are displayed for comparison purposes. These figures also depict the deformed configurations and

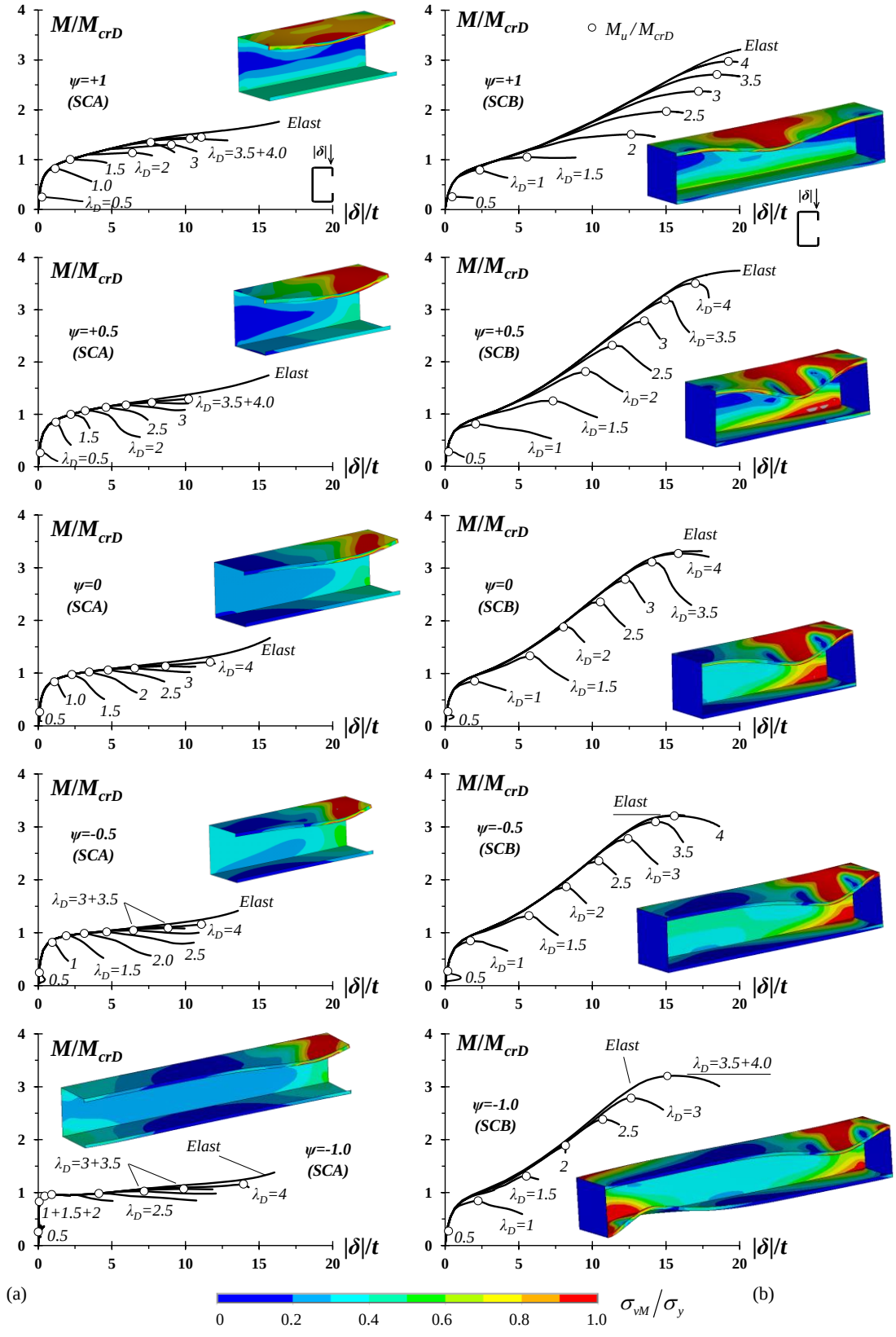

Figure 9. Elastic and elastic-plastic distortional post-buckling equilibrium paths (M/M_{crD} *vs.* $|\delta|/t$), failure modes and von Mises stress contours (for λ_D=*1.5*) concerning (a) SCA and (b) SCB C01 beams exhibiting various ψ and λ_D values

von Mises stress (σ_{VM}) contours, at the peak/failure moments M_u (identified by white circles on the paths), of the beams with λ_D=*1.5* – the distortional nature of the beam collapse modes is clearly visible for all ψ values. The observation of these post-buckling results prompts the following remarks:

(i) As expected, from the elastic post-buckling analyses reported earlier, the SCA and SCB beam elastic-plastic post-buckling and strength behaviors are different, both qualitatively and quantitatively – the SCB beams exhibit a much more pronounced distortional post-buckling strength than their SCA counterparts (particularly for $\lambda_D \geq 1.0$), essentially due the warping fixity – a similar finding was reported by Martins *et al*. (2017a), in the context of beams under uniform bending (ψ=*1*).

(ii) In order to quantify the failure moment variation, Table 4 shows the M_u/M_{crD} values for selected SCA and SCB C01 beams that exhibit all possible combinations of λ_D=1.0/2.0/3.0/4.0 and ψ=+1/+0.5/0/–0.5/–1. These values confirm part of the conclusions drawn earlier, concerning the elastic post-buckling behavior, and show that, for a given λ_D, M_u/M_{crD} either decreases (SCA beams) or increases (SCB beams) as ψ decreases. However, it is worth noting that the M_u/M_{crD} values are very close (differences below 5%) in the SCA beams with "non-positive" ψ values (ψ=*0/–0.5/–1*) and also in the SCB beams under non-uniform bending (ψ=+0.5/0/*–0.5/–1*). Moreover, for λ_D=*1* the M_u/M_{crD} differences are minute regardless of the end support condition and/or ψ value.

(iii) As planned, all beams exhibit clear distortional failure mode configurations, akin to the initial geometrical imperfection (see the buckling mode shapes in Fig.3). The failure modes of each beam pair SCA+SCB sharing the same ψ value are qualitatively similar and involve yielding of the compressed flange-web corner and lip free edge regions.

Table 4. M_u/M_{crD} ratios of SCA+SCB C01 beams exhibiting different distortional slenderness and ψ values

Beam	λ_D	M_u/M_{crD}				
		ψ=*+1.0*	ψ=*+0.5*	ψ=*0*	ψ=*–0.5*	ψ=*–1.0*
SCA	*1.0*	0.82	0.85	0.84	0.82	0.83
	2.0	1.14	1.07	1.02	0.98	0.96
	3.0	1.35	1.18	1.09	1.04	1.03
	4.0	1.45	1.29	1.21	1.16	1.16
SCB	*1.0*	0.79	0.81	0.86	0.85	0.84
	2.0	1.51	1.81	1.88	1.87	1.89
	3.0	2.37	2.78	2.79	2.80	2.81
	4.0	2.97	3.20	3.25	3.25	3.30

At this stage, it should be mentioned that, in order restrict this investigation to beams failing in "pure" distortional modes, all the beams exhibiting M_u/M_{crL} (recall that M_{crL} is the beam critical local buckling moment) values larger than *1.0* (a total of *176* beams out of the 1200 analyzed), were excluded from the failure moment data considered for design purposes. Indeed, such beams are bound to be affected by local-distortional interaction effects (Martins *et al.* 2017b), which fall outside the scope of this work – they are identified, in Tables B1 to B15 presented in Annex B, by an asterisk placed next to the M_u value.

Figures 10(a)-(b) plot the SCA and SCB beam failure moment ratios M_u/M_{crD} against λ_D, for the *1024* beams considered in this work (those failing in "pure" distortional modes). In order to enable an easy assessment of the bending moment diagram (ψ value) influence, the M_u/M_{crD} values are identified by different symbols for each ψ value: (i) white circles, squares and triangles and for ψ=*+1*, ψ=*+0.5* and ψ=*0*, and (ii) gray circles and squares for ψ= *–0.5* and ψ= *–1*. The observation of the results shown in these figures, as well as the failure moment data given in Tables B1-B15, leads to the following conclusions:

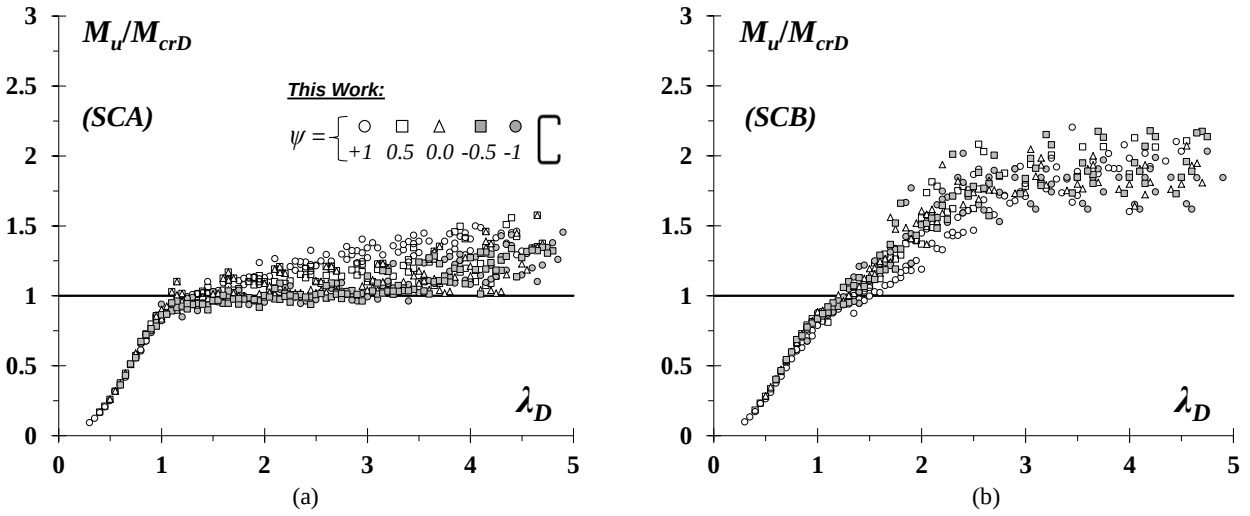

Figure 10. Plots of the (a) SCA and (b) SCB beam M_u/M_{crD} obtained in this work against the distortional slenderness λ_D

(i) Naturally, the failure moment ratios M_u/M_{crD} of all beams increase with the distortional slenderness λ_D, regardless of the ψ value and end support conditions – see also the values given in Table 4 for selected SCA and SCB C01 beams.

(ii) All beams failing visibly below the critical buckling moment level ($M_u/M_{crD} \leq 0.90$) exhibit a minute elastic-plastic strength reserve and very little ductility prior to failure. Moreover, at this applied loading level, there are no visible qualitative differences between the values associated with different combinations of the end support conditions (SCA or SCB) and ψ value – note that the M_u/M_{crD} *vs.* λ_D plots are practically coincident (and linear).

(iii) The above assertion ceases to be valid for $M_u/M_{crD} > 0.90$, as the differences between the values concerning the SCA and SCB beams become clearly visible (regardless of the ψ value) – the latter are consistently higher and the differences increase with λ_D).

(iv) Although the M_u/M_{crD} values are considerable scattered, within the beams sharing the same end support conditions, the influence of ψ is perceptible: the overwhelming majority of the values concerning $\psi=1$ beams are either above (SCA) or below (SCB) their $\psi \neq 1$ counterparts. This scatter is, most likely, due to a combination of several factors, namely the wide variety of beam (iv_1) geometries, (iv_2) critical buckling mode half-wave numbers and (iv_3) post-critical strength reserves dealt with in this works. For instance, recall that the beams analyzed here display quite different combinations of cross-section dimensions (flange-lip and web-flange width ratios) and length. Most likely, the above factors have strong implications on the beam distortional post-buckling behavior and strength (elastic or elastic-plastic) – such implications were previously reported by Martins *et al*. (2017a), but exclusively in the context of beams under uniform bending.

Figures 11(a)-(b) plot the failure moment ratios M_u/M_y (M_y is the yield moment) against the distortional slenderness λ_D for (i) the *1024* SCA or SCB beams considered in this work ($\psi=+1,+0.5,0,-0.5,-1$), (ii) the *26* SCB LC beams numerically analyzed by Yu & Schafer (2005) ($\psi=+1,+0.5,0$) and (iii) the *920* SCA or SCB LC beams numerically analyzed by Martins *et al.* (2017a) ($\psi=+1$). The observation of these plots shows that:

(i) As it would be logical to expect, the M_u/M_y *vs.* λ_D "clouds" follow closely the trends of "Winter-type" strength/design curves, even if there is some "vertical dispersion" associated with the SCB beam, due to differences in elastic-plastic strength reserve – such dispersion is minute for the SCA beams. Like the M_u/M_{crD} values, the M_u/M_y ones are influenced by the ψ value – for instance, the M_u/M_y

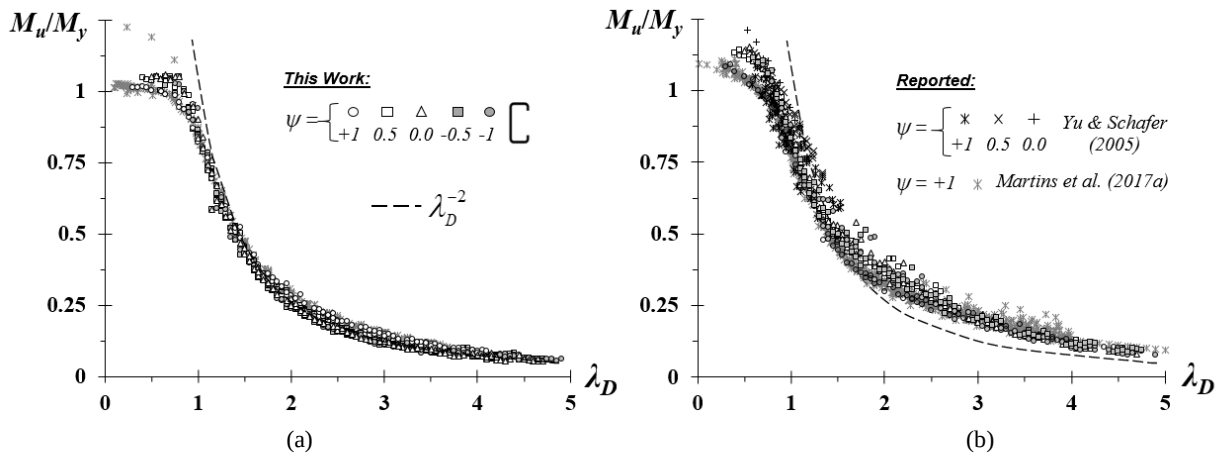

Figure 11. Plots of the (a) SCA and (b) SCB beam failure moment ratios M_u/M_y obtained and gathered in this work against the distortional slenderness λ_D

values concerning the $\psi=+1$ SCA and $\psi=-1$ SCB beams are slightly above all the remaining ones (this is more visible for the SCA beams).

(ii) All the slender SCA beam values are fairly well aligned (very little vertical dispersion) along the elastic buckling strength curve (λ_D^{-2} – dashed curve in Fig. 11(a)) – on the other hand, the slender SCB beams results lie considerably above that same curve (higher post-critical strength reserve).

(iii) The numerical results reported by Yu & Schafer (2005) that are considered here (iii_1) involve built-up beams formed by back-to-back lipped channel profiles, (iii_2) exhibit only low-to-moderate distortional slenderness values (between *0.59* and *1.51*) and (iii_3) comprise mostly beams with $\psi=+1$ (*16* beams – in addition, *5* $\psi=0$ beams and 5 $\psi=+0.5$ beams were analyzed). It is observed that these results "mingle" quite well with those obtained in this work (*i.e.*, they also follow the trend of a "Winter-type" design curve), even if they are a bit above and exhibit a moderate vertical dispersion.

(iv) The values reported by Martins *et al.* (2017a), which concern *410* SCA and *510* SCB uniformly bent LC beams covering a distortional slenderness range comprised between *0.10* and *3.99*, also "mingle" quite well with the other results gathered in this work.

4 Direct Strength Method (DSM) Design Considerations

This section addresses the applicability of the available Direct Strength Method (DSM) distortional design curve to predict the numerical failure moment data concerning the beams considered in this work. It should be noted that the DSM (i) was first proposed by Schafer & Peköz (1998), based on an original idea from Hancock *et al*. (1994), (ii) has been continuously improved since then, mostly due to the efforts of Schafer (2005, 2008), and (iii) is already included in the main body of the North American Specification for cold-formed steel structures (AISI 2016). For beams with (i) cross-sections symmetric with respect to the bending axis or (ii) cross-sections for which first yield occurs in compressed fibers, the currently codified DSM design curve against beam distortional failures is defined as

$$M_{nD} = \begin{cases} M_y + (1 - C_{yd}^{-2})\left(M_p - M_y\right) & \lambda_D \le 0.673 \\ \left(1 - 0.22\lambda_D^{-1}\right)\lambda_D^{-1} M_y & \lambda_D > 0.673 \end{cases}, \quad (1)$$

where M_{nD} is the beam distortional nominal strength, M_y and M_p are the beam yield and plastic moments, respectively, $\lambda_D=(M_y/M_{crD})^{0.5}$ is the beam distortional slenderness and $C_{yd}=(0.673/\lambda_D)^{0.5}\le 3$.

On the other hand, Martins *et al.* (2017a) very recently proposed, in the context of cold-formed steel beams subjected to uniform bending, two novel DSM-based distortional design/strength curves, one intended for SCA beams and the other for SCB beams[12]. They can be cast in the general form

$$M_{nD}^{*}=\begin{cases} M_y+(1-C_{yd}^{-2})\left(M_p-M_y\right) & \lambda_D \le 0.673 \\ \left(1-a\lambda_D^{-b}\right)\lambda_D^{-c}M_y & \lambda_D > 0.673 \end{cases} , \quad (2)$$

where the values of parameters *a*, *b* and *c* are equal to (i) *0.25*, *1.75* and *1.75*, for SCA beams, and (ii) *0.23*, *1.55* and *1.45*, for SCB beams. Figures 12(a)-(b) make it possible to compare the two pairs of DSM distortional strength curves available for the design of SCA and SCB beams: (i) the currently codified curves (solid black lines), which are the same for SCA and SCB beams[13], and (ii) the curves proposed by Martins *et al.* (2017a) (solid red lines), which are different for SCA and SCB beams. It is observed that the two pairs of design curves coincide up to $\lambda_D \approx 1$, when they begin to separate – the differences widen as the slenderness increases.

Figures 13(a)-(b) compare the available DSM distortional design curves (Eqs. (1) and (2)) with the numerical M_u/M_y values (i) obtained in this work (white dots – values given in Tables B1 to B15 of Annex B), concerning *1024* SCA and SCB beams acted by bending moment diagrams associated with ψ=+1/+0.5/0/–0.5/–1, (ii) reported by Yu & Schafer (2005) ("×" symbols –Y&S), concerning *26* SCB beams with ψ=*+1*/*+0.5*/*0* and (iii) determined by Martins *et al.* (2017a) ("+" symbols – Mea), concerning *410* SCA and *510* SCB beams under uniform bending (ψ=*+1*) – separate plots are shown for each combination of ψ value and end support conditions. Moreover, Figures 14(a)-(b) and 15(a)-(b) plot the numerical-to-predicted failure moment ratios M_u/M_{nD} and M_u/M_{nD}^{*} against the distortional slenderness λ_D (values given in Tables B1 to B15), thus providing pictorial assessments of the safety and accuracy of the distortional failure moment estimates yielded by the available strength curves. Distinct plots are again shown for each combination of end support conditions and ψ value, including their

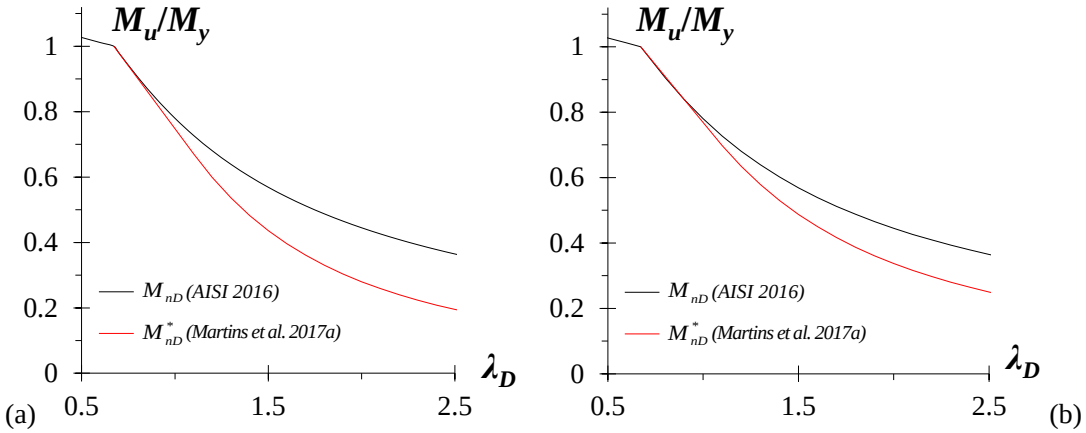

Figure 12. Comparison between the two available DSM distortional design curves for (a) SCA and (b) SCB beams

[12] Recall that Martins *et al.* (2017a) showed that the currently codified DSM beam distortional strength curve (Eq. (1)) is unable to predict adequately (safely and accurately) the distortional failure moments of beams exhibiting moderate-to-high slenderness range.

[13] Since the lipped channel beam inelastic strength reserve depends on the cross-section dimensions, which influence differently the elastic and plastic moments, and *15* distinct lipped channel cross-section dimensions are considered in this work (see Table 1), it was decided to include in the figures representations of the available DSM distortional strength curves that correspond to a "fictitious" cross-section whose dimensions would lead to the average of the 15 "real" plastic-to-elastic moment ratios. However, note that the M_y and M_p values provided in Tables B1 to B15, included in Annex B, are those corresponding to the beam cross-section under consideration.

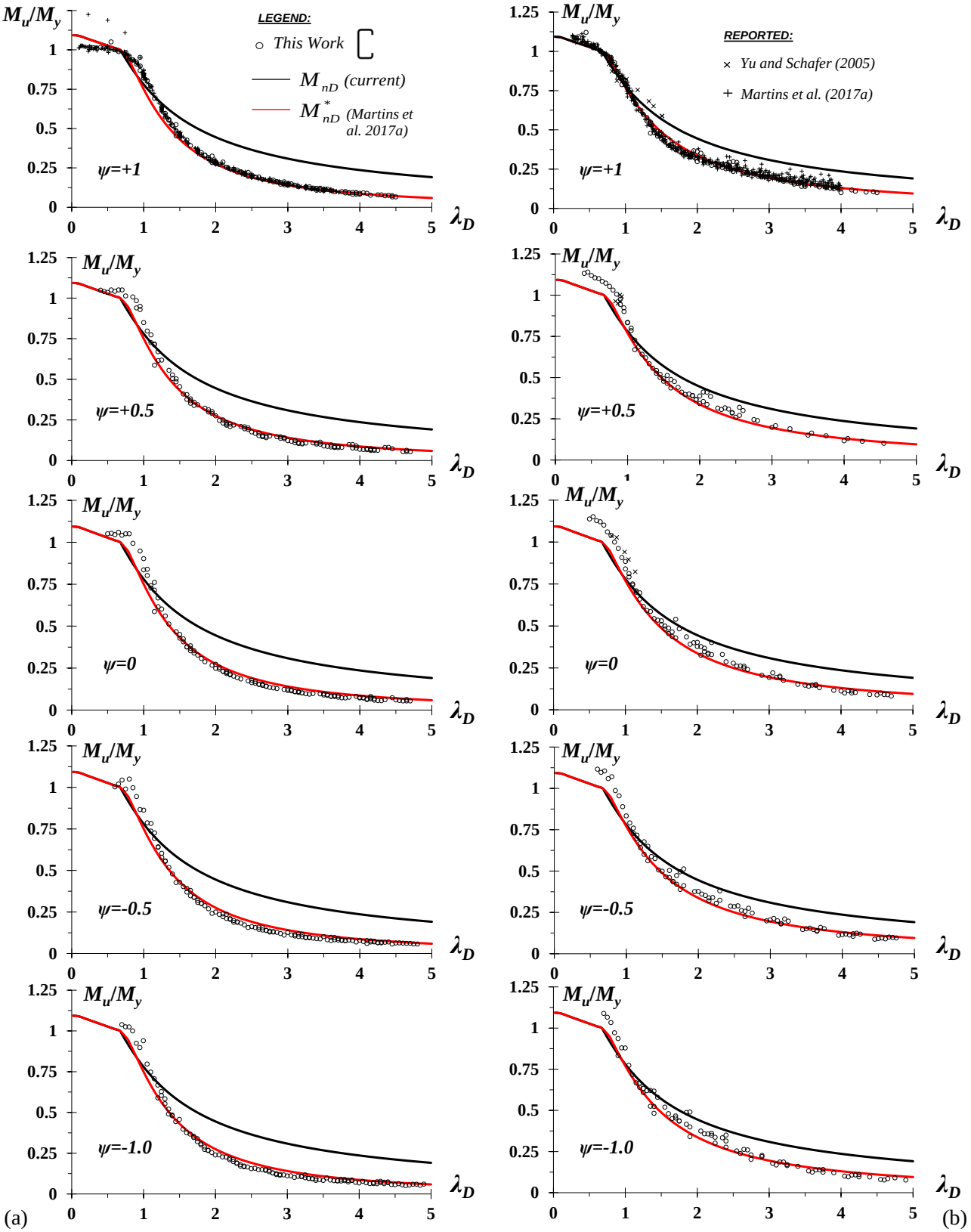

Figure 13. Comparison between the (a) SCA and (b) SCB beam failure moment ratios M_u/M_y obtained and gathered in this work with the available DSM distortional strength curves – *ψ=+1/+0.5/0/–0.5/–1*

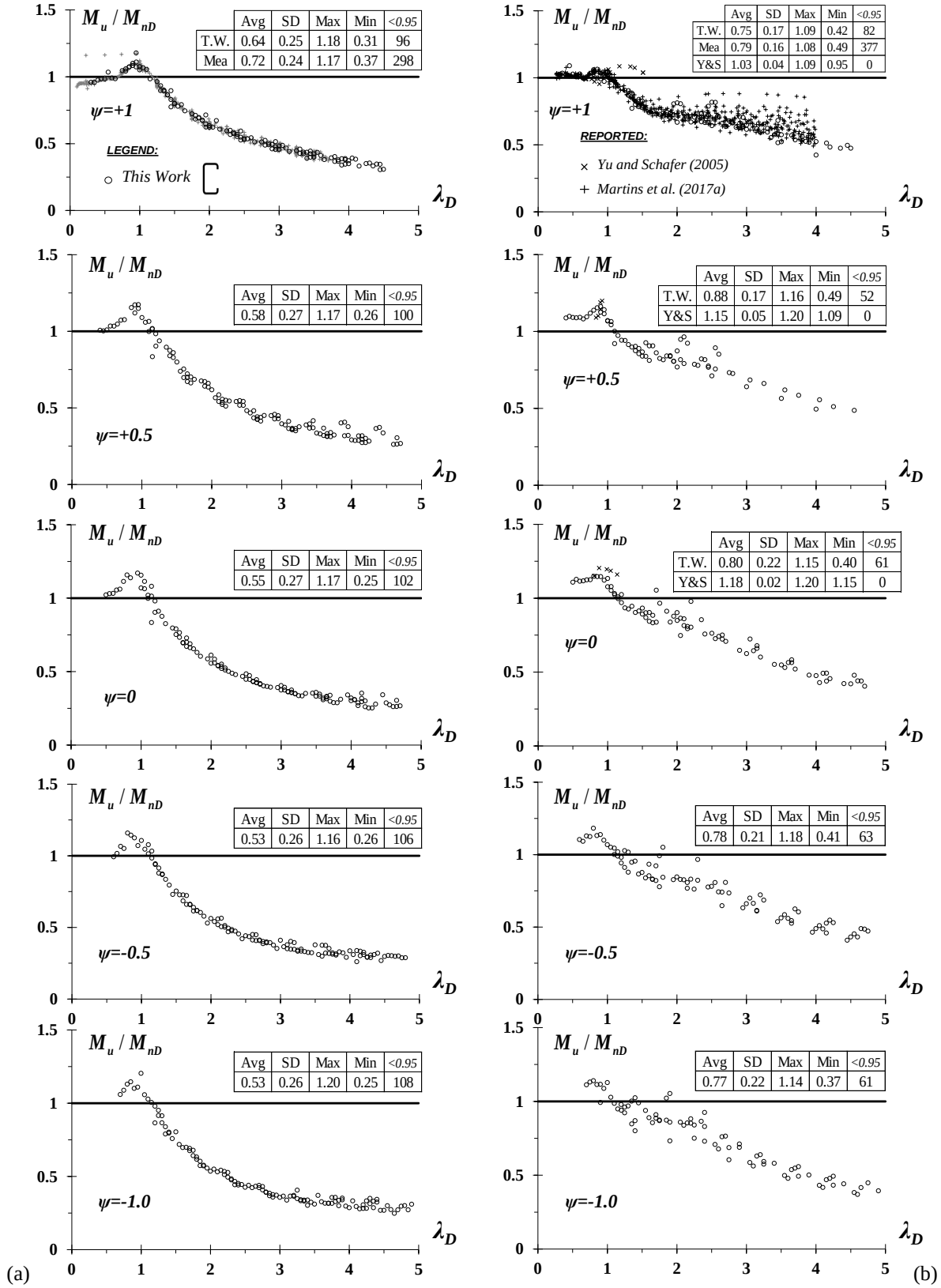

Figure 14. Plots M_u/M_{nD} vs. λ_D for the (a) SCA and (b) SCB beams with $\psi=+1/+0.5/0/0.5/-1$ bending moments

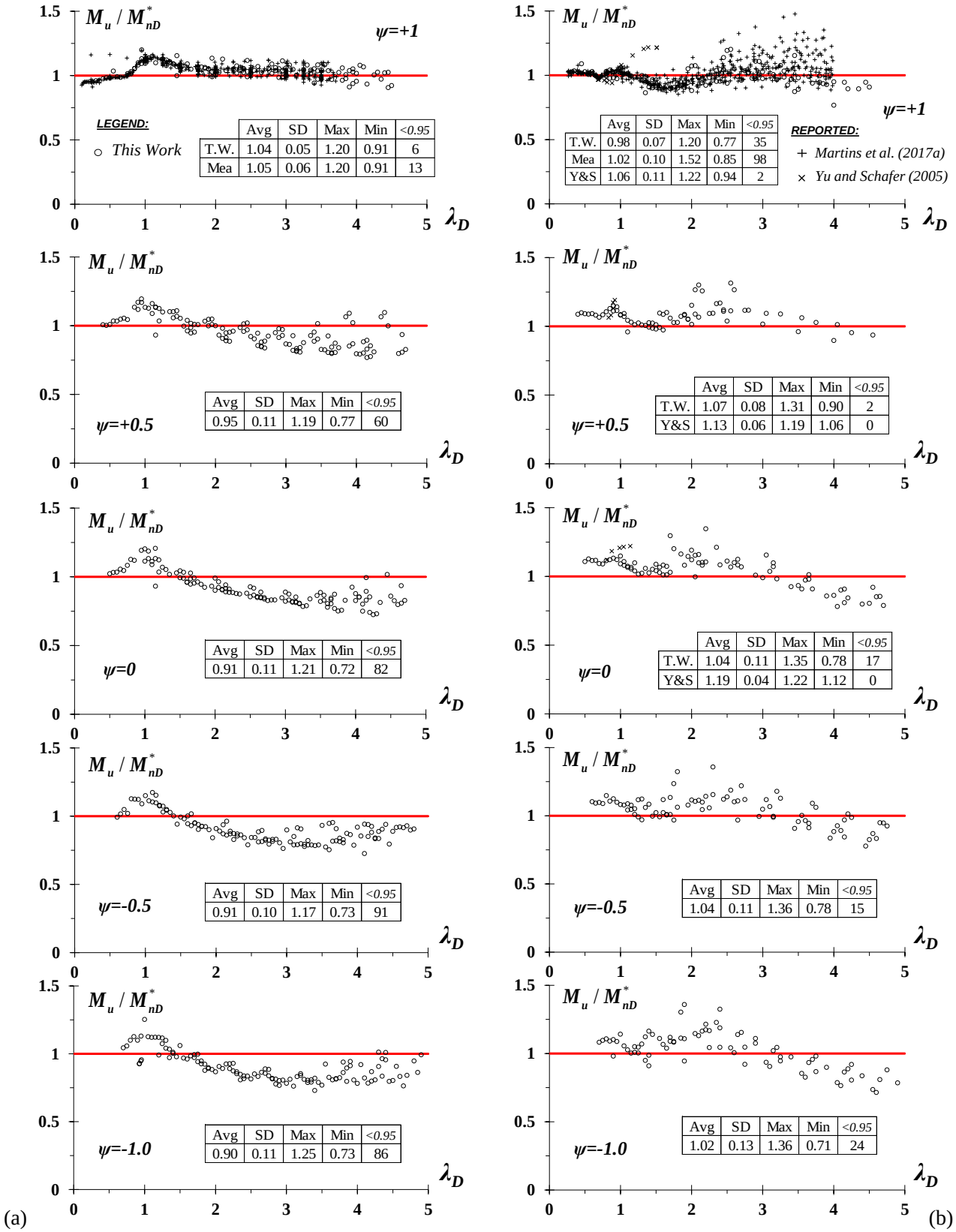

Figure 15. Plots M_u / M^*_{nD} vs. λ_D for the (a) SCA and (b) SCB beams with ψ=+1/+0.5/0/–0.5/–1 bending moments

statistical indicators (averages, standard deviations, maximum/minimum values – the numbers of "visibly unsafe" failure moment predictions, in the sense that $M_u/M_{nD}<0.95$ or $M_u/M_{nD}^*<0.95$, are also provided. The observation of the results shown in these figures and tables prompts the following remarks:

(i) In all the plots displayed in Figures 13(a)-(b), the overwhelming majority of M_u/M_y values are fairly well aligned along "Winter-type" curve with small scatter (vertical dispersion), which is slightly more pronounced in the SCB beams (see Section 3.4).

(ii) The currently codified DSM design curve provides reasonably accurate and mostly safe predictions of all the distortional failure moments reported by Yu & Schafer (2005) (*Y&S*), which is just logical since they were used to develop and calibrate this strength curve – however, recall that all the beams analyzed by these authors exhibit low-to-moderate slenderness values ($\lambda_D \leq 1.51$). Moreover, the amount of overestimation is slightly larger for the beams under non-uniform bending. The above assertions are confirmed by the corresponding M_u/M_{nD} statistical indicators, also given in Figure 14(b): averages, standard deviations, maximum/minimum values equal to *1.03-0.04-1.09-0.95* ($\psi=+1$), *1.15-0.05-1.20-1.09* ($\psi=+0.5$) and *1.18-0.02-1.20-1.1* ($\psi=0$).

(iii) The failure moments obtained in this work, for both the SCA and SCB beams, are also only reasonably accurately and safely predicted by the currently codified DSM design curve in the low-to-moderate slenderness range ($\lambda_D \leq 1.5$), regardless of the bending diagram (ψ value) considered[14]. Again, the M_u/M_{nD} values confirm the above assertions: their averages are, for ψ=+1/+0.5/0/–0.5/–1, *0.98*/*1.00*/*1.00*/*0.98*/*0.96* (SCA beams with $\lambda_D \leq 1.5$), *0.96*/*1.02*/*1.04*/*1.02*/*1.00* (SCB beams with $\lambda_D \leq 1.5$), *0.50*/*0.44*/*0.42*/*0.41*/*0.41* (SCA beams with $\lambda_D > 1.5$) and *0.65*/*0.77*/*0.69*/*0.68*/*0.68* (SCB beams with $\lambda_D > 1.5$). Note that the amount of underestimation tends to grow with λ_D and is particularly severe for the most slender SCA beams subjected to non-uniform bending ($\psi \neq 1$).

(iv) Figures 15(a)-(b) clearly show the failure moment prediction quality improvement achieved by the strength curves proposed by Martins *et al.* (2017a), spanning the whole distortional slenderness range and covering all the ψ values considered (even if they were developed solely in the context of uniformly bent beams). The M_u/M_{nD}^* statistical indicators are significantly better than their M_u/M_{nD} counterparts – indeed, for the beams analyzed in this work, the averages, standard deviations and maximum/minimum values vary (iv_1) between *1.04*/*0.05*/*1.20*/*0.91* ($\psi=1$) and *0.90*/*0.11*/*1.25*/*0.73* ($\psi=-1$), for the SCA beams, and (iv_2) between *0.98*/*0.07*/*1.20*/*0.77* ($\psi=1$) and *1.02*/*0.13*/*1.36*/*0.71* ($\psi=-1$), for the SCB beams[15]. Nevertheless, it must be recognized that there are still fairly high numbers of "visibly unsafe" failure moment predictions ($M_u/M_{nD}^*<0.95$): *19* ($\psi=1$ – *3.6*% of *530*) and *319* ($\psi \neq 1$ – *66.5*% of *480*) SCA beams, and *135* ($\psi=1$ – *21.4*% of *620*) and *58* ($\psi \neq 1$ – *17.6*% of *330*) SCB beams – note that the beams analyzed by Yu & Schafer (2005) and Martins *et al.* (2017a) are included for $\psi=1;0.5;0$ and $\psi=1$, respectively. The failure moment overestimation is particularly severe for (iv_1) fairly slender ($\lambda_D \geq 2.0$) SCA beams under any non-uniform bending ($\psi \neq 1$) and (iv_2) very slender ($\lambda_D \geq 3.5$) SCB beams under uniform ($\psi=1$) and highly non-uniform ($\psi \leq 0$) bending.

In order to improve the quality of the failure moment predictions for beams subjected to non-uniform bending, it was decided to modify the strength curves proposed by Martins *et al.* (2017a), presented in

---

[14] A similar finding was reported by Martins *et al.* (2017a), in the context of uniformly bent beams, and prompted these authors to propose new DSM-based strength curves for SCA and SCB beams, cast in the form given in Eq. (2).

[15] Naturally, the M_{nD}^* failure moment predictions concerning the SCA and SCB $\psi=1$ beams analyzed by Martins *et al.* (2017a) are accurate and mostly safe – their averages, standard deviations and maximum/minimum values are *1.05*/*0.06*/*1.20*/*0.91* and *1.02*/*0.10*/*1.52*/*0.85* for the SCA and SCB beams, respectively. It is worth noting that these SCB beam statistical indicators are superior to those obtained on the basis of the beams analyzed in this work, most likely because of the different cross-section dimensions – Martins *et al.* (2017a) showed that the cross-section dimensions visibly impact the beam post-critical strength. Finally, note also that the numbers of unsafe M_{nD}^* values, for the beams analyzed by Martins *et al.* (2017a), are either minute (SCA beams – *13*, *i.e.*, about *3%*) or reasonably small (SCB beams – *98*, *i.e.*, about *19%*).

Eq. (2), by changing parameters a and c, while keeping parameter b unchanged. The new parameters are either (i) constant (SCB beams) or (ii) explicitly dependent on ψ (SCA beams). Besides improving considerably the failure-to-predicted ratio statistical indicators, this modification leads to a reduction of the numbers of unsafe failure moment predictions by about *45%*. The search for the modified design curves was (i) based on the SCA and SCB beam numerical failure moments obtained and gathered in this work, and (ii) carried out by means of "trial-and-error curve fitting procedures". This search led to DSM-based strength curves providing failure moment estimates denoted by M_{nD}^{**} and obtained from Eq. (2) by replacing the (constant) parameters a and c (providing the M_{nD}^{*} failure moment predictions) by new ones, termed a_1 and c_1. In the case of the SCA beams, a_1 and c_1 are ψ-dependent and given by the expressions

$$a_1 = 0.50\left(1-\left(0.673\right)^{c1}\right) \tag{3}$$

$$c_1 = -0.052\,\psi^2 - 0.082\,\psi + 1.884 \quad . \tag{4}$$

In the case of the SCB beams, the new parameters continue to be constant and read $a_1=1.24$ and $c_1=1.48$. Figures 16(a)-(b) make it possible to compare the proposed strength curves (blue lines) with the available ones, namely the currently codified (black line) and those developed by Martins *et al.* (2017a) (red lines). In order to enable assessing the quality of the failure moment predictions provided by the proposed strength curves Figures 17(a)-(b) plot the M_u / M_{nD}^{**} values against λ_D, for each combination of support conditions and ψ value, and include also the corresponding statistical indicators – these M_u / M_{nD}^{**} values are given, in tabular for, in Annex B (Tables B1 to B15). The close observation and of these two sets of figures prompts the following remarks:

(i) Naturally, for uniformly bent beams ($\psi=1$) the strength curves developed by Martins *et al.* (2017a) either (i_1) remain unchanged (SCA beams) or (i_2) exhibit a minute change (SCB beams). In the latter case, the strength curve is slightly lowered, due to the fact that (i_1) the failure-to-predicted moment

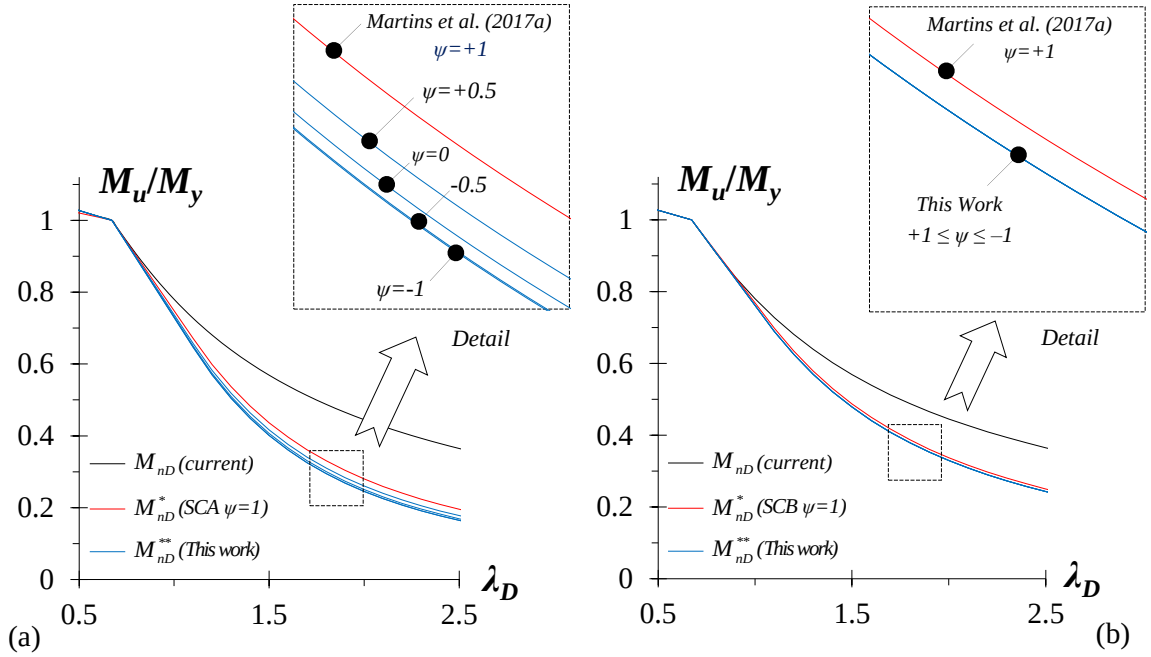

Figure 16. Comparison between the proposed and available DSM distortional design curves for (a) SCA and (b) SCB beams

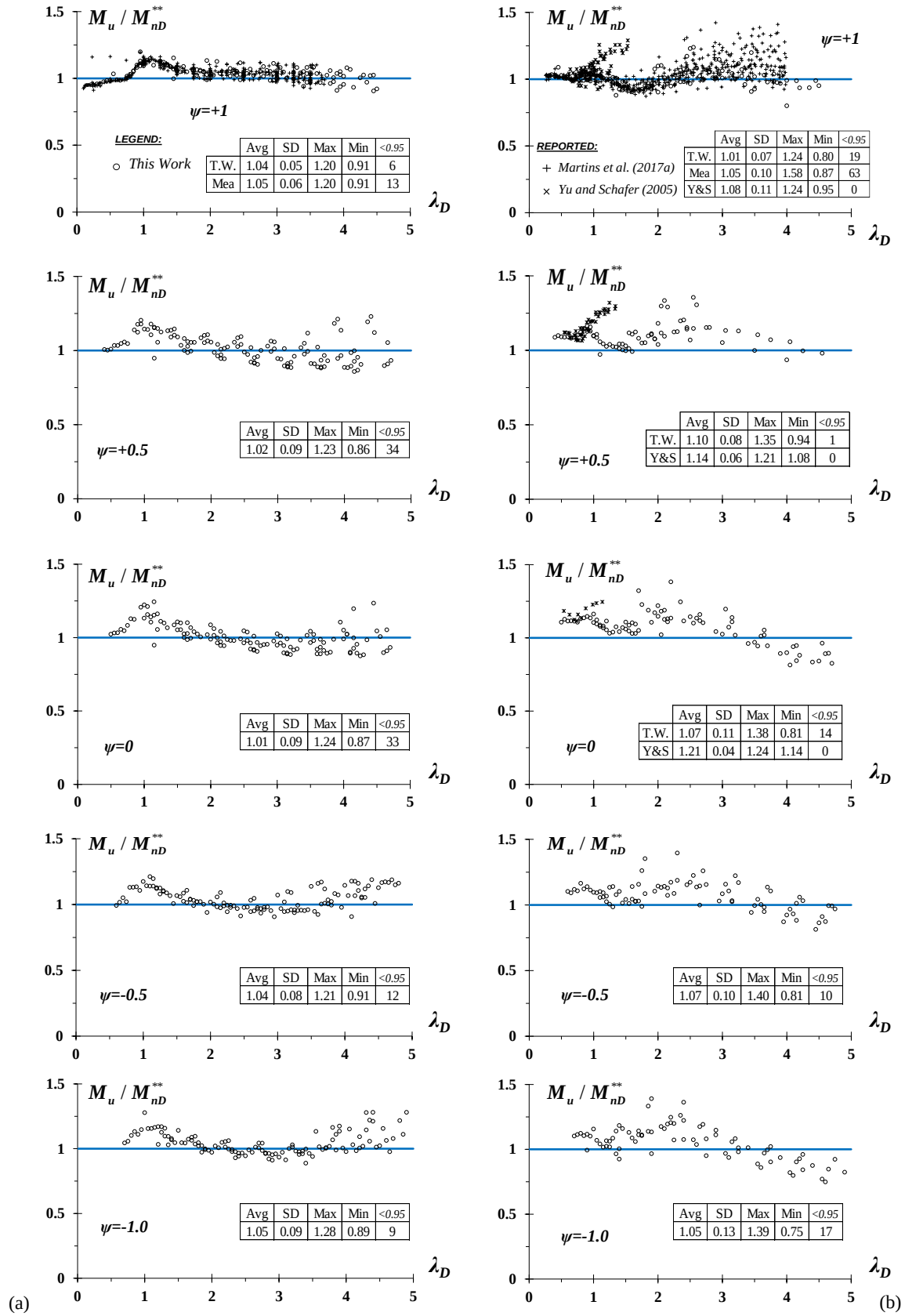

Figure 17. Plots M_u / M^{**}_{nD} vs. λ_D for (a) SCA and (b) SCB beams subjected to ψ=*+1/+0.5/0/–0.5/–1* bending moments

ratios of the beams analyzed in this work have a lower average than those concerning the beams analyzed by Martins *et al.* (2017a) and (i_2) it was intended to lower the number of "visibly unsafe" failure moment predictions ($M_u / M_{nD}^{*} < 0.95$), which was already non-negligible for the beams analyzed by Martins *et al.* (2017a): *98* out of *510* (*19*%).

(ii) Although the proposed M_{nD}^{**} strength curves are different from those developed by Martins *et al.* (2017a) for (ii_1) the SCA beams subjected to non-uniform bending ($\psi \neq 1$) and (ii_2) all the SCB beams with $\lambda_D > 0.673$, the differences only become perceptible in the moderate and high slenderness ranges ($\lambda_D > 1.5$) – see the "zoomed views" in Figures 16(a)-(b). This also means that, for $\lambda_D \leq 1.5$, the M_{nD}^{**} and M_{nD}^{*} values practically coincide.

(iii) In the SCA beams, the strength curve ψ-dependence is such that the various design curves appear, in descending order, according to the sequence $\psi = +1 \rightarrow +0.5 \rightarrow 0 \rightarrow -0.5 \rightarrow -1$, *i.e.*, become lower as the bending moment "non-uniformity" increases – see the "zoomed view" in Figure 16(a). This is perfectly in line with the findings of Section 3.3, where it was shown that the beam elastic post-critical strength also decreases to the sequence $\psi = +1 \rightarrow +0.5 \rightarrow 0 \rightarrow -0.5 \rightarrow -1$ (see Fig. 8(a_2)).

(iv) In the SCA beams, the failure moment prediction quality is very good and, remarkably, almost independent of the bending moment diagram (ψ value), as attested by the fact that the differences between the various M_u / M_{nD}^{**} statistical indicators are quite small. Indeed, the averages vary between *1.01* and *1.05*, the standard deviations vary between *0.05* and *0.09*, the maximum values vary between *1.20* and *1.28*, and the minimum values vary between *0.87* and *0.91*. Moreover, note that the number of "visibly unsafe" failure moment predictions falls from *338* to *107* (*33.5*% to *10.6%* of *1010*), – Figure 17(a) shows that a large portion (about *67*%) of these predictions concerns the beams subjected to $\psi = +0.5$ (*34*) and $\psi = 0$ (*33*) bending moments.

(v) In the SCB beams, the same strength curve applies to all the beams, regardless of the ψ value (see Fig. 16(b)), even if the (quite good) failure moment prediction quality is no longer independent of the bending moment diagram. Indeed, now the averages vary between *1.04* and *1.10*, the standard deviations vary between *0.08* and *0.13*, the maximum values vary between *1.21* and *1.58*, and the minimum values vary between *0.75* and *1.14*. Note also that the number of "visibly unsafe" failure moment predictions falls from *193* to *124* (*20.2*% to *12.9%* of *960*). Figure 17(b) shows that practically all the "visibly unsafe" predictions of beams under non-uniform bending correspond to the high slenderness range ($\lambda_D \geq 3.5$) – they amount to about *40*% of the total number (the remaining *60*% concern uniformly bent beams such that $1.2 < \lambda_D < 2.0$).

5 Concluding Remarks

This paper reported the results of an ongoing numerical (ANSYS SFEA) investigation on the distortional buckling, post-buckling and ultimate strength behaviors, and DSM design of cold-formed steel beams subjected to major-axis uniform and (mostly) non-uniform bending. The beams analyzed consisted of single-span lipped channel members exhibiting (i) *15* geometries, (ii) *two* end support conditions, differing in the warping and local displacement/rotation restraints, (iii) *5* bending moment diagrams and (iv) *8* yield stresses, selected to cover a wide distortional slenderness range.

After presenting the beam geometry selection procedure, aimed at identifying simply supported beams buckling and failing in distortional modes under uniform and non-uniform bending, the ANSYS SFE model employed to perform the non-linear analyses was validated, by replicating numerical results obtained by Yu & Schafer (2005) for lipped channel beams under non-uniform bending. Next, illustrative results concerning the beam (elastic and elastic-plastic) distortional post-buckling behavior and ultimate strength were presented and discussed – particular attention was paid to joint influence of the (i) end

support conditions (SCA of SCB) and (ii) bending moment diagram. An interesting (and surprising) finding was the fact that the variation of the beam distortional post-critical strength with the bending moment diagram (ψ value) is opposite for the SCA and SCB beams: it increases with ψ for the SCA beams, and decreases as ψ grows for the SCB beams.

Then, a fairly extensive parametric study (*1200* beams) was carried out, by means of geometrically non-linear elastic-plastic ANSYS SFEA, in order to assemble substantial distortional failure moment data concerning beams subjected to uniform and non-uniform bending. The above numerical failure moment data, together with other numerical values collected from the literature (Martins *et al.* 2017a and Yu & Schafer 2005), were subsequently used to assess the quality of their prediction by means of the available DSM beam distortional design curves, namely (i) the currently codified one (AISI 2016) and (ii) those proposed by Martins *et al.* (2017a) in the context of beams under uniform bending. It was found that the above prediction quality is (i) poor for the codified design curve (as expected) and (ii) still inadequate for the design curves developed by Martins *et al.* (2017a). Therefore, it was necessary to search for new design curves providing efficient (safe and reliable) failure moment predictions. This goal was successfully achieved by modifying the design curves proposed by Martins *et al.* (2017a), while keeping their format (see Eq. (2)): this was done by replacing the current parameter a and c values by ψ-dependent expressions (SCA beams) or new values (SCB beams). For uniformly bent beams, the design curves of Martins *et al.* (2017a) are either recovered (SCA beams) or slightly lowered/improved (SCB beams).

Finally, one last word to mention that the authors are currently extending the scope of this investigation to cover beams with additional geometries (cross-section shape/dimensions and lengths) and beams subjected to other bending moment diagrams, namely those caused by transverse applied loads. The output of this research effort will be reported in the near future.

Acknowledgments

The first and second authors gratefully acknowledge the financial support of Brazilian Government provided through CAPES (Coordination for the Improvement of Higher Education Personnel) and CNPq (National Council for Scientific and Technological Development), respectively.

References

ABNT (Brazilian Standards Association) (2010). *Brazilian Standard on Design of Cold-Formed Steel Structures* (ABNT NBR 14762:2010), Rio de Janeiro. (Portuguese)

AISI (American Iron and Steel Institute) (2016). *North American Specification* (NAS) *for the Design of Cold-Formed Steel Structural Members* (AISI-S100-16), Washington DC.

AS/NZS (Standards of Australia – SA – and Standards of New Zealand – SNZ) (2005). *Cold-Formed Steel Structures* (AS/NZS 4600 – 2nd ed.), Sydney-Wellington.

Bebiano R, Dinis PB, Silvestre N, Camotim D (2007). On the application of the Direct Strength Method to cold-formed steel beams subjected to non-uniform bending, *Proceedings of 5th International Conference on Advances in Steel Structures* (ICASS 2007 – Singapore 5-7/12), J.Y.R. Liew, Y.S. Choo (eds.), Research Publishing (Singapore), 322-327 (vol. III).

Bebiano R, Camotim D, Gonçalves R (2018). GBTUL 2.0 – a second-generation code for the GBT-based buckling and vibration analysis of thin-walled members, *Thin-Walled Structures*, **124**(March), 235-257.

Camotim D, Dinis PB, Martins AD (2016). Direct Strength Method (DSM) – a general approach for the design of cold-formed steel structures, *Recent Trends in Cold-Formed Steel Construction*, C. Yu (ed.), Woodhead Publishing (Series in Civil and Structural Engineering), Amsterdam, 69-105.

Dinis PB, Camotim D (2010). Local/distortional mode interaction in cold-formed steel lipped channel beams, *Thin-Walled Structures*, **48**(10-11), 771-785.

Hancock GJ, Kwon YB, Bernard ES (1994). Strength design curves for thin-walled sections undergoing distortional buckling, *Journal of Constructional Steel Research*, **31**(2-3), 169-186.

Landesmann A, Camotim D (2016). Distortional failure and DSM design of cold-formed steel lipped channel beams under elevated temperatures, *Thin-Walled Structures*, **98A**(January), 75-93.

Martins AD, Landesmann A, Camotim D, Dinis PB (2017a). Distortional failure of cold-formed steel beams under uniform bending: behaviour, strength and DSM design, *Thin-Walled Structures*, **118**(September), 196-213.

Martins AD, Camotim D, Dinis PB (2017b). Local-distortional interaction in cold-formed steel beams: behaviour, strength and DSM design, *Thin-Walled Structures*, **119**(October), 879-901.

SAS (Swanson Analysis Systems Inc.) (2009). Ansys Reference Manual (version 12).

Schafer BW (2008). Review: the Direct Strength Method of cold-formed steel member design, *Journal of Constructional Steel Research*, **64**(7-8), 766-788.

Schafer BW, Peköz T (1998). Direct strength prediction of cold-formed steel members using numerical elastic buckling solutions, *Proceedings of 14th International Specialty Conference on Cold-formed Steel Structures* (St. Louis, 15-16/10), R LaBoube, W-W Yu (eds.), 69-76.

Shifferaw Y, Schafer BW (2012). Inelastic bending capacity of cold-formed steel members, *Journal of Structural Engineering* (ASCE), **138**(4), 468-480.

Wang L, Young B (2014). Design of cold-formed steel channel with stiffened webs subjected to bending, *Thin-Walled Structures*, **85**(December), 81-92.

Yu C, Schafer BW (2005). *Distortional Buckling of Cold-Formed Steel Members in Bending*, Final Report, American Iron and Steel Institute (AISI), Baltimore, Maryland.

Yu C, Schafer BW (2006). Distortional buckling tests on cold-formed steel beams, *Journal of Structural Engineering* (ASCE), **132**(4), 515-528.

Yu C, Schafer BW (2007). Simulation of cold-formed steel beams in local and distortional buckling with applications to the Direct Strength Method, *Journal of Constructional Steel Research*, **63**(5), 581-590.

ANNEX A – DATA CONCERNING THE BUCKLING BEHAVIOR OF THE SELECTED BEAMS

Tables A1 to A5 presents the GBT-based results concerning the buckling behavior of selected beams. Each table is associated with a given bending moment diagram ($\psi = +1.0/+0.5/0/-0.5/-1.0$) and includes the *15* beam geometries (C01-C15) and the *two* end support conditions considered (SCA and SCB). The information provided consists of (i) the length associated with critical distortional buckling (L_D), (ii) the corresponding critical distortional buckling moment (M_{crD}), (iii) its ratios with respect to the lowest local (M_{crL}) and global (M_{crG}) buckling moments, and (iv) the critical distortional half-wave number (n_D).

Table A1: SCA and SCB beam critical buckling lengths, moments, buckling moment ratios and half-wave numbers – ***ψ=+1.0***

Beam	SCA					SCB				
	L_D (cm)	M_{crD} (kNcm)	$\frac{M_{crL}}{M_{crD}}$	$\frac{M_{crG}}{M_{crD}}$	n_D	L_D (cm)	M_{crD} (kNcm)	$\frac{M_{crL}}{M_{crD}}$	$\frac{M_{crG}}{M_{crD}}$	n_D
C01	20	301.77	4.19	128.57	1	35	422.09	3.04	68.01	1
C02	30	283.20	3.18	103.80	1	45	404.30	2.22	129.18	1
C03	45	2049.44	2.88	17.40	1	55	2556.83	2.31	37.23	1
C04	35	996.85	2.82	73.02	1	60	1435.91	1.98	83.76	1
C05	35	2073.76	3.42	56.68	1	55	2693.56	2.70	60.96	1
C06	35	1566.80	3.09	39.11	1	55	2262.71	2.18	43.84	1
C07	35	2844.95	2.81	43.99	1	60	4086.80	2.00	44.09	1
C08	45	1062.21	2.87	74.76	1	70	1528.27	2.03	74.81	1
C09	40	843.14	2.63	89.92	1	40	1220.86	1.84	78.59	1
C10	45	1100.49	2.81	52.05	1	75	1593.06	1.98	48.92	1
C11	55	1358.92	2.94	42.72	1	70	2375.53	1.73	97.64	1
C12	45	1803.09	3.31	42.17	1	80	2583.19	2.36	47.64	1
C13	40	1493.07	3.16	57.76	1	65	2143.05	2.23	54.76	1
C14	45	1260.95	2.89	57.84	1	75	1826.58	2.03	60.47	1
C15	55	3204.07	2.73	58.39	1	95	4592.14	1.95	54.62	1

Table A2: SCA and SCB beam critical buckling lengths, moments, buckling moment ratios and half-wave numbers – ***ψ=+0.5***

Beam	SCA					SCB				
	L_D (cm)	M_{crD} (kNcm)	$\frac{M_{crL}}{M_{crD}}$	$\frac{M_{crG}}{M_{crD}}$	n_D	L_D (cm)	M_{crD} (kNcm)	$\frac{M_{crL}}{M_{crD}}$	$\frac{M_{crG}}{M_{crD}}$	n_D
C01	20	387.40	3.63	132.33	1	25	616.25	2.58	120.72	1
C02	30	360.60	2.75	107.71	1	45	516.89	1.89	133.41	1
C03	40	2341.30	2.75	25.44	1	55	3204.03	2.01	39.23	1
C04	40	1271.81	2.45	75.62	1	55	1857.01	1.66	99.16	1
C05	35	2458.66	3.16	45.28	1	55	3424.04	2.52	63.45	1
C06	35	2006.01	2.66	40.37	1	55	2969.06	1.95	53.37	1
C07	40	3643.76	2.36	45.38	1	55	5257.71	1.78	51.94	1
C08	45	1356.79	2.48	77.33	1	65	1999.30	1.83	100.49	1
C09	40	1078.53	2.26	75.25	1	60	1245.00	2.15	38.59	1
C10	45	1410.37	2.41	41.11	1	65	2074.55	1.77	59.01	1
C11	65	1733.36	2.53	44.25	1	70	2507.49	1.87	54.31	1
C12	50	2304.74	2.86	43.59	1	130	3297.56	2.15	49.28	2
C13	40	1911.53	2.69	45.67	1	60	2794.15	2.00	65.98	1
C14	45	1617.68	2.48	59.57	1	70	2380.89	1.81	71.88	1
C15	55	4101.62	2.30	60.27	1	90	5840.27	1.76	63.18	1

Table A3: SCA and SCB beam critical buckling lengths, moments, buckling moment ratios and half-wave numbers – ***ψ=0.0***

Beam	SCA					SCB				
	L_D (cm)	M_{crD} (kNcm)	$\frac{M_{crL}}{M_{crD}}$	$\frac{M_{crG}}{M_{crD}}$	n_D	L_D (cm)	M_{crD} (kNcm)	$\frac{M_{crL}}{M_{crD}}$	$\frac{M_{crG}}{M_{crD}}$	n_D
C01	25	454.91	3.23	101.41	1	25	806.82	2.23	130.80	1
C02	40	417.84	2.47	73.54	1	55	591.53	1.75	109.12	1
C03	45	2664.67	2.53	24.84	1	55	3977.82	1.70	44.16	1
C04	55	1460.88	2.22	44.40	1	100	2312.25	1.40	111.30	2
C05	40	2757.90	2.97	56.70	1	50	4299.40	2.21	71.68	1
C06	50	2324.97	2.39	24.03	1	85	2958.65	2.15	25.95	2
C07	40	4228.27	1.91	26.36	1	55	4388.01	2.38	9.72	1
C08	65	1585.51	2.22	52.35	1	65	1750.16	2.29	26.58	1
C09	45	1260.04	2.03	53.58	1	60	1397.94	2.09	28.13	1
C10	60	1617.65	2.20	26.69	1	160	2006.82	2.02	25.86	2
C11	70	2070.51	2.20	41.14	1	70	3129.97	1.63	60.81	1
C12	65	2753.23	2.50	39.28	1	170	4315.03	1.82	63.66	2
C13	40	2304.11	2.35	53.22	1	65	3546.33	1.73	72.65	1
C14	65	1990.15	2.06	68.02	1	210	2897.68	1.60	70.34	2
C15	85	4697.14	1.93	30.99	1	170	5548.85	1.98	26.08	2

Table A4: SCA and SCB beam critical buckling lengths, moments, buckling moment ratios and half-wave numbers – ***ψ=–1.0***

Beam	SCA					SCB				
	L_D (cm)	M_{crD} (kNcm)	$\frac{M_{crL}}{M_{crD}}$	$\frac{M_{crG}}{M_{crD}}$	n_D	L_D (cm)	M_{crD} (kNcm)	$\frac{M_{crL}}{M_{crD}}$	$\frac{M_{crG}}{M_{crD}}$	n_D
C01	25	515.55	2.96	126.40	1	35	824.66	2.22	96.92	1
C02	50	436.23	2.46	63.79	1	55	707.92	1.52	125.94	1
C03	60	2743.34	2.57	19.25	1	55	4755.20	1.48	51.02	1
C04	60	1574.66	2.15	50.20	1	110	2712.85	1.25	131.03	2
C05	30	3173.17	2.71	97.11	1	140	5245.46	1.95	87.16	1
C06	55	2504.16	2.29	26.06	1	95	3373.83	2.00	25.18	2
C07	40	4561.51	1.37	34.52	1	60	5000.82	2.18	11.77	2
C08	70	1716.21	2.13	58.24	1	65	1828.55	2.57	18.66	1
C09	45	1362.92	1.95	60.36	1	150	1429.17	2.54	17.64	2
C10	65	1741.20	2.13	29.46	1	220	2297.62	1.88	25.81	2
C11	55	2323.51	1.77	51.78	1	70	2523.56	2.25	16.75	1
C12	70	3444.98	1.68	78.71	1	250	3296.78	2.58	14.80	2
C13	60	2629.07	2.08	65.88	2	160	4120.39	1.57	72.59	2
C14	65	2053.01	2.00	41.46	1	210	2359.84	2.19	19.77	2
C15	90	5025.99	1.51	36.50	1	230	5828.42	2.00	18.77	2

Table A5: SCA and SCB beam critical buckling lengths, moments, buckling moment ratios and half-wave numbers – ***ψ=–0.5***

Beam	SCA					SCB				
	L_D (cm)	M_{crD} (kNcm)	$\frac{M_{crL}}{M_{crD}}$	$\frac{M_{crG}}{M_{crD}}$	n_D	L_D (cm)	M_{crD} (kNcm)	$\frac{M_{crL}}{M_{crD}}$	$\frac{M_{crG}}{M_{crD}}$	n_D
C01	45	472.62	3.27	36.37	1	50	798.31	2.34	58.03	1
C02	50	467.04	2.37	62.34	1	55	815.93	1.36	110.48	1
C03	60	2954.83	2.44	18.70	1	55	5381.64	1.33	45.58	1
C04	70	1682.75	2.07	49.16	1	130	3073.41	1.13	137.22	2
C05	100	3945.90	1.96	154.27	1	75	5915.65	1.81	79.55	1
C06	65	2585.69	2.22	18.95	1	110	3641.18	1.95	17.62	2
C07	110	4597.27	1.18	26.94	2	120	5883.07	1.75	13.75	2
C08	70	1775.16	2.12	44.30	1	60	1927.37	2.89	13.89	1
C09	160	1393.76	1.96	41.93	1	140	1822.53	1.88	26.88	2
C10	75	1802.35	2.11	21.93	1	250	2459.09	1.90	17.49	2
C11	40	1863.55	2.62	5.48	1	75	2948.08	2.03	16.63	1
C12	85	2652.44	2.74	9.81	1	180	4985.39	1.73	34.25	2
C13	170	2187.30	2.61	11.13	2	160	3436.36	2.02	22.09	2
C14	75	1741.51	2.55	6.50	1	180	2677.59	2.06	17.61	2
C15	160	4730.07	1.94	12.90	2	220	6618.43	1.71	18.26	2

ANNEX B – DATA CONCERNING THE SELECTED BEAM FAILURE MOMENTS AND DSM ESTIMATES

Tables B1 to B15 provide the numerical beam failure moments and their DSM estimates. Each table concerns one beam geometry (C01 to C15 – see Table 1), the two end support conditions (SCA and SCB), *5* bending moment diagrams (ψ=+1/+0.5/0/ –0.5/ –1) and *8* slenderness values (yield stresses) considered. The information provided consists of (i) distortional slenderness (λ_D), (ii) yield and plastic moments (M_y and M_p), (iii) failure moment (M_u), (iv) failure to-yield moment ratio M_u / M_y and (vi) failure to-predicted moment ratios M_u / M_{nD}, M_u / M^*_{nD} and M_u / M^{**}_{nD}.

Table B1: Failure moments and their DSM estimates for SCA and SCB ***C01*** beams

	SCA								SCB							
ψ	λ_D	M_u (kNcm)	M_y (kNcm)	M_p (kNcm)	$\frac{M_u}{M_y}$	$\frac{M_u}{M_{nD}}$	$\frac{M_u}{M^*_{nD}}$	$\frac{M_u}{M^{**}_{nD}}$	λ_D	M_u (kNcm)	M_y (kNcm)	M_p (kNcm)	$\frac{M_u}{M_y}$	$\frac{M_u}{M_{nD}}$	$\frac{M_u}{M^*_{nD}}$	$\frac{M_u}{M^{**}_{nD}}$
+1	0.50	75.2	74.9	80.9	1.00	0.98	0.98	0.98	0.50	110.8	105.6	114.1	1.05	1.03	1.03	1.03
	1.00	247.8	302.1	326.3	0.82	1.05	1.09	1.09	1.00	344.2	422.5	456.2	0.81	1.04	1.06	1.07
	1.50	309.0	679.2	733.4	0.45	0.80	1.05	1.05	1.50	446.0	949.4	1025.2	0.47	0.83	0.96	0.98
	2.00	333.8	1207.3	1303.7	0.28	0.62	1.00	1.00	2.00	610.5	1688.7	1823.6	0.36	0.81	1.07	1.10
	2.50	367.6	1886.5	2037.1	0.19	0.53	1.02	1.02	2.50	787.0	2638.1	2848.8	0.30	0.82	1.19	1.23
	3.00	404.8	2715.5	2932.3	0.15	0.48	1.06	1.06	3.00	759.7	3798.7	4102.1	0.20	0.65	1.03	1.06
	3.50	419.1	3696.8	3992.0	0.11	0.42	1.04	1.04	3.50	723.9	5170.6	5583.5	0.14	0.52	0.89	0.93
	4.00	424.1	4828.0	5213.5	0.09	0.37	1.02	1.02	4.00	675.4	6753.7	7293.0	0.10	0.42	0.77	0.80
+0.5	0.60	145.9	140.0	151.2	1.04	1.03	1.03	1.03	0.60	244.8	222.3	240.1	1.10	1.09	1.09	1.09
	1.10	363.1	469.2	506.6	0.77	1.06	1.16	1.18	1.10	499.2	745.5	805.0	0.67	0.92	0.96	0.97
	1.60	402.7	991.1	1070.3	0.41	0.75	1.04	1.08	1.60	770.8	1578.2	1704.2	0.49	0.91	1.09	1.11
	2.10	426.3	1708.4	1844.8	0.25	0.59	0.98	1.04	2.10	1117.2	2718.0	2935.0	0.41	0.96	1.30	1.33
	2.60	443.3	2618.5	2827.6	0.17	0.48	0.95	1.02	2.60	1249.8	4166.0	4498.6	0.30	0.85	1.27	1.31
	3.10	460.0	3722.6	4019.9	0.12	0.41	0.93	1.01	3.10	1714.5*	5922.3	6395.2	0.29	0.97	1.56	1.61
	3.60	480.7	5020.8	5421.7	0.10	0.37	0.93	1.02	3.60	1961.7*	7986.8	8624.6	0.25	0.94	1.62	1.69
	4.10	476.4	6511.8	7031.8	0.07	0.32	0.88	0.99	4.10	2155.5*	10359.7	11186.9	0.21	0.90	1.65	1.73
0	0.70	231.3	222.3	240.1	1.04	1.06	1.04	1.05	0.70	435.1	395.5	427.1	1.10	1.12	1.09	1.11
	1.20	437.0	654.6	706.9	0.67	0.98	1.12	1.16	1.20	810.0	1161.9	1254.6	0.70	1.02	1.10	1.11
	1.70	464.1	1314.1	1419.1	0.35	0.69	0.99	1.07	1.70	1258.1	2332.3	2518.5	0.54	1.05	1.30	1.32
	2.20	472.6	2202.1	2378.0	0.21	0.52	0.91	1.01	2.20	1562.2	3905.6	4217.5	0.40	0.98	1.35	1.38
	2.70	472.6	3316.1	3580.9	0.14	0.42	0.85	0.97	2.70	2042.7*	5881.7	6351.4	0.35	1.02	1.54	1.59
	3.20	472.6	4658.5	5030.5	0.10	0.35	0.80	0.94	3.20	2363.3*	8261.9	8921.7	0.29	0.98	1.61	1.67
	3.70	472.6	6228.1	6725.4	0.08	0.30	0.77	0.91	3.70	2586.8*	11045.0	11927.0	0.23	0.92	1.61	1.68
	4.20	472.6	8024.9	8665.7	0.06	0.26	0.74	0.89	4.20	2667.7*	14232.1	15368.6	0.19	0.83	1.54	1.61
-0.5	0.80	346.9	330.4	356.8	1.05	1.16	1.13	1.13	0.80	565.4	528.1	570.3	1.07	1.18	1.15	1.16
	1.30	486.0	870.8	940.3	0.56	0.87	1.05	1.10	1.30	905.6	1394.0	1505.3	0.65	1.02	1.12	1.14
	1.80	503.6	1670.3	1803.7	0.30	0.62	0.93	1.02	1.80	1368.4	2672.5	2885.9	0.51	1.05	1.32	1.35
	2.30	519.9	2727.8	2945.6	0.19	0.48	0.87	0.99	2.30	1657.7	4362.5	4710.8	0.38	0.97	1.36	1.40
	2.80	530.7	4041.9	4364.7	0.13	0.40	0.83	0.98	2.80	2160.0*	6465.1	6981.4	0.33	1.02	1.56	1.61
	3.30	553.3	5614.0	6062.3	0.10	0.35	0.82	0.99	3.30	2468.1*	8980.4	9697.5	0.27	0.97	1.61	1.67
	3.80	581.4	7444.0	8038.4	0.08	0.32	0.83	1.02	3.80	2633.4*	11908.4	12859.3	0.22	0.89	1.58	1.64
	4.30	646.2	9531.9	10293.0	0.07	0.31	0.89	1.12	4.30	2659.0*	15247.8	16465.4	0.17	0.79	1.48	1.55
-1	0.90	354.2	383.2	413.8	0.92	1.10	1.10	1.11	0.90	605.0	646.0	697.6	0.94	1.12	1.10	1.12
	1.40	447.8	926.0	1000.0	0.48	0.80	1.01	1.08	1.40	965.1	1564.7	1689.6	0.62	1.02	1.16	1.18
	1.90	454.5	1705.9	1842.2	0.27	0.57	0.89	0.99	1.90	1412.2	2881.3	3111.4	0.49	1.05	1.36	1.39
	2.40	454.5	2722.9	2940.3	0.17	0.44	0.82	0.94	2.40	1609.4	4598.3	4965.5	0.35	0.92	1.32	1.36
	2.90	454.5	3974.4	4291.7	0.11	0.36	0.77	0.91	2.90	2163.0*	6713.2	7249.3	0.32	1.01	1.58	1.63
	3.40	454.5	5462.9	5899.2	0.08	0.30	0.73	0.89	3.40	2297.7*	9228.5	9965.4	0.25	0.91	1.52	1.58
	3.90	612.2	7188.5	7762.5	0.09	0.35	0.94	1.17	3.90	2298.2*	12141.7	13111.3	0.19	0.78	1.40	1.46
	4.40	678.0	9149.9	9880.6	0.07	0.34	1.01	1.28	4.40	2298.3*	15455.4	16689.5	0.15	0.69	1.30	1.37

Table B2: Failure moments and their DSM estimates for SCA and SCB ***C02*** beams

	SCA								*SCB*							
ψ	λ_D	M_u *(kNcm)*	M_y *(kNcm)*	M_p *(kNcm)*	$\frac{M_u}{M_y}$	$\frac{M_u}{M_{nD}}$	$\frac{M_u}{M^*_{nD}}$	$\frac{M_u}{M^{**}_{nD}}$	λ_D	M_u *(kNcm)*	M_y *(kNcm)*	M_p *(kNcm)*	$\frac{M_u}{M_y}$	$\frac{M_u}{M_{nD}}$	$\frac{M_u}{M^*_{nD}}$	$\frac{M_u}{M^{**}_{nD}}$
+1	0.55	89.3	85.0	92.1	1.05	1.03	1.03	1.03	0.55	124.8	122.1	132.2	1.02	1.01	1.01	1.01
	1.05	251.2	312.3	338.1	0.80	1.07	1.14	1.14	1.05	330.3	445.2	482.0	0.74	0.98	1.01	1.02
	1.55	293.3	680.2	736.4	0.43	0.78	1.05	1.05	1.55	415.4	970.9	1051.1	0.43	0.77	0.91	0.93
	2.05	322.8	1190.4	1288.8	0.27	0.62	1.03	1.02	2.05	596.5	1699.1	1839.4	0.35	0.81	1.08	1.10
	2.55	353.4	1841.3	1993.4	0.19	0.54	1.04	1.04	2.55	769.1	2629.7	2847.0	0.29	0.82	1.20	1.24
	3.05	390.4	2634.4	2852.0	0.15	0.49	1.08	1.08	3.05	933.9*	3761.4	4072.2	0.25	0.82	1.30	1.35
	3.55	409.8	3569.7	3864.6	0.11	0.43	1.08	1.08	3.55	1077.7*	5095.6	5516.6	0.21	0.80	1.37	1.43
	4.05	424.4	4645.7	5029.5	0.09	0.39	1.08	1.08	4.05	1172.0*	6632.3	7180.3	0.18	0.76	1.38	1.44
+0.5	0.65	160.7	153.1	165.7	1.05	1.05	1.05	1.05	0.65	236.3	218.0	236.0	1.08	1.08	1.08	1.08
	1.15	341.1	476.2	515.5	0.72	1.02	1.14	1.16	1.15	468.0	683.3	739.8	0.68	0.97	1.03	1.04
	1.65	372.3	981.7	1062.8	0.38	0.72	1.02	1.06	1.65	669.9	1406.9	1523.1	0.48	0.91	1.10	1.12
	2.15	387.0	1666.6	1804.3	0.23	0.56	0.95	1.01	2.15	920.5	2388.6	2585.9	0.39	0.92	1.26	1.29
	2.65	387.0	2532.3	2741.6	0.15	0.44	0.88	0.95	2.65	1161.9*	3630.0	3929.9	0.32	0.93	1.39	1.43
	3.15	387.0	3577.4	3873.0	0.11	0.37	0.83	0.91	3.15	1382.8*	5128.1	5551.7	0.27	0.91	1.48	1.54
	3.65	387.0	4803.4	5200.2	0.08	0.31	0.80	0.88	3.65	1557.9*	6885.9	7454.7	0.23	0.88	1.53	1.59
	4.15	387.0	6210.3	6723.3	0.06	0.27	0.77	0.86	4.15	1652.7*	8901.9	9637.3	0.19	0.81	1.50	1.57
0	0.75	246.7	235.0	254.4	1.05	1.11	1.08	1.08	0.75	352.3	332.4	359.8	1.06	1.12	1.09	1.11
	1.25	392.1	652.4	706.3	0.60	0.91	1.07	1.11	1.25	569.1	924.5	1000.9	0.62	0.93	1.02	1.03
	1.75	419.0	1280.1	1385.8	0.33	0.66	0.96	1.04	1.75	873.3	1811.9	1961.6	0.48	0.96	1.20	1.23
	2.25	425.9	2114.9	2289.6	0.20	0.50	0.89	0.99	2.25	1169.7*	2994.6	3242.0	0.39	0.97	1.35	1.39
	2.75	425.9	3160.0	3421.1	0.13	0.40	0.83	0.94	2.75	1446.8*	4474.1	4843.7	0.32	0.97	1.47	1.52
	3.25	425.9	4413.8	4778.5	0.10	0.34	0.78	0.92	3.25	1693.1*	6247.4	6763.5	0.27	0.94	1.55	1.61
	3.75	425.9	5876.3	6361.8	0.07	0.29	0.75	0.89	3.75	1896.9*	8319.0	9006.3	0.23	0.91	1.60	1.66
	4.25	425.9	7547.6	8171.1	0.06	0.25	0.72	0.87	4.25	1963.3*	10684.4	11567.1	0.18	0.82	1.54	1.60
-0.5	0.85	314.7	315.4	341.4	1.00	1.14	1.12	1.13	0.85	504.6	511.7	554.0	0.99	1.13	1.11	1.12
	1.35	411.8	794.6	860.3	0.52	0.84	1.03	1.09	1.35	758.0	1290.9	1397.6	0.59	0.95	1.06	1.08
	1.85	429.6	1493.4	1616.8	0.29	0.60	0.92	1.02	1.85	1121.3*	2422.6	2622.7	0.46	0.97	1.24	1.27
	2.35	439.9	2408.7	2607.7	0.18	0.47	0.86	0.99	2.35	1451.3*	3909.8	4232.8	0.37	0.96	1.36	1.40
	2.85	451.9	3543.4	3836.2	0.13	0.39	0.83	0.98	2.85	1746.5*	5749.6	6224.6	0.30	0.94	1.45	1.50
	3.35	451.9	4896.2	5300.7	0.09	0.33	0.79	0.96	3.35	2010.0*	7944.9	8601.2	0.25	0.91	1.51	1.57
	3.85	521.8	6465.4	6999.5	0.08	0.33	0.87	1.08	3.85	2224.5*	10492.7	11359.5	0.21	0.87	1.54	1.61
	4.35	559.0	8254.1	8936.0	0.07	0.31	0.90	1.14	4.35	2287.1*	13396.1	14502.8	0.17	0.78	1.47	1.54
-1	0.95	378.7	422.1	456.9	0.90	1.11	1.13	1.15	0.95	647.5	735.9	796.7	0.88	1.09	1.09	1.10
	1.45	435.7	981.7	1062.8	0.44	0.76	0.98	1.05	1.45	993.1	1716.1	1857.8	0.58	0.99	1.14	1.16
	1.95	450.0	1776.4	1923.1	0.25	0.56	0.88	0.99	1.95	1398.2*	3102.8	3359.2	0.45	0.99	1.29	1.32
	2.45	462.8	2802.9	3034.5	0.17	0.44	0.84	0.97	2.45	1740.3*	4897.7	5302.3	0.36	0.96	1.38	1.42
	2.95	474.6	4064.4	4400.2	0.12	0.37	0.81	0.96	2.95	2041.2*	7100.8	7687.4	0.29	0.92	1.44	1.49
	3.45	488.2	5559.4	6018.7	0.09	0.32	0.79	0.96	3.45	2061.6*	9712.0	10514.3	0.21	0.78	1.32	1.38
	3.95	519.0	7286.3	7888.2	0.07	0.30	0.81	1.01	3.95	2061.3*	12731.3	13783.1	0.16	0.68	1.22	1.27
	4.45	530.7	9248.2	10012.2	0.06	0.27	0.80	1.01	4.45	2061.3*	16157.3	17492.0	0.13	0.60	1.14	1.19

Table B3: Failure moments and their DSM estimates for SCA and SCB ***C03*** beams

	SCA								*SCB*							
ψ	λ_D	M_u *(kNcm)*	M_y *(kNcm)*	M_p *(kNcm)*	$\frac{M_u}{M_y}$	$\frac{M_u}{M_{nD}}$	$\frac{M_u}{M^*_{nD}}$	$\frac{M_u}{M^{**}_{nD}}$	λ_D	M_u *(kNcm)*	M_y *(kNcm)*	M_p *(kNcm)*	$\frac{M_u}{M_y}$	$\frac{M_u}{M_{nD}}$	$\frac{M_u}{M^*_{nD}}$	$\frac{M_u}{M^{**}_{nD}}$
+1	0.40	310.2	305.4	337.0	1.02	0.97	0.97	0.97	0.40	440.2	413.4	456.2	1.07	1.02	1.02	1.02
	0.90	1399.2	1538.0	1697.4	0.91	1.08	1.08	1.08	0.90	1812.0	2085.4	2301.6	0.87	1.04	1.02	1.04
	1.40	1941.7	3723.9	4110.0	0.52	0.87	1.09	1.09	1.40	2509.5	5045.9	5569.1	0.50	0.83	0.94	0.95
	1.90	2156.7	6855.7	7566.5	0.31	0.68	1.05	1.05	1.90	3033.5	9294.8	10258.6	0.33	0.70	0.90	0.93
	2.40	2290.1	10940.8	12075.2	0.21	0.55	1.02	1.02	2.40	3737.9	14828.6	16366.0	0.25	0.67	0.95	0.98
	2.90	2346.5	15975.5	17631.9	0.15	0.46	0.98	0.98	2.90	4318.9	21650.7	23895.5	0.20	0.63	0.98	1.01
	3.40	2355.8	21956.1	24232.6	0.11	0.39	0.94	0.94	3.40	4716.9	29761.4	32847.1	0.16	0.58	0.97	1.01
	3.90	2374.6	28890.0	31885.4	0.08	0.34	0.91	0.91	3.90	4910.5	39156.8	43216.7	0.13	0.52	0.93	0.97
+0.5	0.50	605.4	584.7	645.3	1.04	1.01	1.01	1.01	0.50	896.5	800.6	883.7	1.12	1.09	1.09	1.09
	1.00	1989.9	2342.3	2585.2	0.85	1.09	1.13	1.14	1.00	2667.0	3202.6	3534.6	0.83	1.07	1.08	1.10
	1.50	2394.9	5269.3	5815.7	0.45	0.80	1.05	1.09	1.50	3441.1	7209.5	7957.0	0.48	0.84	0.98	1.00
	2.00	2575.2	9365.6	10336.7	0.27	0.62	1.00	1.06	2.00	4383.4	12817.6	14146.6	0.34	0.77	1.01	1.04
	2.50	2575.4	14634.9	16152.3	0.18	0.48	0.92	0.99	2.50	5195.3	20023.4	22099.5	0.26	0.71	1.04	1.07
	3.00	2575.4	21073.5	23258.5	0.12	0.40	0.87	0.95	3.00	5705.1	28837.8	31827.8	0.20	0.64	1.02	1.05
	3.50	2575.4	28681.4	31655.2	0.09	0.34	0.83	0.91	3.50	5929.4	39249.9	43319.4	0.15	0.56	0.96	1.00
	4.00	2575.4	37462.4	41346.6	0.07	0.29	0.80	0.89	4.00	5990.6	51263.2	56578.3	0.12	0.49	0.90	0.94
0	0.60	1003.6	960.8	1060.4	1.04	1.03	1.03	1.03	0.60	1616.0	1433.7	1582.4	1.13	1.11	1.11	1.11
	1.10	2391.6	3224.9	3559.3	0.74	1.02	1.11	1.14	1.10	3579.4	4815.0	5314.2	0.74	1.02	1.07	1.08
	1.60	2557.6	6822.2	7529.5	0.37	0.70	0.96	1.02	1.60	4955.6	10184.9	11240.9	0.49	0.90	1.08	1.10
	2.10	2701.2	11752.6	12971.2	0.23	0.54	0.90	1.00	2.10	6429.4	17543.3	19362.2	0.37	0.86	1.16	1.19
	2.60	2736.3	18012.5	19880.1	0.15	0.43	0.85	0.96	2.60	7411.5*	26890.3	29678.3	0.28	0.78	1.16	1.20
	3.10	2780.8	25609.2	28264.5	0.11	0.36	0.81	0.95	3.10	7724.9*	38225.8	42189.2	0.20	0.67	1.09	1.13
	3.60	2780.8	34535.4	38116.1	0.08	0.31	0.78	0.92	3.60	7761.9*	51553.6	56898.8	0.15	0.58	1.00	1.04
	4.10	2780.8	44794.7	49439.2	0.06	0.27	0.75	0.90	4.10	7761.9*	66866.3	73799.2	0.12	0.50	0.92	0.96
-0.5	0.70	1404.2	1344.3	1483.7	1.04	1.07	1.05	1.05	0.70	2576.1	2331.2	2572.9	1.11	1.13	1.10	1.12
	1.20	2525.4	3951.1	4360.7	0.64	0.94	1.07	1.12	1.20	4569.6	6848.2	7558.3	0.67	0.98	1.05	1.07
	1.70	2687.0	7928.2	8750.2	0.34	0.66	0.95	1.04	1.70	6488.9	13741.2	15165.9	0.47	0.92	1.13	1.16
	2.20	2786.4	13279.4	14656.3	0.21	0.51	0.89	1.01	2.20	8044.4*	23013.7	25399.8	0.35	0.85	1.18	1.21
	2.70	2804.0	19997.3	22070.7	0.14	0.41	0.83	0.98	2.70	8944.0*	34665.7	38260.0	0.26	0.76	1.15	1.18
	3.20	3218.2	28093.1	31005.8	0.11	0.39	0.91	1.09	3.20	9068.6*	48693.7	53742.4	0.19	0.64	1.05	1.08
	3.70	3369.9	37555.5	41449.4	0.09	0.35	0.91	1.12	3.70	9071.5*	65097.4	71846.9	0.14	0.55	0.96	1.00
	4.20	3560.0	48392.0	53409.5	0.07	0.33	0.93	1.16	4.20	9070.1*	83880.8	92577.8	0.11	0.48	0.89	0.93
-1	0.80	1937.9	1891.7	2087.9	1.02	1.13	1.10	1.10	0.80	3557.7	3444.6	3801.8	1.03	1.14	1.11	1.12
	1.30	2917.4	4993.7	5511.5	0.58	0.91	1.10	1.16	1.30	5628.7	9093.8	10036.6	0.62	0.97	1.07	1.09
	1.80	2952.7	9574.1	10566.8	0.31	0.63	0.95	1.05	1.80	7600.5*	17435.3	19243.0	0.44	0.89	1.13	1.15
	2.30	2972.9	15629.2	17249.7	0.19	0.48	0.87	0.99	2.30	8369.5*	28469.2	31421.0	0.29	0.75	1.05	1.08
	2.80	3000.6	23166.4	25568.3	0.13	0.39	0.82	0.97	2.80	8513.8*	42191.7	46566.3	0.20	0.61	0.94	0.97
	3.30	3043.5	32178.2	35514.5	0.09	0.33	0.79	0.96	3.30	8513.8*	58606.7	64683.2	0.15	0.51	0.85	0.88
	3.80	3780.4	42668.4	47092.4	0.09	0.36	0.94	1.16	3.80	8513.8*	77710.3	85767.5	0.11	0.44	0.78	0.81
	4.30	4221.3	54633.3	60297.8	0.08	0.35	1.01	1.28	4.30	8513.8*	99506.2	109823	0.09	0.39	0.73	0.76

Table B4: Failure moments and their DSM estimates for SCA and SCB ***C04*** beams

	SCA								*SCB*							
ψ	λ_D	M_u *(kNcm)*	M_y *(kNcm)*	M_p *(kNcm)*	$\frac{M_u}{M_y}$	$\frac{M_u}{M_{nD}}$	$\frac{M_u}{M^*_{nD}}$	$\frac{M_u}{M^{**}_{nD}}$	λ_D	M_u *(kNcm)*	M_y *(kNcm)*	M_p *(kNcm)*	$\frac{M_u}{M_y}$	$\frac{M_u}{M_{nD}}$	$\frac{M_u}{M^*_{nD}}$	$\frac{M_u}{M^{**}_{nD}}$
+1	1.00	923.0	1099.6	1208.4	0.84	1.08	1.12	1.12	1.00	1253.1	1594.0	1751.8	0.79	1.01	1.02	1.03
	1.50	1129.4	2475.6	2720.6	0.46	0.80	1.06	1.06	1.50	1585.9	3584.9	3939.7	0.44	0.78	0.91	0.92
	2.00	1241.6	4401.5	4837.0	0.28	0.63	1.02	1.02	2.00	1893.2	6372.9	7003.4	0.30	0.67	0.88	0.90
	2.50	1335.2	6877.1	7557.6	0.19	0.53	1.02	1.02	2.50	2335.4	9957.8	10943.1	0.23	0.64	0.94	0.97
	3.00	1399.4	9905.8	10885.9	0.14	0.46	1.00	1.00	3.00	2721.6	14336.5	15755.0	0.19	0.61	0.97	1.01
	3.50	1439.4	13481.0	14814.8	0.11	0.40	0.98	0.98	3.50	3005.8	19515.5	21446.4	0.15	0.58	0.98	1.02
	4.00	1454.1	17609.2	19351.5	0.08	0.35	0.96	0.96	4.00	3155.5	25488.2	28010.1	0.12	0.52	0.95	0.99
	4.50	1451.0	22283.9	24488.8	0.07	0.31	0.92	0.92	4.50	3235.7	32258.0	35449.7	0.10	0.47	0.91	0.95
+0.5	1.20	1432.3	2329.2	2559.7	0.61	0.90	1.03	1.06	1.10	1828.4	2511.4	2759.9	0.73	1.00	1.04	1.06
	1.70	1586.5	4674.7	5137.3	0.34	0.66	0.95	1.00	1.60	2323.1	5312.4	5838.0	0.44	0.81	0.97	0.99
	2.20	1637.2	7830.3	8605.0	0.21	0.51	0.89	0.94	2.10	3084.9	9147.8	10052.9	0.34	0.79	1.07	1.09
	2.70	1661.2	11792.6	12959.4	0.14	0.41	0.84	0.91	2.60	3749.5*	14024.2	15411.8	0.27	0.76	1.13	1.16
	3.20	1690.8	16564.9	18203.9	0.10	0.35	0.81	0.88	3.10	4213.0*	19935.2	21907.6	0.21	0.71	1.14	1.18
	3.70	1908.3	22144.0	24335.0	0.09	0.34	0.87	0.97	3.60	4431.2*	26887.1	29547.4	0.16	0.63	1.09	1.13
	4.20	1936.5	28536.4	31359.9	0.07	0.30	0.85	0.95	4.10	4496.8*	34873.5	38324.0	0.13	0.56	1.02	1.07
	4.70	1937.6	35732.3	39267.8	0.05	0.27	0.83	0.93	4.60	4498.7*	43897.7	48241.1	0.10	0.50	0.96	1.00
0	1.20	1432.3	2329.2	2559.7	0.61	0.90	1.03	1.07	1.20	1905.5	2888.8	3174.6	0.66	0.97	1.04	1.05
	1.70	1586.5	4674.7	5137.3	0.34	0.66	0.95	1.03	1.70	2486.1	5800.3	6374.2	0.43	0.84	1.03	1.05
	2.20	1637.2	7830.3	8605.0	0.21	0.51	0.89	0.99	2.20	3190.0	9713.8	10675.0	0.33	0.80	1.11	1.14
	2.70	1661.2	11792.6	12959.4	0.14	0.41	0.84	0.96	2.70	3520.8	14629.3	16076.8	0.24	0.71	1.07	1.10
	3.20	1690.8	16564.9	18203.9	0.10	0.35	0.81	0.94	3.20	3594.4	20550.0	22583.3	0.17	0.60	0.98	1.02
	3.70	1908.3	22144.0	24335.0	0.09	0.34	0.87	1.04	3.70	3631.3	27472.6	30190.9	0.13	0.52	0.91	0.95
	4.20	1936.5	28536.4	31359.9	0.07	0.30	0.85	1.03	4.20	3634.2	35400.5	38903.2	0.10	0.45	0.84	0.88
	4.70	1937.6	35732.3	39267.8	0.05	0.27	0.83	1.01	4.70	3627.1	44330.3	48716.5	0.08	0.40	0.79	0.83
-0.5	1.30	1633.5	2944.1	3235.4	0.55	0.87	1.04	1.10	1.30	2180.7	3884.2	4268.6	0.56	0.88	0.97	0.99
	1.80	1698.8	5640.9	6199.1	0.30	0.62	0.93	1.02	1.80	3060.2	7443.2	8179.6	0.41	0.84	1.06	1.09
	2.30	1725.7	9209.6	10120.8	0.19	0.48	0.85	0.98	2.30	3931.0	12153.7	13356.2	0.32	0.82	1.16	1.19
	2.80	1762.8	13650.1	15000.7	0.13	0.39	0.82	0.96	2.80	4568.6*	18012.6	19794.8	0.25	0.77	1.18	1.22
	3.30	1795.3	18962.5	20838.7	0.09	0.33	0.79	0.95	3.30	4631.6*	25019.8	27495.3	0.19	0.65	1.08	1.13
	3.80	1910.4	25143.4	27631.2	0.08	0.31	0.81	0.99	3.80	4634.8*	33178.6	36461.4	0.14	0.56	1.00	1.04
	4.30	2056.0	32196.2	35381.8	0.06	0.29	0.84	1.05	4.30	4633.4*	42482.6	46685.9	0.11	0.49	0.93	0.97
	4.80	2299.8	40117.5	44086.9	0.06	0.29	0.91	1.16	4.80	4633.4*	52938.1	58176.0	0.09	0.44	0.87	0.91
-1	1.40	1692.7	3532.9	3882.5	0.48	0.80	1.00	1.07	1.40	2521.8	4821.1	5298.2	0.52	0.87	0.99	1.00
	1.90	1745.3	6506.3	7150.0	0.27	0.58	0.90	1.00	1.90	3547.5	8877.8	9756.2	0.40	0.86	1.11	1.13
	2.40	1775.9	10380.7	11407.8	0.17	0.45	0.84	0.97	2.40	4447.0	14164.1	15565.6	0.31	0.83	1.19	1.22
	2.90	1814.2	15156.3	16655.9	0.12	0.38	0.80	0.95	2.90	4535.3	20680.1	22726.3	0.22	0.69	1.07	1.11
	3.40	1946.4	20836.3	22897.9	0.09	0.34	0.82	1.00	3.40	4537.5	28425.8	31238.4	0.16	0.58	0.97	1.01
	3.90	2256.5	27414.1	30126.5	0.08	0.34	0.91	1.14	3.90	4537.5	37401.2	41101.8	0.12	0.50	0.90	0.94
	4.40	2447.1	34893.0	38345.5	0.07	0.32	0.96	1.21	4.40	4537.0	47609.5	52320.1	0.10	0.44	0.84	0.88
	4.90	2621.2	43273.1	47554.7	0.06	0.31	0.99	1.28	4.90	4534.1	59044.2	64886.3	0.08	0.39	0.78	0.82

Table B5: Failure moments and their DSM estimates for SCA and SCB ***C05*** beams

	SCA								*SCB*							
ψ	λ_D	M_u *(kNcm)*	M_y *(kNcm)*	M_p *(kNcm)*	$\frac{M_u}{M_y}$	$\frac{M_u}{M_{nD}}$	$\frac{M_u}{M^*_{nD}}$	$\frac{M_u}{M^{**}_{nD}}$	λ_D	M_u *(kNcm)*	M_y *(kNcm)*	M_p *(kNcm)*	$\frac{M_u}{M_y}$	$\frac{M_u}{M_{nD}}$	$\frac{M_u}{M^*_{nD}}$	$\frac{M_u}{M^{**}_{nD}}$
+1	0.65	752.6	760.9	840.3	0.99	0.99	0.99	0.99	0.65	1092.5	1091.9	1205.9	1.00	1.00	1.00	1.00
	1.15	1651.5	2385.7	2634.9	0.69	0.98	1.10	1.10	1.15	2260.8	3417.4	3774.3	0.66	0.94	0.99	1.01
	1.65	1921.2	4909.0	5421.6	0.39	0.75	1.05	1.05	1.65	2768.9	7032.6	7766.9	0.39	0.75	0.91	0.93
	2.15	2115.9	8335.0	9205.4	0.25	0.61	1.04	1.04	2.15	3449.3	11941.6	13188.6	0.29	0.69	0.94	0.97
	2.65	2248.1	12663.8	13986.1	0.18	0.51	1.02	1.02	2.65	4149.9	18140.2	20034.5	0.23	0.66	0.99	1.02
	3.15	2329.6	17890.9	19759.1	0.13	0.44	1.00	1.00	3.15	4693.7	25632.7	28309.3	0.18	0.62	1.01	1.04
	3.65	2352.5	24020.7	26529.0	0.10	0.38	0.97	0.97	3.65	5052.0	34414.8	38008.5	0.15	0.57	0.99	1.03
	4.15	2352.5	31053.3	34295.9	0.08	0.33	0.93	0.93	4.15	5209.3	44490.8	49136.6	0.12	0.51	0.95	0.99
+0.5	0.75	1315.3	1298.2	1433.7	1.01	1.08	1.04	1.05	0.75	1956.5	1857.0	2050.9	1.05	1.12	1.08	1.10
	1.25	2225.6	3602.3	3978.4	0.62	0.94	1.10	1.12	1.25	3197.5	5154.1	5692.3	0.62	0.94	1.02	1.04
	1.75	2419.7	7058.4	7795.4	0.34	0.69	1.01	1.05	1.75	4158.9	10097.5	11151.9	0.41	0.82	1.03	1.05
	2.25	2546.7	11666.5	12884.7	0.22	0.54	0.96	1.02	2.25	5262.2	16695.9	18439.3	0.32	0.79	1.09	1.12
	2.75	2626.0	17430.9	19251.1	0.15	0.45	0.92	1.00	2.75	6109.7	24936.4	27540.2	0.25	0.73	1.12	1.15
	3.25	2626.0	24343.1	26885.1	0.11	0.38	0.88	0.96	3.25	6610.9	34831.8	38469.0	0.19	0.66	1.09	1.13
	3.75	2626.0	32411.7	35796.2	0.08	0.32	0.84	0.93	3.75	6804.8	46373.6	51216.0	0.15	0.58	1.03	1.07
	4.25	2626.0	41627.9	45974.8	0.06	0.28	0.81	0.91	4.25	6795.3	59561.8	65781.4	0.11	0.51	0.95	1.00
0	0.85	1975.9	1990.3	2198.1	0.99	1.14	1.12	1.12	0.85	3113.9	3116.5	3441.9	1.00	1.15	1.12	1.14
	1.35	2572.4	5016.5	5540.3	0.51	0.83	1.02	1.07	1.35	4607.6	7862.2	8683.2	0.59	0.95	1.06	1.08
	1.85	2712.6	9422.6	10406.5	0.29	0.60	0.92	1.00	1.85	6411.7	14770.1	16312.4	0.43	0.91	1.16	1.19
	2.35	2813.8	15204.3	16791.9	0.19	0.48	0.87	0.98	2.35	7849.9	23831.6	26320.1	0.33	0.85	1.21	1.25
	2.85	2855.4	22361.5	24696.5	0.13	0.39	0.83	0.95	2.85	8797.5*	35046.7	38706.4	0.25	0.78	1.20	1.24
	3.35	3030.5	30898.6	34125.0	0.10	0.35	0.84	0.98	3.35	9023.2*	48424.1	53480.6	0.19	0.67	1.11	1.16
	3.85	3119.4	40811.2	45072.8	0.08	0.31	0.83	0.99	3.85	9032.2*	63959.3	70638.1	0.14	0.58	1.03	1.07
	4.35	3169.5	52099.4	57539.7	0.06	0.28	0.81	0.98	4.35	9030.1*	81652.5	90178.8	0.11	0.51	0.95	1.00
-0.5	0.95	2693.7	3107.9	3432.4	0.87	1.07	1.09	1.11	0.95	2644.9	2974.7	3285.3	0.89	1.10	1.10	1.11
	1.45	3095.3	7243.2	7999.5	0.43	0.73	0.94	1.01	1.45	3509.8	6929.4	7653.0	0.51	0.87	1.00	1.01
	1.95	3159.3	13097.9	14465.6	0.24	0.53	0.84	0.94	1.95	4715.1	12534.8	13843.7	0.38	0.83	1.08	1.10
	2.45	3229.3	20676.4	22835.5	0.16	0.42	0.79	0.91	2.45	5701.5	19790.9	21857.5	0.29	0.78	1.12	1.15
	2.95	3315.6	29978.7	33109.1	0.11	0.35	0.76	0.91	2.95	5692.2	28689.1	31684.8	0.20	0.63	1.00	1.03
	3.45	3597.3	41004.6	45286.4	0.09	0.32	0.79	0.96	3.45	5710.7	39237.9	43335.2	0.15	0.54	0.91	0.94
	3.95	3736.8	53750.1	59362.7	0.07	0.29	0.79	0.98	3.95	5704.4	51437.4	56808.6	0.11	0.46	0.84	0.87
	4.45	3910.4	68219.3	75342.8	0.06	0.27	0.80	1.01	4.45	5694.2	65283.3	72100.3	0.09	0.41	0.78	0.81
-1	1.05	2327.8	2923.1	3228.3	0.80	1.06	1.13	1.16	1.05	4252.3	5497.9	6072.1	0.77	1.03	1.06	1.07
	1.55	2533.4	6370.6	7035.8	0.40	0.72	0.97	1.05	1.55	6218.3	11976.0	13226.5	0.52	0.94	1.11	1.13
	2.05	2672.3	11146.3	12310.3	0.24	0.55	0.91	1.02	2.05	7839.5	20951.5	23139.3	0.37	0.86	1.15	1.18
	2.55	2715.3	17246.1	19047.0	0.16	0.44	0.85	0.99	2.55	8219.9	32416.0	35800.9	0.25	0.71	1.04	1.07
	3.05	2745.0	24674.1	27250.7	0.11	0.37	0.81	0.97	3.05	8255.8	46377.9	51220.8	0.18	0.59	0.93	0.97
	3.55	3273.4	33426.2	36916.6	0.10	0.37	0.92	1.13	3.55	8264.3	62828.8	69389.5	0.13	0.50	0.85	0.89
	4.05	3386.9	43506.4	48049.4	0.08	0.33	0.92	1.15	4.05	8233.4	81772.9	90311.7	0.10	0.43	0.79	0.82
	4.55	3451.4	54910.7	60644.6	0.06	0.30	0.91	1.16	4.55	8255.8	103210	113988	0.08	0.38	0.74	0.77

Table B6: Failure moments and their DSM estimates for SCA and SCB ***C06*** beams

ψ	SCA								SCB							
	λ_D	M_u (kNcm)	M_y (kNcm)	M_p (kNcm)	$\frac{M_u}{M_y}$	$\frac{M_u}{M_{nD}}$	$\frac{M_u}{M^*_{nD}}$	$\frac{M_u}{M^{**}_{nD}}$	λ_D	M_u (kNcm)	M_y (kNcm)	M_p (kNcm)	$\frac{M_u}{M_y}$	$\frac{M_u}{M_{nD}}$	$\frac{M_u}{M^*_{nD}}$	$\frac{M_u}{M^{**}_{nD}}$
+1	0.95	1229.4	1415.5	1574.3	0.87	1.07	1.09	1.09	0.70	1094.7	1109.9	1234.5	0.99	1.01	0.98	1.00
	1.45	1492.6	3295.0	3664.8	0.45	0.77	1.00	1.00	1.20	2041.4	3260.2	3626.1	0.63	0.92	0.99	1.00
	1.95	1691.1	5959.7	6628.5	0.28	0.62	0.99	0.99	1.70	2444.4	6539.8	7273.7	0.37	0.73	0.90	0.92
	2.45	1840.8	9405.5	10461.1	0.20	0.53	0.99	0.99	2.20	3002.6	10952.5	12181.7	0.27	0.67	0.92	0.95
	2.95	1949.4	13636.5	15166.9	0.14	0.46	0.99	0.99	2.70	3569.9	16494.5	18345.6	0.22	0.64	0.96	0.99
	3.45	2014.3	18648.6	20741.5	0.11	0.40	0.97	0.97	3.20	3988.2	23169.6	25769.9	0.17	0.59	0.97	1.00
	3.95	2024.2	24445.9	27189.4	0.08	0.35	0.94	0.94	3.70	4231.7	30977.9	34454.5	0.14	0.54	0.94	0.98
	4.45	2024.2	31028.2	34510.4	0.07	0.31	0.91	0.91	4.20	4348.5	39915.5	44395.1	0.11	0.48	0.90	0.94
+0.5	1.15	1803.0	3074.6	3419.6	0.59	0.83	0.93	0.95	0.80	1958.6	1898.9	2112.0	1.03	1.14	1.11	1.12
	1.65	2232.8	6330.9	7041.5	0.35	0.67	0.95	0.99	1.30	2931.8	5016.0	5579.0	0.58	0.91	1.01	1.03
	2.15	2340.8	10747.5	11953.7	0.22	0.52	0.89	0.95	1.80	3826.5	9618.2	10697.7	0.40	0.82	1.03	1.05
	2.65	2395.7	16328.2	18160.7	0.15	0.42	0.85	0.91	2.30	4812.6	15705.5	17468.1	0.31	0.78	1.09	1.13
	3.15	2430.1	23069.1	25658.1	0.11	0.36	0.81	0.89	2.80	5567.0	23277.9	25890.4	0.24	0.73	1.12	1.15
	3.65	2643.5	30974.1	34450.2	0.09	0.33	0.84	0.93	3.30	5947.0*	32331.5	35960.0	0.18	0.65	1.08	1.12
	4.15	2696.3	40043.1	44537.1	0.07	0.30	0.83	0.93	3.80	6051.5*	42874.1	47685.7	0.14	0.57	1.01	1.05
	4.65	2708.6	50272.4	55914.4	0.05	0.26	0.81	0.91	4.30	6051.5*	54897.8	61058.9	0.11	0.50	0.94	0.98
0	1.15	1803.0	3074.6	3419.6	0.59	0.83	0.93	0.96	0.90	2305.0	2397.8	2666.9	0.96	1.15	1.13	1.15
	1.65	2232.8	6330.9	7041.5	0.35	0.67	0.95	1.01	1.40	3150.4	5797.2	6447.9	0.54	0.90	1.02	1.04
	2.15	2340.8	10747.5	11953.7	0.22	0.52	0.89	0.99	1.90	4166.4	10681.8	11880.6	0.39	0.84	1.08	1.11
	2.65	2395.7	16328.2	18160.7	0.15	0.42	0.85	0.96	2.40	4883.3	17043.7	18956.4	0.29	0.76	1.08	1.12
	3.15	2430.1	23069.1	25658.1	0.11	0.36	0.81	0.94	2.90	5122.6	24882.9	27675.4	0.21	0.65	1.01	1.04
	3.65	2643.5	30974.1	34450.2	0.09	0.33	0.84	1.00	3.40	5181.2	34203.3	38041.9	0.15	0.55	0.93	0.96
	4.15	2696.3	40043.1	44537.1	0.07	0.30	0.83	1.00	3.90	5209.6	45001.1	50051.5	0.12	0.48	0.86	0.89
	4.65	2708.6	50272.4	55914.4	0.05	0.26	0.81	0.99	4.40	5208.7	57280.2	63708.6	0.09	0.42	0.80	0.83
-0.5	1.00	2162.6	2506.1	2787.3	0.86	1.11	1.15	1.17	1.00	2811.3	3372.4	3750.9	0.83	1.07	1.08	1.10
	1.50	2414.8	5634.8	6267.2	0.43	0.75	0.99	1.07	1.50	3784.1	7591.7	8443.7	0.50	0.88	1.02	1.04
	2.00	2505.9	10016.6	11140.7	0.25	0.56	0.91	1.02	2.00	5078.6	13497.2	15012.0	0.38	0.85	1.12	1.14
	2.50	2522.7	15651.4	17407.9	0.16	0.44	0.84	0.98	2.50	6003.7	21085.1	23451.4	0.28	0.78	1.14	1.17
	3.00	2856.0	22539.2	25068.8	0.13	0.41	0.90	1.07	3.00	6197.1	30363.0	33770.6	0.20	0.66	1.05	1.08
	3.50	3105.4	30676.3	34119.0	0.10	0.38	0.93	1.14	3.50	6223.4	41331.0	45969.5	0.15	0.56	0.96	1.00
	4.00	3185.3	40066.3	44562.9	0.08	0.34	0.92	1.15	4.00	6225.7	53981.3	60039.5	0.12	0.49	0.88	0.92
	4.50	3183.8	50709.4	56400.4	0.06	0.30	0.89	1.13	4.50	6225.7	68321.6	75989.2	0.09	0.43	0.83	0.86
-1	1.10	2339.0	3128.7	3479.9	0.75	1.03	1.12	1.16	1.10	3158.7	4405.0	4899.3	0.72	0.99	1.03	1.04
	1.60	2488.5	6621.0	7364.1	0.38	0.70	0.96	1.04	1.60	4469.5	9320.4	10366.5	0.48	0.89	1.07	1.09
	2.10	2584.6	11401.1	12680.6	0.23	0.53	0.89	1.01	2.10	5737.0	16057.5	17859.6	0.36	0.84	1.13	1.16
	2.60	2605.6	17480.7	19442.5	0.15	0.42	0.83	0.97	2.60	5868.1	24616.0	27378.6	0.24	0.68	1.01	1.04
	3.10	2521.5	24848.1	27636.7	0.10	0.34	0.76	0.91	3.10	5891.4	34992.3	38919.4	0.17	0.56	0.90	0.94
	3.60	2864.2	33511.1	37272.0	0.09	0.33	0.83	1.02	3.60	5891.4	47190.1	52486.1	0.12	0.48	0.83	0.86
	4.10	2959.1	43465.8	48343.9	0.07	0.29	0.82	1.03	4.10	5891.4	61209.4	68078.9	0.10	0.42	0.76	0.80
	4.60	3097.7	54712.2	60852.4	0.06	0.27	0.83	1.06	4.60	5891.1	77046.5	85693.2	0.08	0.37	0.71	0.75

Table B7: Failure moments and their DSM estimates for SCA and SCB ***C07*** beams

	SCA								*SCB*							
ψ	λ_D	M_u *(kNcm)*	M_y *(kNcm)*	M_p *(kNcm)*	$\frac{M_u}{M_y}$	$\frac{M_u}{M_{nD}}$	$\frac{M_u}{M^*_{nD}}$	$\frac{M_u}{M^{**}_{nD}}$	λ_D	M_u *(kNcm)*	M_y *(kNcm)*	M_p *(kNcm)*	$\frac{M_u}{M_y}$	$\frac{M_u}{M_{nD}}$	$\frac{M_u}{M^*_{nD}}$	$\frac{M_u}{M^{**}_{nD}}$
+1	0.30	137.8	136.1	150.0	1.01	0.96	0.96	0.96	0.30	209.2	193.1	212.9	1.08	1.03	1.03	1.03
	0.80	903.2	956.7	1054.8	0.94	1.04	1.01	1.01	0.80	1295.0	1373.7	1514.5	0.94	1.04	1.01	1.03
	1.30	1446.4	2523.5	2782.3	0.57	0.90	1.08	1.08	1.30	2013.4	3620.7	3992.0	0.56	0.87	0.96	0.98
	1.80	1610.7	4836.4	5332.3	0.33	0.68	1.02	1.02	1.80	2419.7	6943.0	7654.9	0.35	0.71	0.90	0.92
	2.30	1762.9	7899.7	8709.8	0.22	0.57	1.02	1.02	2.30	3059.0	11336.1	12498.5	0.27	0.69	0.96	0.99
	2.80	1881.3	11704.7	12904.9	0.16	0.49	1.02	1.02	2.80	3677.7	16800.0	18522.7	0.22	0.67	1.02	1.06
	3.30	1957.9	16260.2	17927.6	0.12	0.43	1.00	1.00	3.30	4113.8	23339.2	25732.5	0.18	0.62	1.03	1.07
	3.80	1957.9	21561.8	23772.8	0.09	0.37	0.96	0.96	3.80	4318.7	30944.9	34118.0	0.14	0.56	1.00	1.04
+0.5	0.40	322.1	307.2	338.7	1.05	1.01	1.01	1.01	0.40	506.9	447.7	493.6	1.13	1.09	1.09	1.09
	0.90	1455.3	1549.2	1708.1	0.94	1.12	1.12	1.12	0.90	2137.7	2264.6	2496.8	0.94	1.12	1.11	1.13
	1.40	1893.8	3748.0	4132.3	0.51	0.84	1.06	1.09	1.40	2884.7	5477.1	6038.8	0.53	0.87	0.99	1.01
	1.90	2059.3	6899.1	7606.5	0.30	0.64	1.00	1.05	1.90	3951.5	10085.3	11119.4	0.39	0.84	1.09	1.11
	2.40	2155.6	11011.3	12140.4	0.20	0.52	0.96	1.03	2.40	4974.1	16093.5	17743.7	0.31	0.82	1.17	1.20
	2.90	2191.8	16075.9	17724.3	0.14	0.43	0.91	0.99	2.90	5816.6*	23497.2	25906.7	0.25	0.78	1.21	1.25
	3.40	2234.2	22097.2	24363.1	0.10	0.37	0.89	0.98	3.40	6285.4*	32301.0	35613.2	0.19	0.71	1.19	1.23
	3.90	2234.2	29075.3	32056.7	0.08	0.32	0.85	0.95	3.90	6385.2*	42500.4	46858.5	0.15	0.62	1.11	1.16
0	0.50	603.4	574.9	633.9	1.05	1.02	1.02	1.02	0.50	1007.8	886.5	977.4	1.14	1.11	1.11	1.11
	1.00	1923.4	2304.1	2540.3	0.83	1.07	1.11	1.13	1.00	2978.7	3546.1	3909.7	0.84	1.08	1.09	1.11
	1.50	2219.5	5183.1	5714.6	0.43	0.75	0.99	1.05	1.50	4231.1	7978.7	8796.8	0.53	0.93	1.09	1.11
	2.00	2284.3	9216.3	10161.4	0.25	0.56	0.90	0.99	2.00	5694.3	14184.4	15638.8	0.40	0.90	1.19	1.22
	2.50	2349.3	14399.4	15875.9	0.16	0.45	0.85	0.96	2.50	6896.9*	22163.1	24435.7	0.31	0.85	1.24	1.28
	3.00	2398.3	20736.7	22863.1	0.12	0.37	0.82	0.95	3.00	7751.9*	31914.8	35187.4	0.24	0.79	1.25	1.29
	3.50	2511.7	28223.9	31118.0	0.09	0.33	0.82	0.97	3.50	7985.6*	43444.0	47898.8	0.18	0.69	1.17	1.22
	4.00	2633.1	36865.3	40645.5	0.07	0.30	0.83	0.99	4.00	7990.9*	56741.8	62560.2	0.14	0.60	1.08	1.13
-0.5	0.60	951.5	948.0	1045.2	1.00	0.99	0.99	0.99	0.60	1655.0	1483.4	1635.5	1.12	1.10	1.10	1.10
	1.10	2345.5	3181.8	3508.1	0.74	1.01	1.10	1.14	1.10	3626.9	4985.6	5496.8	0.73	1.00	1.04	1.06
	1.60	2487.3	6732.3	7422.6	0.37	0.69	0.94	1.02	1.60	5305.0	10546.1	11627.5	0.50	0.93	1.12	1.14
	2.10	2566.4	11595.0	12784.0	0.22	0.52	0.87	0.98	2.10	6850.1*	18169.3	20032.4	0.38	0.88	1.19	1.22
	2.60	2580.8	17774.3	19596.9	0.15	0.41	0.81	0.95	2.60	8072.7*	27855.2	30711.5	0.29	0.82	1.22	1.26
	3.10	2659.0	25265.9	27856.7	0.11	0.35	0.79	0.95	3.10	8667.7*	39595.1	43655.2	0.22	0.73	1.18	1.22
	3.60	2659.0	34074.1	37568.1	0.08	0.30	0.75	0.92	3.60	8719.6*	53402.0	58877.9	0.16	0.63	1.08	1.12
	4.10	2659.0	44194.5	48726.2	0.06	0.26	0.73	0.91	4.10	8724.1*	69262.9	76365.2	0.13	0.55	1.00	1.04
-1	0.70	1112.3	1070.8	1180.7	1.04	1.06	1.04	1.04	0.70	1835.7	1685.3	1858.1	1.09	1.11	1.08	1.10
	1.20	1855.8	3151.1	3474.2	0.59	0.87	0.99	1.03	1.20	3167.4	4950.5	5458.1	0.64	0.94	1.01	1.02
	1.70	2187.5	6319.8	6967.8	0.35	0.68	0.97	1.06	1.70	4624.3	9931.7	10950.1	0.47	0.91	1.12	1.14
	2.20	2221.6	10585.6	11671.1	0.21	0.51	0.89	1.01	2.20	6001.3	16633.3	18338.9	0.36	0.88	1.21	1.25
	2.70	2294.9	15944.2	17579.2	0.14	0.42	0.86	1.01	2.70	6511.2	25050.8	27619.6	0.26	0.76	1.15	1.19
	3.20	2377.4	22400.1	24697.0	0.11	0.36	0.84	1.01	3.20	6542.8	35188.8	38797.1	0.19	0.64	1.04	1.08
	3.70	2405.2	29944.3	33014.8	0.08	0.32	0.81	1.00	3.70	6547.3	47042.8	51866.6	0.14	0.55	0.96	1.00
	4.20	2448.5	38585.7	42542.3	0.06	0.28	0.80	1.01	4.20	6547.3	60617.1	66832.8	0.11	0.48	0.89	0.93

Table B8: Failure moments and their DSM estimates for SCA and SCB ***C08*** beams

	SCA								*SCB*							
ψ	λ_D	M_u *(kNcm)*	M_y *(kNcm)*	M_p *(kNcm)*	$\frac{M_u}{M_y}$	$\frac{M_u}{M_{nD}}$	$\frac{M_u}{M^*_{nD}}$	$\frac{M_u}{M^{**}_{nD}}$	λ_D	M_u *(kNcm)*	M_y *(kNcm)*	M_p *(kNcm)*	$\frac{M_u}{M_y}$	$\frac{M_u}{M_{nD}}$	$\frac{M_u}{M^*_{nD}}$	$\frac{M_u}{M^{**}_{nD}}$
+1	0.60	360.4	360.3	393.9	1.00	0.99	0.99	0.99	0.60	537.6	517.4	565.6	1.04	1.03	1.03	1.03
	1.10	925.2	1205.7	1318.1	0.77	1.06	1.15	1.15	1.10	1229.9	1736.9	1898.8	0.71	0.97	1.01	1.03
	1.60	1088.0	2549.9	2787.6	0.43	0.79	1.09	1.09	1.60	1467.4	3677.1	4019.8	0.40	0.74	0.89	0.91
	2.10	1260.6	4397.7	4807.6	0.29	0.67	1.13	1.13	2.10	1971.1	6333.2	6923.6	0.31	0.73	0.98	1.01
	2.60	1290.8	6739.7	7368.0	0.19	0.54	1.07	1.07	2.60	2418.8	9705.4	10610.1	0.25	0.71	1.05	1.08
	3.10	1337.9	9580.7	10473.7	0.14	0.47	1.05	1.05	3.10	2924.4*	13798.2	15084.4	0.21	0.71	1.14	1.18
	3.60	1386.2	12920.5	14124.9	0.11	0.41	1.04	1.04	3.60	3346.4*	18611.6	20346.5	0.18	0.69	1.19	1.24
	4.10	1481.8	16759.3	18321.4	0.09	0.38	1.07	1.07	4.10	3427.4*	24136.5	26386.3	0.14	0.62	1.13	1.18
+0.5	0.70	654.8	623.6	681.8	1.05	1.07	1.05	1.06	0.70	976.2	910.0	994.9	1.07	1.10	1.07	1.09
	1.20	1225.3	1829.3	1999.8	0.67	0.98	1.13	1.15	1.20	1716.1	2674.6	2924.0	0.64	0.94	1.01	1.03
	1.70	1320.9	3677.1	4019.8	0.36	0.70	1.01	1.05	1.70	2366.6	5367.8	5868.1	0.44	0.86	1.06	1.08
	2.20	1383.2	6157.7	6731.7	0.22	0.55	0.95	1.01	2.20	3180.5*	8989.4	9827.3	0.35	0.86	1.19	1.22
	2.70	1383.2	9271.2	10135.4	0.15	0.44	0.89	0.96	2.70	3934.4*	13539.5	14801.6	0.29	0.85	1.29	1.33
	3.20	1383.2	13022.1	14236.0	0.11	0.36	0.84	0.92	3.20	4568.2*	19013.5	20785.8	0.24	0.83	1.35	1.40
	3.70	1383.2	17410.6	19033.5	0.08	0.31	0.80	0.89	3.70	5023.8*	25420.7	27790.2	0.20	0.78	1.36	1.41
	4.20	1383.2	22436.5	24527.9	0.06	0.27	0.78	0.87	4.20	5210.0*	32756.3	35809.6	0.16	0.70	1.31	1.37
0	0.80	979.8	933.1	1020.1	1.05	1.16	1.13	1.13	0.80	1536.9	1478.2	1616.0	1.04	1.15	1.11	1.13
	1.30	1382.1	2466.8	2696.7	0.56	0.88	1.05	1.10	1.30	2314.3	3908.0	4272.3	0.59	0.93	1.02	1.04
	1.80	1456.1	4734.9	5176.3	0.31	0.63	0.94	1.02	1.80	3333.3*	7492.7	8191.1	0.44	0.91	1.15	1.18
	2.30	1487.5	7728.3	8448.7	0.19	0.49	0.88	0.98	2.30	4348.7*	12232.2	13372.4	0.36	0.90	1.27	1.31
	2.80	1505.7	11451.5	12519.0	0.13	0.40	0.83	0.95	2.80	5224.3*	18126.6	19816.2	0.29	0.88	1.35	1.39
	3.30	1505.7	15909.3	17392.2	0.09	0.33	0.79	0.92	3.30	5943.9*	25180.5	27527.6	0.24	0.83	1.38	1.44
	3.80	1505.7	21096.9	23063.4	0.07	0.29	0.76	0.90	3.80	6402.2*	33389.2	36501.4	0.19	0.77	1.37	1.43
	4.30	1505.7	27009.7	29527.4	0.06	0.25	0.73	0.88	4.30	6456.7*	42752.7	46737.8	0.15	0.68	1.28	1.34
-0.5	0.90	1204.5	1275.0	1393.8	0.94	1.13	1.12	1.13	0.90	2099.7	2198.8	2403.8	0.95	1.14	1.12	1.14
	1.40	1478.3	3085.8	3373.4	0.48	0.80	1.00	1.07	1.40	3057.4	5317.0	5812.6	0.58	0.96	1.08	1.10
	1.90	1530.2	5686.5	6216.6	0.27	0.58	0.90	1.00	1.90	4265.7*	9793.2	10706.0	0.44	0.94	1.21	1.24
	2.40	1560.1	9067.9	9913.2	0.17	0.45	0.84	0.97	2.40	5319.1*	15627.5	17084.2	0.34	0.90	1.29	1.33
	2.90	1589.1	13243.9	14478.4	0.12	0.38	0.80	0.95	2.90	6227.3*	22815.3	24942.0	0.27	0.86	1.34	1.38
	3.40	1629.1	18205.1	19902.1	0.09	0.33	0.78	0.95	3.40	6972.6*	31361.2	34284.5	0.22	0.81	1.36	1.41
	3.90	1869.7	23951.7	26184.3	0.08	0.32	0.86	1.07	3.90	7249.5*	41260.7	45106.6	0.18	0.73	1.30	1.36
	4.40	2104.2	30483.6	33325.0	0.07	0.32	0.94	1.19	4.40	7262.6*	52522.8	57418.5	0.14	0.64	1.21	1.27
-1	1.00	1580.0	1681.5	1838.2	0.94	1.20	1.25	1.28	1.00	2700.5	3071.9	3358.3	0.88	1.13	1.14	1.16
	1.50	1732.7	3787.9	4141.0	0.46	0.80	1.06	1.14	1.50	3832.5*	6915.3	7559.9	0.55	0.97	1.14	1.16
	2.00	1605.6	6730.5	7357.9	0.24	0.54	0.87	0.97	2.00	5061.6*	12292.3	13438.1	0.41	0.93	1.22	1.25
	2.50	1635.4	10518.4	11498.9	0.16	0.43	0.81	0.94	2.50	6166.5*	19207.5	20997.9	0.32	0.88	1.28	1.32
	3.00	1669.8	15147.1	16559.0	0.11	0.36	0.78	0.93	3.00	7107.9*	27661.1	30239.4	0.26	0.83	1.32	1.37
	3.50	1719.1	20611.9	22533.1	0.08	0.31	0.77	0.94	3.50	7674.0*	37648.3	41157.5	0.20	0.76	1.30	1.35
	4.00	1819.9	26922.0	29431.4	0.07	0.29	0.78	0.98	4.00	7906.0*	49173.7	53757.3	0.16	0.68	1.23	1.29
	4.50	1933.7	34077.5	37253.9	0.06	0.27	0.80	1.02	4.50	7898.4*	62237.4	68038.7	0.13	0.60	1.15	1.20

Table B9: Failure moments and their DSM estimates for SCA and SCB ***C09*** beams

	SCA								*SCB*							
ψ	λ_D	M_u *(kNcm)*	M_y *(kNcm)*	M_p *(kNcm)*	$\frac{M_u}{M_y}$	$\frac{M_u}{M_{nD}}$	$\frac{M_u}{M^*_{nD}}$	$\frac{M_u}{M^{**}_{nD}}$	λ_D	M_u *(kNcm)*	M_y *(kNcm)*	M_p *(kNcm)*	$\frac{M_u}{M_y}$	$\frac{M_u}{M_{nD}}$	$\frac{M_u}{M^*_{nD}}$	$\frac{M_u}{M^{**}_{nD}}$
+1	0.35	168.1	166.3	185.5	1.01	0.96	0.96	0.96	0.35	316.5	290.0	323.4	1.09	1.03	1.03	1.03
	0.85	917.6	981.0	1093.9	0.94	1.07	1.05	1.05	0.85	1494.2	1714.5	1912.0	0.87	1.00	0.98	0.99
	1.35	1370.3	2478.0	2763.4	0.55	0.89	1.10	1.10	1.35	2072.6	4329.0	4827.6	0.48	0.77	0.86	0.88
	1.85	1529.7	4648.9	5184.3	0.33	0.69	1.06	1.05	1.85	2874.4	8129.1	9065.4	0.35	0.74	0.95	0.97
	2.35	1663.1	7506.4	8371.0	0.22	0.57	1.05	1.05	2.35	3702.7	13119.1	14630.2	0.28	0.73	1.04	1.07
	2.85	1757.8	11037.8	12309.2	0.16	0.49	1.04	1.04	2.85	4463.2*	19294.9	21517.3	0.23	0.71	1.11	1.14
	3.35	1805.3	15251.6	17008.4	0.12	0.42	1.01	1.01	3.35	5067.5*	26660.5	29731.3	0.19	0.68	1.14	1.18
	3.85	1813.5	20143.6	22463.8	0.09	0.37	0.98	0.98	3.85	5425.7*	35211.8	39267.6	0.15	0.63	1.12	1.17
+0.5	0.45	363.9	349.7	390.0	1.04	1.00	1.00	1.00	0.45	578.8	507.5	566.0	1.14	1.10	1.10	1.10
	0.95	1454.2	1565.3	1745.5	0.93	1.15	1.17	1.18	0.95	2040.1	2264.7	2525.6	0.90	1.11	1.11	1.13
	1.45	1766.1	3642.3	4061.8	0.48	0.83	1.07	1.10	1.45	2638.6	5271.5	5878.7	0.50	0.86	0.99	1.00
	1.95	1905.3	6589.4	7348.4	0.29	0.64	1.01	1.06	1.95	3490.9	9536.5	10635.0	0.37	0.80	1.05	1.08
	2.45	1994.4	10406.6	11605.3	0.19	0.52	0.97	1.04	2.45	4331.4	15051.2	16784.8	0.29	0.77	1.12	1.15
	2.95	2030.6	15085.3	16822.9	0.13	0.43	0.93	1.01	2.95	4942.3*	21819.7	24333.0	0.23	0.72	1.14	1.18
	3.45	2072.6	20629.8	23006.0	0.10	0.37	0.90	0.99	3.45	5234.9*	29846.5	33284.2	0.18	0.65	1.09	1.14
	3.95	2072.6	27044.4	30159.4	0.08	0.32	0.87	0.97	3.95	5339.9*	39122.8	43629.1	0.14	0.57	1.03	1.07
0	0.55	660.2	627.0	699.2	1.05	1.03	1.03	1.03	0.55	1089.6	946.8	1055.9	1.15	1.13	1.13	1.13
	1.05	1828.2	2281.8	2544.6	0.80	1.06	1.13	1.16	1.05	2732.1	3450.4	3847.8	0.79	1.05	1.08	1.09
	1.55	2019.5	4973.0	5545.8	0.41	0.73	0.99	1.05	1.55	3751.9	7519.2	8385.3	0.50	0.90	1.07	1.09
	2.05	2121.2	8700.6	9702.8	0.24	0.56	0.92	1.02	2.05	4950.7	13153.3	14668.3	0.38	0.86	1.15	1.18
	2.55	2157.1	13464.6	15015.5	0.16	0.45	0.87	0.98	2.55	5910.6*	20352.6	22696.8	0.29	0.81	1.19	1.23
	3.05	2194.5	19260.7	21479.2	0.11	0.37	0.83	0.96	3.05	6462.4*	29117.2	32470.9	0.22	0.73	1.17	1.21
	3.55	2294.3	26093.3	29098.7	0.09	0.33	0.83	0.98	3.55	6564.8*	39447.0	43990.6	0.17	0.63	1.08	1.12
	4.05	2449.4	33962.2	37874.0	0.07	0.31	0.85	1.02	4.05	6567.6*	51337.8	57251.0	0.13	0.55	1.00	1.04
-0.5	0.65	1001.0	981.0	1093.9	1.02	1.02	1.02	1.02	0.65	1168.9	1066.3	1189.1	1.10	1.09	1.09	1.09
	1.15	2124.9	3070.8	3424.5	0.69	0.98	1.10	1.14	1.15	2322.6	3339.5	3724.1	0.70	0.99	1.05	1.06
	1.65	2196.1	6325.0	7053.5	0.35	0.66	0.93	1.01	1.65	2998.5	6870.9	7662.3	0.44	0.83	1.01	1.03
	2.15	2263.7	10739.3	11976.2	0.21	0.50	0.86	0.97	2.15	3930.2	11664.8	13008.3	0.34	0.81	1.10	1.13
	2.65	2304.2	16317.9	18197.4	0.14	0.41	0.81	0.95	2.65	4540.1	17721.1	19762.2	0.26	0.74	1.11	1.14
	3.15	2366.3	23056.6	25712.3	0.10	0.35	0.79	0.95	3.15	4541.1	25039.8	27923.9	0.18	0.61	1.00	1.03
	3.65	2555.9	30955.4	34520.9	0.08	0.32	0.82	1.00	3.65	4545.2	33621.0	37493.5	0.14	0.53	0.91	0.95
	4.15	2765.7	40018.5	44627.9	0.07	0.30	0.85	1.07	4.15	4545.2	43460.4	48466.2	0.10	0.46	0.84	0.88
-1	0.75	1159.0	1130.2	1260.4	1.03	1.09	1.06	1.06	0.75	1767.5	1659.1	1850.2	1.07	1.13	1.10	1.11
	1.25	1893.6	3134.8	3495.8	0.60	0.92	1.07	1.13	1.25	2800.1	4606.2	5136.8	0.61	0.92	1.00	1.02
	1.75	1970.4	6145.9	6853.8	0.32	0.64	0.94	1.04	1.75	3940.4	9029.0	10069.0	0.44	0.87	1.09	1.11
	2.25	2017.5	10163.5	11334.1	0.20	0.50	0.87	1.00	2.25	5021.8	14923.2	16642.1	0.34	0.84	1.17	1.20
	2.75	2071.7	15183.4	16932.3	0.14	0.41	0.84	0.99	2.75	5122.6	22293.2	24860.9	0.23	0.69	1.05	1.08
	3.25	2118.1	21205.6	23648.1	0.10	0.35	0.81	0.98	3.25	5130.5	31138.8	34725.4	0.16	0.57	0.95	0.98
	3.75	2242.4	28230.0	31481.6	0.08	0.32	0.82	1.02	3.75	5130.5	41455.8	46230.8	0.12	0.49	0.87	0.90
	4.25	2282.7	36261.0	40437.6	0.06	0.28	0.81	1.02	4.25	5131.4	53248.5	59381.8	0.10	0.43	0.81	0.84

Table B10: Failure moments and their DSM estimates for SCA and SCB ***C10*** beams

ψ	SCA								SCB							
	λ_D	M_u (kNcm)	M_y (kNcm)	M_p (kNcm)	$\frac{M_u}{M_y}$	$\frac{M_u}{M_{nD}}$	$\frac{M_u}{M^*_{nD}}$	$\frac{M_u}{M^{**}_{nD}}$	λ_D	M_u (kNcm)	M_y (kNcm)	M_p (kNcm)	$\frac{M_u}{M_y}$	$\frac{M_u}{M_{nD}}$	$\frac{M_u}{M^*_{nD}}$	$\frac{M_u}{M^{**}_{nD}}$
+1	0.90	796.6	862.6	947.1	0.92	1.10	1.10	1.10	0.90	1031.5	1238.7	1360.0	0.83	0.99	0.98	0.99
	1.40	1083.1	2081.3	2285.1	0.52	0.86	1.09	1.09	1.40	1443.5	2994.0	3287.2	0.48	0.80	0.91	0.92
	1.90	1201.3	3836.5	4212.3	0.31	0.67	1.05	1.05	1.90	1879.2	5516.6	6056.9	0.34	0.73	0.94	0.97
	2.40	1317.4	6118.4	6717.6	0.22	0.57	1.05	1.05	2.40	2431.0	8801.4	9663.5	0.28	0.73	1.04	1.08
	2.90	1403.3	8931.8	9806.6	0.16	0.49	1.05	1.05	2.90	2911.5	12853.6	14112.5	0.23	0.71	1.11	1.15
	3.40	1472.3	12276.9	13479.3	0.12	0.44	1.05	1.05	3.40	3311.9*	17668.1	19398.5	0.19	0.68	1.15	1.19
	3.90	1513.1	16158.6	17741.1	0.09	0.39	1.04	1.04	3.90	3623.2*	23244.8	25521.5	0.16	0.64	1.15	1.20
	4.40	1541.0	20566.8	22581.1	0.07	0.35	1.02	1.02	4.40	3692.3*	29588.9	32486.9	0.12	0.58	1.09	1.15
+0.5	1.10	1394.1	1920.8	2108.9	0.73	1.00	1.09	1.11	1.00	1670.8	2001.0	2197.0	0.83	1.07	1.08	1.10
	1.60	1526.3	4057.2	4454.6	0.38	0.70	0.96	1.00	1.50	2217.2	4498.5	4939.1	0.49	0.87	1.01	1.03
	2.10	1614.7	6991.0	7675.7	0.23	0.54	0.91	0.96	2.00	3108.3	7999.0	8782.5	0.39	0.87	1.15	1.18
	2.60	1641.0	10717.2	11766.9	0.15	0.43	0.86	0.92	2.50	3944.0*	12497.6	13721.6	0.32	0.87	1.26	1.30
	3.10	1665.6	15235.8	16728.0	0.11	0.36	0.82	0.90	3.00	4675.8*	17994.1	19756.4	0.26	0.84	1.33	1.38
	3.60	1710.8	20546.7	22559.1	0.08	0.32	0.80	0.89	3.50	5273.1*	24493.6	26892.5	0.22	0.80	1.37	1.42
	4.10	1768.5	26650.1	29260.2	0.07	0.29	0.80	0.89	4.00	5592.2*	31991.1	35124.4	0.17	0.74	1.34	1.40
	4.60	1819.2	33550.8	36836.8	0.05	0.26	0.80	0.90	4.50	5698.0*	40486.7	44452.0	0.14	0.67	1.27	1.33
0	1.10	1394.1	1920.8	2108.9	0.73	1.00	1.09	1.12	1.10	1586.6	2116.4	2323.6	0.75	1.03	1.07	1.09
	1.60	1526.3	4057.2	4454.6	0.38	0.70	0.96	1.03	1.60	2034.4	4478.5	4917.1	0.45	0.84	1.01	1.03
	2.10	1614.7	6991.0	7675.7	0.23	0.54	0.91	1.00	2.10	2679.5	7718.2	8474.1	0.35	0.81	1.10	1.13
	2.60	1641.0	10717.2	11766.9	0.15	0.43	0.86	0.97	2.60	3086.4	11830.5	12989.2	0.26	0.74	1.10	1.13
	3.10	1665.6	15235.8	16728.0	0.11	0.36	0.82	0.95	3.10	3243.4	16820.5	18468.0	0.19	0.64	1.04	1.07
	3.60	1710.8	20546.7	22559.1	0.08	0.32	0.80	0.95	3.60	3334.9	22683.2	24904.8	0.15	0.56	0.97	1.01
	4.10	1768.5	26650.1	29260.2	0.07	0.29	0.80	0.96	4.10	3334.9	29418.4	32299.7	0.11	0.49	0.90	0.94
	4.60	1819.2	33550.8	36836.8	0.05	0.26	0.80	0.97	4.60	3374.1	37031.3	40658.2	0.09	0.44	0.85	0.89
-0.5	1.20	1588.9	2472.4	2714.6	0.64	0.94	1.08	1.13	1.20	1687.4	2632.9	2890.8	0.64	0.94	1.01	1.02
	1.70	1674.4	4959.9	5445.7	0.34	0.66	0.95	1.04	1.70	2221.0	5285.9	5803.6	0.42	0.82	1.01	1.03
	2.20	1705.5	8305.0	9118.4	0.21	0.50	0.87	0.99	2.20	3004.1	8851.6	9718.5	0.34	0.83	1.14	1.17
	2.70	1733.7	12512.6	13738.1	0.14	0.41	0.82	0.97	2.70	3662.4	13330.1	14635.6	0.27	0.81	1.22	1.26
	3.20	1772.3	17572.8	19293.9	0.10	0.35	0.80	0.96	3.20	3932.5	18726.3	20560.3	0.21	0.72	1.18	1.22
	3.70	1902.1	23495.6	25796.8	0.08	0.32	0.82	1.01	3.70	3972.9	25035.2	27487.2	0.16	0.62	1.09	1.14
	4.20	2121.4	30276.0	33241.2	0.07	0.31	0.88	1.11	4.20	3979.8	32256.9	35416.2	0.12	0.55	1.01	1.06
	4.70	2310.5	37908.9	41621.7	0.06	0.30	0.93	1.19	4.70	3972.9	40391.4	44347.3	0.10	0.48	0.95	0.99
-1	1.30	1660.6	2999.0	3292.7	0.55	0.87	1.04	1.10	0.90	1031.5	1238.7	1360.0	0.83	0.86	0.95	0.97
	1.80	1732.8	5752.3	6315.7	0.30	0.62	0.93	1.02	1.40	1443.5	2994.0	3287.2	0.48	0.82	1.03	1.05
	2.30	1756.9	9388.2	10307.7	0.19	0.48	0.85	0.98	1.90	1879.2	5516.6	6056.9	0.34	0.84	1.18	1.21
	2.80	1792.4	13916.8	15279.8	0.13	0.39	0.81	0.96	2.40	2431.0	8801.4	9663.5	0.28	0.78	1.19	1.23
	3.30	1865.7	19333.1	21226.6	0.10	0.34	0.80	0.98	2.90	2911.5	12853.6	14112.5	0.23	0.71	1.17	1.22
	3.80	2084.4	25632.0	28142.4	0.08	0.33	0.86	1.07	3.40	3311.9*	17668.1	19398.5	0.19	0.61	1.07	1.12
	4.30	2271.1	32823.6	36038.4	0.07	0.31	0.91	1.15	3.90	3623.2*	23244.8	25521.5	0.16	0.53	1.00	1.04
	4.80	2447.6	40897.9	44903.5	0.06	0.30	0.95	1.22	4.40	3692.3*	29588.9	32486.9	0.12	0.47	0.94	0.98

Table B11: Failure moments and their DSM estimates for SCA and SCB ***C11*** beams

	SCA								SCB							
ψ	λ_D	M_u (kNcm)	M_y (kNcm)	M_p (kNcm)	$\frac{M_u}{M_y}$	$\frac{M_u}{M_{nD}}$	$\frac{M_u}{M^*_{nD}}$	$\frac{M_u}{M^{**}_{nD}}$	λ_D	M_u (kNcm)	M_y (kNcm)	M_p (kNcm)	$\frac{M_u}{M_y}$	$\frac{M_u}{M_{nD}}$	$\frac{M_u}{M^*_{nD}}$	$\frac{M_u}{M^{**}_{nD}}$
+1	0.45	424.6	419.7	455.5	1.01	0.98	0.98	0.98	0.45	614.7	548.9	595.6	1.12	1.09	1.09	1.09
	0.95	1783.5	1872.6	2032.0	0.95	1.18	1.20	1.20	0.95	2022.1	2429.6	2636.4	0.83	1.03	1.03	1.04
	1.45	2283.4	4358.7	4729.7	0.52	0.90	1.15	1.15	1.45	2780.6	5666.4	6148.6	0.49	0.84	0.97	0.98
	1.95	2563.6	7886.1	8557.3	0.33	0.71	1.13	1.13	1.95	3752.4	10243.1	11114.9	0.37	0.81	1.05	1.08
	2.45	2746.7	12446.6	13506.0	0.22	0.59	1.12	1.12	2.45	4730.2	16167.7	17543.8	0.29	0.79	1.14	1.17
	2.95	2912.0	18048.4	19584.6	0.16	0.51	1.11	1.11	2.95	4688.1	23440.4	25435.4	0.20	0.64	1.00	1.04
	3.45	2971.5	24683.4	26784.3	0.12	0.44	1.08	1.08	3.45	4488.5	32061.0	34789.8	0.14	0.52	0.87	0.91
	3.95	3003.8	32359.7	35113.8	0.09	0.39	1.05	1.05	3.95	7389.8	42029.6	45606.8	0.18	0.74	1.32	1.38
+0.5	0.55	779.7	742.6	805.8	1.05	1.03	1.03	1.03	0.55	1142.3	1033.2	1121.1	1.11	1.09	1.09	1.09
	1.05	2161.6	2712.1	2942.9	0.80	1.06	1.13	1.14	1.05	3024.7	3777.6	4099.1	0.80	1.06	1.09	1.11
	1.55	2417.7	5908.5	6411.4	0.41	0.74	1.00	1.03	1.55	4218.4	8225.1	8925.2	0.51	0.93	1.10	1.12
	2.05	2545.2	10331.8	11211.2	0.25	0.57	0.93	0.99	2.05	5942.4	14391.9	15616.9	0.41	0.95	1.26	1.30
	2.55	2672.8	15990.1	17351.1	0.17	0.47	0.90	0.97	2.55	7123.8	22261.9	24156.6	0.32	0.89	1.31	1.35
	3.05	2705.5	22875.4	24822.3	0.12	0.39	0.86	0.94	3.05	8926.1	31851.1	34562.0	0.28	0.92	1.47	1.52
	3.55	2705.5	30987.5	33624.8	0.09	0.33	0.82	0.91	3.55	9974.2	43151.6	46824.3	0.23	0.87	1.50	1.56
	4.05	2705.5	40326.5	43758.7	0.07	0.29	0.79	0.88	4.05	10469.7	56163.3	60943.4	0.19	0.80	1.46	1.52
0	0.65	1213.4	1146.2	1243.7	1.06	1.06	1.06	1.06	0.65	2034.1	1816.1	1970.7	1.12	1.12	1.12	1.12
	1.15	2725.4	3583.9	3888.9	0.76	1.08	1.21	1.24	1.15	4029.8	5682.5	6166.2	0.71	1.01	1.07	1.08
	1.65	2827.2	7385.7	8014.3	0.38	0.73	1.03	1.10	1.65	5430.6	11704.0	12700.2	0.46	0.88	1.07	1.09
	2.15	2886.8	12543.5	13611.1	0.23	0.55	0.94	1.04	2.15	6707.5	19872.7	21564.0	0.34	0.81	1.10	1.13
	2.65	2933.2	19049.3	20670.7	0.15	0.44	0.89	1.01	2.65	7549.1	30196.4	32766.5	0.25	0.72	1.08	1.12
	3.15	2978.3	26919.3	29210.4	0.11	0.37	0.85	0.99	3.15	8531.8	42659.2	46290.0	0.20	0.68	1.10	1.14
	3.65	3046.9	36145.3	39221.7	0.08	0.33	0.83	0.99	3.65	8591.6	57277.2	62152.1	0.15	0.58	1.01	1.05
	4.15	3769.6	46727.4	50704.4	0.08	0.35	0.99	1.20	4.15	7405.0	74050.3	80352.8	0.10	0.44	0.81	0.84
-0.5	0.75	1766.8	1783.9	1935.7	0.99	1.05	1.02	1.02	0.75	3128.9	2954.3	3205.7	1.06	1.12	1.09	1.11
	1.25	2871.1	4956.1	5377.9	0.58	0.88	1.03	1.08	1.25	5547.6*	8192.8	8890.1	0.68	1.03	1.12	1.13
	1.75	2984.8	9718.4	10545.5	0.31	0.61	0.90	0.99	1.75	7962.6*	16062.8	17429.9	0.50	0.99	1.24	1.26
	2.25	3025.3	16062.8	17429.9	0.19	0.47	0.83	0.94	2.25	10651*	26556.1	28816.3	0.40	1.00	1.39	1.43
	2.75	3108.5	23997.3	26039.8	0.13	0.39	0.79	0.93	2.75	12712.9	39672.7	43049.3	0.32	0.96	1.46	1.51
	3.25	3208.7	33513.9	36366.3	0.10	0.33	0.78	0.94	3.25	14447.6	55404.5	60120.1	0.26	0.91	1.50	1.55
	3.75	3613.6	44620.7	48418.4	0.08	0.32	0.84	1.03	3.75	15459.4	73767.8	80046.2	0.21	0.83	1.47	1.53
	4.25	3726.6	57317.5	62195.9	0.07	0.29	0.83	1.05	4.25	15562*	94746.3	102810	0.16	0.74	1.37	1.43
-1	0.85	2849.3	2849.3	3091.8	1.00	1.15	1.13	1.13	0.85	4154.4*	4278.0	4642.1	0.97	1.11	1.09	1.11
	1.35	3521.2	7191.9	7804.0	0.49	0.79	0.97	1.03	1.35	6697.7*	10783.9	11701.7	0.62	1.00	1.12	1.14
	1.85	3692.5	13504.0	14653.4	0.27	0.57	0.88	0.97	1.85	9853.1*	20244.0	21966.9	0.49	1.02	1.30	1.33
	2.35	3726.3	21793.7	23648.6	0.17	0.44	0.81	0.93	2.35	12281*	32666.4	35446.7	0.38	0.97	1.38	1.42
	2.85	3824.6	32052.9	34781.0	0.12	0.37	0.78	0.92	2.85	13840.8	48051.2	52140.8	0.29	0.89	1.38	1.42
	3.35	4180.3	44281.6	48050.5	0.09	0.34	0.81	0.98	3.35	14124.8	66390.2	72040.7	0.21	0.76	1.27	1.32
	3.85	4828.2	58487.9	63465.9	0.08	0.34	0.89	1.11	3.85	14148.5	87683.5	95146.3	0.16	0.66	1.17	1.22
	4.35	5389.3	74663.7	81018.4	0.07	0.33	0.96	1.22	4.35	14148.5	111939	121466	0.13	0.58	1.09	1.14

Table B12: Failure moments and their DSM estimates for SCA and SCB ***C12*** beams

ψ	SCA								SCB							
	λ_D	M_u (kNcm)	M_y (kNcm)	M_p (kNcm)	$\frac{M_u}{M_y}$	$\frac{M_u}{M_{nD}}$	$\frac{M_u}{M^*_{nD}}$	$\frac{M_u}{M^{**}_{nD}}$	λ_D	M_u (kNcm)	M_y (kNcm)	M_p (kNcm)	$\frac{M_u}{M_y}$	$\frac{M_u}{M_{nD}}$	$\frac{M_u}{M^*_{nD}}$	$\frac{M_u}{M^{**}_{nD}}$
+1	0.95	684.4	763.0	841.3	0.90	1.11	1.13	1.13	0.95	867.2	1101.6	1214.6	0.79	0.97	0.97	0.99
	1.45	861.0	1774.0	1956.0	0.49	0.83	1.07	1.07	1.45	1176.8	2565.6	2828.8	0.46	0.78	0.90	0.92
	1.95	944.9	3204.6	3533.4	0.29	0.65	1.03	1.03	1.95	1526.9	4640.0	5116.0	0.33	0.72	0.94	0.97
	2.45	1029.9	5059.6	5578.7	0.20	0.55	1.03	1.03	2.45	1962.4	7329.5	8081.5	0.27	0.72	1.04	1.07
	2.95	1102.2	7339.1	8092.1	0.15	0.48	1.04	1.04	2.95	2347.8	10624.7	11714.8	0.22	0.70	1.11	1.15
	3.45	1156.4	10033.4	11062.8	0.12	0.42	1.04	1.04	3.45	2688.7	14530.3	16021.1	0.19	0.68	1.15	1.20
	3.95	1194.2	13156.9	14506.8	0.09	0.38	1.03	1.03	3.95	2535.6	19046.3	21000.5	0.13	0.56	1.00	1.05
	4.45	1232.2	16695.3	18408.3	0.07	0.35	1.02	1.02	4.45	2563.7	24177.4	26658.1	0.11	0.50	0.95	0.99
+0.5	1.15	1187.6	1664.3	1835.0	0.71	1.01	1.13	1.15	1.05	1077.8	1373.4	1514.3	0.78	1.04	1.07	1.09
	1.65	1260.8	3428.7	3780.5	0.37	0.70	0.99	1.03	1.55	1387.7	2990.0	3296.8	0.46	0.84	0.99	1.01
	2.15	1302.5	5822.6	6420.0	0.22	0.54	0.91	0.97	2.05	1858.9	5231.3	5768.0	0.36	0.82	1.09	1.12
	2.65	1306.2	8850.7	9758.8	0.15	0.43	0.85	0.92	2.55	2192.7	8097.3	8928.1	0.27	0.76	1.11	1.15
	3.15	1327.7	12503.6	13786.5	0.11	0.36	0.82	0.90	3.05	2411.7	11583.2	12771.7	0.21	0.68	1.09	1.13
	3.65	1362.9	16785.9	18508.2	0.08	0.32	0.80	0.89	3.55	2567.1	15689.1	17298.8	0.16	0.62	1.06	1.10
	4.15	1573.7	21702.5	23929.2	0.07	0.32	0.89	1.00	4.05	2648.6	20419.7	22514.8	0.13	0.56	1.01	1.06
	4.65	1700.0	27243.7	30039.0	0.06	0.30	0.93	1.05	4.55	2621.6	25774.9	28419.5	0.10	0.49	0.94	0.98
0	1.15	1187.6	1664.3	1835.0	0.71	1.01	1.13	1.17	1.15	1296.0	1850.3	2040.1	0.70	1.00	1.05	1.07
	1.65	1260.8	3428.7	3780.5	0.37	0.70	0.99	1.06	1.65	1663.8	3805.4	4195.9	0.44	0.83	1.01	1.03
	2.15	1302.5	5822.6	6420.0	0.22	0.54	0.91	1.01	2.15	2140.2	6461.6	7124.6	0.33	0.79	1.08	1.11
	2.65	1306.2	8850.7	9758.8	0.15	0.43	0.85	0.97	2.65	2548.9	9818.8	10826.2	0.26	0.75	1.12	1.16
	3.15	1327.7	12503.6	13786.5	0.11	0.36	0.82	0.95	3.15	2703.5	13872.2	15295.5	0.19	0.66	1.07	1.11
	3.65	1362.9	16785.9	18508.2	0.08	0.32	0.80	0.95	3.65	2703.5	18621.9	20532.5	0.15	0.56	0.98	1.02
	4.15	1573.7	21702.5	23929.2	0.07	0.32	0.89	1.08	4.15	2703.5	24077.3	26547.6	0.11	0.49	0.91	0.95
	4.65	1700.0	27243.7	30039.0	0.06	0.30	0.93	1.14	4.65	2720.8	30228.9	33330.5	0.09	0.44	0.85	0.90
-0.5	1.25	1285.2	2131.6	2350.3	0.60	0.91	1.07	1.12	1.25	1340.4	2231.8	2460.7	0.60	0.91	0.99	1.01
	1.75	1333.3	4172.6	4600.8	0.32	0.64	0.94	1.03	1.75	1700.3	4377.7	4826.8	0.39	0.78	0.97	0.99
	2.25	1368.8	6900.3	7608.3	0.20	0.49	0.87	1.00	2.25	2207.4	7234.2	7976.4	0.31	0.76	1.06	1.09
	2.75	1384.5	10305.2	11362.5	0.13	0.40	0.82	0.97	2.75	2655.7	10805.9	11914.6	0.25	0.73	1.12	1.16
	3.25	1407.2	14396.8	15873.9	0.10	0.34	0.79	0.96	3.25	2969.0	15097.8	16646.8	0.20	0.69	1.13	1.17
	3.75	1506.3	19165.5	21131.9	0.08	0.31	0.81	1.00	3.75	3046.7	20095.4	22157.2	0.15	0.60	1.06	1.11
	4.25	1612.2	24616.1	27141.8	0.07	0.29	0.84	1.06	4.25	3051.0	25813.1	28461.6	0.12	0.53	0.99	1.03
	4.75	1777.5	30748.7	33903.6	0.06	0.29	0.90	1.15	4.75	3051.0	32246.1	35554.6	0.09	0.47	0.93	0.97
-1	1.35	1323.0	2541.7	2802.5	0.52	0.84	1.03	1.10	1.35	1745.3	3323.8	3664.8	0.53	0.85	0.95	0.96
	1.85	1372.4	4768.7	5258.0	0.29	0.60	0.92	1.02	1.85	2592.2	6237.5	6877.5	0.42	0.87	1.11	1.14
	2.35	1383.0	7696.7	8486.4	0.18	0.47	0.85	0.98	2.35	3358.4	10066.8	11099.6	0.33	0.87	1.23	1.26
	2.85	1413.1	11320.9	12482.5	0.12	0.39	0.81	0.96	2.85	4064.8*	14802.1	16320.8	0.27	0.85	1.31	1.36
	3.35	1446.7	15641.4	17246.2	0.09	0.33	0.79	0.96	3.35	4207.1*	20453.0	22551.6	0.21	0.74	1.23	1.28
	3.85	1518.9	20658.1	22777.7	0.07	0.30	0.80	0.99	3.85	4182.2*	27014.8	29786.6	0.15	0.63	1.13	1.17
	4.35	1648.7	26371.0	29076.7	0.06	0.29	0.84	1.06	4.35	4180.3*	34487.4	38025.9	0.12	0.56	1.05	1.09
	4.85	1755.0	32785.0	36148.8	0.05	0.27	0.86	1.11	4.85	4180.0*	42870.8	47269.4	0.10	0.50	0.98	1.03

Table B13: Failure moments and their DSM estimates for SCA and SCB ***C13*** beams

	SCA								SCB							
ψ	λ_D	M_u (kNcm)	M_y (kNcm)	M_p (kNcm)	$\frac{M_u}{M_y}$	$\frac{M_u}{M_{nD}}$	$\frac{M_u}{M^*_{nD}}$	$\frac{M_u}{M^{**}_{nD}}$	λ_D	M_u (kNcm)	M_y (kNcm)	M_p (kNcm)	$\frac{M_u}{M_y}$	$\frac{M_u}{M_{nD}}$	$\frac{M_u}{M^*_{nD}}$	$\frac{M_u}{M^{**}_{nD}}$
+1	0.75	699.9	711.2	795.0	0.98	1.05	1.02	1.02	0.75	999.6	1028.3	1149.5	0.97	1.03	1.00	1.02
	1.25	1251.5	1970.1	2202.3	0.64	0.96	1.13	1.13	1.25	1705.2	2854.3	3190.7	0.60	0.91	0.99	1.00
	1.75	1395.9	3863.4	4318.7	0.36	0.72	1.06	1.06	1.75	2032.4	5593.2	6252.4	0.36	0.73	0.91	0.93
	2.25	1523.5	6381.3	7133.4	0.24	0.60	1.05	1.05	2.25	2617.9	9245.2	10334.8	0.28	0.71	0.98	1.01
	2.75	1635.4	9538.3	10662.4	0.17	0.51	1.05	1.05	2.75	3140.4	13814.9	15443.1	0.23	0.68	1.04	1.07
	3.25	1711.5	13320.0	14889.8	0.13	0.45	1.04	1.04	3.25	3618.8	19292.8	21566.6	0.19	0.65	1.08	1.12
	3.75	1752.3	17731.1	19820.8	0.10	0.39	1.02	1.02	3.75	3953.1*	25688.5	28716.0	0.15	0.61	1.08	1.12
	4.25	1782.2	22776.5	25460.9	0.08	0.35	1.00	1.00	4.25	4126.2*	32992.3	36880.7	0.13	0.56	1.04	1.09
+0.5	0.85	1176.1	1167.7	1305.3	1.01	1.15	1.13	1.14	0.85	1730.7	1720.3	1923.0	1.01	1.15	1.13	1.14
	1.35	1637.7	2950.4	3298.1	0.56	0.90	1.10	1.13	1.35	2415.9	4339.1	4850.5	0.56	0.90	1.01	1.02
	1.85	1781.4	5535.6	6188.0	0.32	0.68	1.03	1.09	1.85	3262.3	8149.6	9110.1	0.40	0.84	1.07	1.10
	2.35	1865.0	8932.8	9985.6	0.21	0.54	0.99	1.06	2.35	4162.8	13147.0	14696.4	0.32	0.82	1.16	1.20
	2.85	1913.9	13137.4	14685.7	0.15	0.45	0.95	1.03	2.85	4945.6*	19340.8	21620.3	0.26	0.79	1.22	1.26
	3.35	1968.4	18154.0	20293.5	0.11	0.39	0.93	1.02	3.35	5429.6*	26721.6	29870.9	0.20	0.73	1.22	1.26
	3.85	2355.8	23977.8	26803.8	0.10	0.40	1.06	1.18	3.85	5536.3*	35289.2	39448.3	0.16	0.64	1.14	1.19
	4.35	2438.8	30609.0	34216.5	0.08	0.37	1.06	1.19	4.35	5546.0*	45053.3	50363.2	0.12	0.56	1.06	1.11
0	0.95	1701.9	1797.1	2008.9	0.95	1.17	1.19	1.21	0.95	2371.7	2614.0	2922.1	0.91	1.12	1.12	1.14
	1.45	1950.8	4185.3	4678.6	0.47	0.80	1.03	1.09	1.45	3254.1	6093.0	6811.1	0.53	0.91	1.05	1.07
	1.95	2020.8	7568.2	8460.1	0.27	0.59	0.93	1.02	1.95	4397.8	11018.3	12316.8	0.40	0.88	1.14	1.17
	2.45	2077.1	11945.7	13353.5	0.17	0.47	0.88	0.99	2.45	5421.6*	17394.7	19444.8	0.31	0.84	1.21	1.25
	2.95	2126.1	17317.9	19358.9	0.12	0.39	0.85	0.98	2.95	6184.2*	25217.6	28189.6	0.25	0.78	1.23	1.27
	3.45	2274.5	23689.5	26481.5	0.10	0.35	0.86	1.02	3.45	6436.6*	34491.6	38556.6	0.19	0.69	1.16	1.21
	3.95	2532.9	31051.1	34710.6	0.08	0.34	0.92	1.11	3.95	6459.2*	45211.9	50540.4	0.14	0.60	1.08	1.12
	4.45	2883.5	39412.1	44057.0	0.07	0.34	1.02	1.23	4.45	6459.5*	57383.4	64146.5	0.11	0.53	1.00	1.05
-0.5	1.05	1781.6	2263.2	2530.0	0.79	1.05	1.11	1.14	1.05	2055.5	2599.6	2906.0	0.79	1.05	1.08	1.09
	1.55	1985.9	4930.1	5511.2	0.40	0.73	0.98	1.06	1.55	2631.9	5670.1	6338.4	0.46	0.84	0.99	1.01
	2.05	2033.2	8630.1	9647.2	0.24	0.54	0.89	1.00	2.05	3577.3	9917.9	11086.8	0.36	0.83	1.10	1.13
	2.55	2081.8	13348.8	14922.0	0.16	0.44	0.84	0.98	2.55	4436.3	15342.9	17151.2	0.29	0.81	1.19	1.22
	3.05	2123.2	19095.8	21346.3	0.11	0.37	0.81	0.97	3.05	4671.8	21950.0	24537.0	0.21	0.70	1.12	1.16
	3.55	2123.2	25871.1	28920.2	0.08	0.31	0.77	0.95	3.55	4596.0	29739.2	33244.2	0.15	0.58	1.00	1.04
	4.05	2436.9	33674.7	37643.5	0.07	0.31	0.86	1.07	4.05	4597.4	38705.7	43267.4	0.12	0.51	0.93	0.97
	4.55	2702.6	42501.8	47510.9	0.06	0.30	0.92	1.17	4.55	4619.4	48854.2	54612.0	0.09	0.45	0.87	0.91
-1	1.15	1627.0	2301.7	2572.9	0.71	1.00	1.12	1.16	1.15	2362.6	3541.4	3958.8	0.67	0.95	1.00	1.02
	1.65	1741.0	4742.7	5301.7	0.37	0.70	0.98	1.07	1.65	3276.0	7289.5	8148.6	0.45	0.86	1.04	1.06
	2.15	1822.1	8048.7	8997.3	0.23	0.54	0.92	1.05	2.15	4414.0	12378.1	13837.0	0.36	0.85	1.16	1.19
	2.65	1832.1	12229.2	13670.5	0.15	0.43	0.86	1.01	2.65	4943.6	18802.7	21018.7	0.26	0.76	1.14	1.17
	3.15	1865.7	17279.4	19315.9	0.11	0.37	0.83	1.00	3.15	4934.5	26567.8	29699.0	0.19	0.63	1.02	1.06
	3.65	1893.0	23199.4	25933.6	0.08	0.32	0.81	0.99	3.65	4934.0	35673.6	39878.0	0.14	0.54	0.93	0.97
	4.15	1906.1	29993.9	33528.9	0.06	0.28	0.78	0.98	4.15	4934.0	46115.3	51550.3	0.11	0.47	0.86	0.90
	4.65	1917.9	37658.2	42096.4	0.05	0.25	0.76	0.98	4.65	4933.5	57897.6	64721.2	0.09	0.42	0.81	0.85

Table B14: Failure moments and their DSM estimates for SCA and SCB ***C14*** beams

	SCA								SCB							
ψ	λ_D	M_u (kNcm)	M_y (kNcm)	M_p (kNcm)	$\frac{M_u}{M_y}$	$\frac{M_u}{M_{nD}}$	$\frac{M_u}{M^*_{nD}}$	$\frac{M_u}{M^{**}_{nD}}$	λ_D	M_u (kNcm)	M_y (kNcm)	M_p (kNcm)	$\frac{M_u}{M_y}$	$\frac{M_u}{M_{nD}}$	$\frac{M_u}{M^*_{nD}}$	$\frac{M_u}{M^{**}_{nD}}$
+1	0.85	1925.9	2057.1	2344.8	0.94	1.07	1.06	1.06	0.85	2737.1	2950.2	3362.9	0.93	1.06	1.04	1.05
	1.35	2892.2	5187.7	5913.3	0.56	0.90	1.11	1.11	1.35	4088.4	7452.3	8494.6	0.55	0.89	0.99	1.01
	1.85	3224.5	9734.9	11096.5	0.33	0.70	1.06	1.06	1.85	4821.6	13984.3	15940.3	0.34	0.72	0.92	0.94
	2.35	3538.0	15707.6	17904.5	0.23	0.58	1.06	1.06	2.35	5844.5	22573.4	25730.7	0.26	0.67	0.95	0.98
	2.85	3763.3	23105.7	26337.5	0.16	0.50	1.06	1.06	2.85	6783.7	33192.5	37835.0	0.20	0.63	0.98	1.01
	3.35	3887.1	31929.4	36395.3	0.12	0.44	1.04	1.04	3.35	7086.1	45859.6	52273.8	0.15	0.55	0.92	0.96
	3.85	3914.9	42169.5	48067.7	0.09	0.38	1.01	1.01	3.85	7793.9	60574.7	69047.1	0.13	0.53	0.94	0.98
	4.35	3914.9	53835.2	61364.9	0.07	0.33	0.97	0.97	4.35	8012.2	77328.8	88144.6	0.10	0.47	0.89	0.94
+0.5	0.95	3120.2	3284.1	3743.4	0.95	1.17	1.19	1.20	0.95	4381.1	4745.7	5409.4	0.92	1.14	1.14	1.16
	1.45	3853.3	7659.8	8731.2	0.50	0.86	1.11	1.15	1.45	5747.2	11052.1	12598.0	0.52	0.89	1.02	1.04
	1.95	4163.0	13858.0	15796.3	0.30	0.66	1.05	1.11	1.95	7334.0	19993.1	22789.5	0.37	0.81	1.05	1.08
	2.45	4403.8	21869.7	24928.5	0.20	0.54	1.02	1.09	2.45	8995.9	31559.5	35973.6	0.29	0.77	1.11	1.14
	2.95	4464.7	31712.9	36148.4	0.14	0.45	0.97	1.06	2.95	10156*	45751.3	52150.4	0.22	0.71	1.11	1.15
	3.45	4894.3	43369.5	49435.4	0.11	0.42	1.01	1.12	3.45	10673*	62577.6	71330.2	0.17	0.63	1.06	1.11
	3.95	5127.5	56848.6	64799.8	0.09	0.38	1.02	1.14	3.95	10793*	82029.4	93502.6	0.13	0.55	0.99	1.03
	4.45	5185.1	72159.2	82251.9	0.07	0.34	1.00	1.12	4.45	10798*	104116	118678	0.10	0.49	0.92	0.97
0	1.05	3912.5	4664.5	5316.9	0.84	1.11	1.19	1.21	1.05	3926.4	4835.9	5512.3	0.81	1.08	1.11	1.12
	1.55	4306.1	10158.9	11579.8	0.42	0.77	1.03	1.10	1.55	5066.4	10537.9	12011.8	0.48	0.87	1.03	1.05
	2.05	4525.5	17773.6	20259.6	0.25	0.58	0.96	1.06	2.05	5996.2	18441.3	21020.6	0.33	0.75	1.00	1.02
	2.55	4659.1	27490.5	31335.5	0.17	0.47	0.92	1.04	2.55	7419.6	28537.1	32528.5	0.26	0.73	1.07	1.10
	3.05	4706.1	39336.6	44838.5	0.12	0.39	0.87	1.01	3.05	8979.6	40816.2	46525.1	0.22	0.72	1.16	1.20
	3.55	4885.8	53284.8	60737.6	0.09	0.35	0.87	1.02	3.55	7741.5	55296.8	63031.0	0.14	0.53	0.91	0.94
	4.05	5003.3	69353.3	79053.5	0.07	0.31	0.85	1.02	4.05	7197.9	71978.7	82046.2	0.10	0.43	0.78	0.81
	4.55	5011.3	87532.9	99775.9	0.06	0.27	0.83	1.01	4.55	9084.4	90844.0	103550	0.10	0.48	0.92	0.96
-0.5	1.15	4382.3	6035.8	6880.0	0.73	1.03	1.15	1.20	1.15	4740.9	6613.2	7538.2	0.72	1.02	1.08	1.09
	1.65	4712.5	12414.5	14150.9	0.38	0.72	1.02	1.11	1.65	5923.5	13614.4	15518.6	0.44	0.83	1.01	1.03
	2.15	4970.2	21084.8	24033.8	0.24	0.56	0.96	1.09	2.15	7405.2	23114.7	26347.7	0.32	0.77	1.05	1.07
	2.65	4975.7	32037.7	36518.7	0.16	0.45	0.90	1.05	2.65	7856.3	35114.2	40025.5	0.22	0.65	0.97	1.00
	3.15	5375.3	45264.1	51595.1	0.12	0.40	0.92	1.10	3.15	8931.9	49621.8	56562.3	0.18	0.61	0.99	1.03
	3.65	5856.5	60773.2	69273.4	0.10	0.37	0.95	1.17	3.65	9326.7	66619.6	75937.4	0.14	0.54	0.94	0.98
	4.15	5987.4	78564.9	89553.5	0.08	0.33	0.94	1.18	4.15	10335.1	86125.4	98171.6	0.12	0.53	0.97	1.01
	4.65	6028.5	98630.1	112425	0.06	0.30	0.92	1.17	4.65	10813.0	108131	123254	0.10	0.49	0.95	0.99
-1	1.25	4506.2	7181.6	8186.1	0.63	0.95	1.12	1.17	1.25	5825.1	9193.6	10479.4	0.63	0.96	1.05	1.06
	1.75	4776.1	14083.6	16053.4	0.34	0.68	1.00	1.10	1.75	7823.9	18017.2	20537.3	0.43	0.87	1.08	1.11
	2.25	4917.7	23277.1	26532.9	0.21	0.53	0.93	1.06	2.25	8959.9	29782.1	33947.7	0.30	0.75	1.04	1.07
	2.75	5016.5	34771.4	39634.7	0.14	0.43	0.89	1.04	2.75	8990.5	44488.2	50710.7	0.20	0.60	0.92	0.95
	3.25	5656.0	48557.2	55348.8	0.12	0.41	0.95	1.14	3.25	10563.0	62135.5	70826.3	0.17	0.59	0.98	1.01
	3.75	5788.0	64652.7	73695.5	0.09	0.36	0.93	1.15	3.75	11582.6	82733.1	94304.8	0.14	0.56	0.98	1.02
	4.25	6182.4	83039.9	94654.4	0.07	0.33	0.96	1.21	4.25	11688.9	106263	121126	0.11	0.49	0.92	0.96
	4.75	6182.4	103728	118236	0.06	0.30	0.93	1.19	4.75	11946.0	132734	151299	0.09	0.45	0.88	0.92

Table B15: Failure moments and their DSM estimates for SCA and SCB ***C15*** beams

ψ	SCA								SCB							
	λ_D	M_u (kNcm)	M_y (kNcm)	M_p (kNcm)	$\frac{M_u}{M_y}$	$\frac{M_u}{M_{nD}}$	$\frac{M_u}{M^*_{nD}}$	$\frac{M_u}{M^{**}_{nD}}$	λ_D	M_u (kNcm)	M_y (kNcm)	M_p (kNcm)	$\frac{M_u}{M_y}$	$\frac{M_u}{M_{nD}}$	$\frac{M_u}{M^*_{nD}}$	$\frac{M_u}{M^{**}_{nD}}$
+1	0.80	1964.4	2047.0	2333.8	0.96	1.06	1.03	1.03	0.80	2818.2	2932.2	3343.0	0.96	1.06	1.03	1.04
	1.30	3231.0	5421.7	6181.3	0.60	0.93	1.12	1.12	1.30	4482.4	7759.1	8846.2	0.58	0.90	1.00	1.01
	1.80	3601.7	10387.0	11842.3	0.35	0.71	1.07	1.07	1.80	5352.6	14882.1	16967.1	0.36	0.74	0.93	0.95
	2.30	3994.8	16942.9	19316.6	0.24	0.60	1.08	1.07	2.30	6665.9	24287.1	27689.8	0.27	0.70	0.98	1.01
	2.80	4328.7	25116.9	28635.9	0.17	0.52	1.09	1.09	2.80	7856.2	36001.8	41045.9	0.22	0.66	1.02	1.05
	3.30	4527.0	34895.4	39784.4	0.13	0.46	1.08	1.08	3.30	8414.6	50012.6	57019.5	0.17	0.59	0.99	1.02
	3.80	4620.9	46264.4	52746.2	0.10	0.40	1.06	1.06	3.80	8782.0	66305.4	75595.0	0.13	0.53	0.95	0.99
	4.30	4639.2	59237.8	67537.2	0.08	0.35	1.03	1.03	4.30	9125.0*	84907.9	96803.9	0.11	0.49	0.91	0.95
+0.5	0.90	3267.8	3319.4	3784.5	0.98	1.17	1.17	1.18	0.90	4612.4	4730.2	5392.9	0.98	1.16	1.15	1.16
	1.40	4234.5	8035.8	9161.6	0.53	0.88	1.10	1.14	1.40	6223.4	11452.0	13056.5	0.54	0.90	1.03	1.04
	1.90	4629.5	14812.9	16888.3	0.31	0.67	1.05	1.10	1.90	8212.0	21078.3	24031.5	0.39	0.84	1.08	1.11
	2.40	4891.2	23623.2	26932.9	0.21	0.55	1.01	1.09	2.40	10380*	33636.8	38349.4	0.31	0.82	1.17	1.20
	2.90	5029.8	34494.3	39327.1	0.15	0.46	0.98	1.06	2.90	12120*	49113.5	55994.6	0.25	0.77	1.21	1.25
	3.40	5152.9	47412.3	54055.0	0.11	0.40	0.95	1.05	3.40	13157*	67508.7	76966.9	0.19	0.71	1.19	1.24
	3.90	6136.0	62391.2	71132.5	0.10	0.41	1.09	1.21	3.90	13538*	88835.9	101282	0.15	0.63	1.13	1.18
	4.40	6386.6	79403.2	90528.0	0.08	0.37	1.10	1.23	4.40	13619*	113068	128909	0.12	0.56	1.06	1.11
0	1.00	4238.8	4702.5	5361.3	0.90	1.16	1.20	1.22	1.00	4901.3	5546.2	6323.2	0.88	1.13	1.15	1.16
	1.50	4756.8	10566.8	12047.3	0.45	0.79	1.04	1.11	1.50	6335.7	12489.3	14239.1	0.51	0.89	1.04	1.06
	2.00	5118.0	18782.4	21413.9	0.27	0.61	0.99	1.09	2.00	8384.3	22198.6	25308.7	0.38	0.85	1.12	1.15
	2.50	5196.4	29363.0	33476.9	0.18	0.49	0.93	1.05	2.50	9634.5	34674.1	39532.1	0.28	0.76	1.11	1.14
	3.00	5289.0	42281.1	48204.8	0.13	0.41	0.89	1.03	3.00	9634.5	49943.4	56940.7	0.19	0.62	0.99	1.03
	3.50	5529.5	57536.6	65597.7	0.10	0.36	0.89	1.04	3.50	9970.2	67978.9	77503.0	0.15	0.55	0.93	0.97
	4.00	5696.2	75157.1	85687.0	0.08	0.32	0.88	1.05	4.00	9972.4	88780.6	101219	0.11	0.48	0.86	0.90
	4.50	5770.4	95115.1	108441	0.06	0.29	0.86	1.05	4.50	9972.4	112362	128105	0.09	0.42	0.80	0.84
-0.5	1.10	4765.9	6085.6	6938.2	0.78	1.08	1.17	1.21	1.10	5355.9	7053.8	8042.0	0.76	1.04	1.09	1.10
	1.60	5040.6	12862.7	14664.9	0.39	0.73	1.00	1.09	1.60	6867.0	14923.5	17014.4	0.46	0.85	1.02	1.04
	2.10	5282.3	22170.9	25277.2	0.24	0.56	0.94	1.06	2.10	9048.0	25697.8	29298.2	0.35	0.83	1.11	1.14
	2.60	5385.3	33982.5	38743.6	0.16	0.45	0.89	1.03	2.60	10298.8	39404.3	44925.0	0.26	0.74	1.10	1.14
	3.10	5479.8	48297.5	55064.2	0.11	0.38	0.85	1.02	3.10	11132.3	56015.2	63863.1	0.20	0.66	1.07	1.11
	3.60	6382.5	65143.6	74270.5	0.10	0.38	0.95	1.16	3.60	11008.7	75530.6	86112.7	0.15	0.56	0.96	1.00
	4.10	6592.1	84493.0	96330.8	0.08	0.34	0.94	1.18	4.10	11004.1	97978.1	111705	0.11	0.49	0.89	0.93
	4.60	6663.5	106346	121245	0.06	0.30	0.92	1.17	4.60	11004.1	123330	140609	0.09	0.43	0.83	0.87
-1	1.20	4540.7	6804.8	7758.2	0.67	0.98	1.12	1.17	1.20	6350.0	9529.5	10864.6	0.67	0.98	1.05	1.07
	1.70	4837.4	13664.9	15579.5	0.35	0.69	0.99	1.09	1.70	8676.1	19128.1	21808.1	0.45	0.89	1.09	1.11
	2.20	5003.0	22890.1	26097.2	0.22	0.53	0.93	1.06	2.20	11170.6	32032.4	36520.3	0.35	0.85	1.17	1.21
	2.70	5149.1	34480.4	39311.3	0.15	0.44	0.89	1.04	2.70	11446*	48242.2	55001.1	0.24	0.70	1.05	1.09
	3.20	5223.4	48435.8	55221.9	0.11	0.37	0.85	1.03	3.20	11408*	67771.4	77266.5	0.17	0.58	0.94	0.98
	3.70	5223.4	64756.3	73828.9	0.08	0.32	0.82	1.01	3.70	11408*	90606.3	103301	0.13	0.50	0.87	0.90
	4.20	5757.9	83441.9	95132.4	0.07	0.31	0.87	1.09	4.20	11439*	116747	133103	0.10	0.43	0.81	0.84
	4.70	5762.2	104493	119132	0.06	0.27	0.84	1.08	4.70	11440*	146207	166691	0.08	0.39	0.75	0.79